INTEGRATIVE ANALYSIS OF POLICY CHANGES FOR A COASTAL WATERSHED: IMPLICATIONS FOR AGRICULTURE AND ECOSYSTEM HEALTH

By

Mahesh Ramesh Tapas

July, 2024

Director of Dissertation: Randall Etheridge, PhD

Major Department: Coastal Studies

**ABSTRACT**

This dissertation explores the integration of hydrological modeling, the effects of sea level rise, and socio-economic factors influencing watershed management in North Carolina, primarily utilizing the Soil and Water Assessment Tool Plus (SWAT+) with four independent publication chapters. The first chapter assesses the effectiveness of various satellite precipitation products and autocalibration techniques on river flow prediction, highlighting the superior performance of the Global Precipitation Measurement Integrated Multi-satellitE Retrievals (GPM IMERG) dataset when combined with the Generalized Likelihood Uncertainty Estimation (GLUE) technique. The second study investigates the effects of sea level rise on nitrate dynamics within the Tar-Pamlico coastal watershed, with adjustments made to SWAT+ parameters to simulate changes in nitrogen processes and their impacts on ecosystem health. This reveals increased nitrate loads under sea

level rise scenarios. The third chapter merges econometric and engineering frameworks to evaluate the efficacy of agricultural best management practices (BMPs) as influenced by farmers' behavioral responses. It reveals that despite potential incentives, significant reductions in nitrate loading are not achieved, underscoring the limitations of current models and the importance of comprehensive socio-hydrological frameworks. Collectively, this dissertation enhances our understanding of hydrological processes and their interactions with environmental changes and human factors, offering crucial insights for effective watershed management and policy development.

# Integrative Analysis of Policy Changes for a Coastal Watershed: Implications for Agriculture and Ecosystem Health

A Dissertation

Presented to the Faculty of the Department of Coastal Studies

East Carolina University

In Partial Fulfillment of the Requirements for the Degree of

Doctor of Philosophy in Integrated Coastal Sciences

By

Mahesh Ramesh Tapas

July, 2024

Director of Dissertation: Randall Etheridge, PhD

Dissertation Committee Members:

Ariane Peralta, PhD

Gregory Howard, PhD

Natasha Bell, PhD

Venkataraman Lakshmi, PhD

# DEDICATION

I dedicate this dissertation to my family, who have been my greatest support. My mother, Sangita Tapas, has always been there for me with her love and strength. My sister, Ankita Tapas, has been a constant source of support and joy. And to my late father, Ramesh Tapas, I am forever grateful for his wisdom and guidance. Their support has been invaluable, and this achievement is because of their belief in me.

## ACKNOWLEDGMENTS

I would like to express my sincere gratitude to everyone who has supported me throughout my PhD journey. A heartfelt thank you to my dissertation committee members—Dr. Randall Etheridge, Dr. Gregory Howard, Dr. Ariane Peralta, Dr. Natasha Bell, and Dr. Venkataraman Lakshmi—for their invaluable guidance and support. A special acknowledgment to Dr. Randall Etheridge, who has been the best advisor in the world, providing unparalleled mentorship and encouragement. I am also grateful to the SWAT+ developers and my collaborators for their contributions and teamwork that have enriched my research. Additionally, I want to thank my fellow PhD students and the faculty in the ICS PhD cohort for their encouragement. I also acknowledge the generous funding from the National Science Foundation and the Environmental Protection Agency, which was crucial to my research. Your collective support has been crucial to my success.

TABLE OF CONTENTS

LIST OF TABLES

LIST OF FIGURES

# Chapter 1: Satellite-Based Rainfall Datasets and Autocalibration Techniques' Effects on SWAT+ Flow Simulation

Mahesh R Tapas[1*,†], Randall Etheridge[2,†], Thanh-Nhan-Duc Tran[3], Manh-Hung Le[4,5], Brian Hinckley[2], Van Tam Nguyen[6], Venkataraman Lakshmi[3]

[1] Integrated Coastal Program, East Carolina University, Greenville, NC 27858, USA

[2] Department of Engineering, Center for Sustainable Energy and Environmental Engineering, East Carolina University, Greenville, NC 27858, USA

[3] Department of Civil and Environment Engineering, University of Virginia, Charlottesville, VA 22904, USA

[4] NASA Goddard Space Flight Center Hydrological Sciences Laboratory, MD 20771, USA

[5] Science Applications International Corporation, Greenbelt, MD 20771, USA

[6] Helmholtz Centre for Environmental Research – UFZ, Saxony 04138, Germany

***Corresponding author:** Mahesh R Tapas (tapasm21@students.ecu.edu), 3101, Life Sciences and Biotechnology Building, East Carolina University, Greenville, North Carolina, USA, 27858

[†]This author contributes equally to this paper.

**Highlights**

- Cn2, revap_co, flo_min, revap_min, and awc are the most sensitive parameters.
- Flow simulation is influenced more by rainfall forcing than autocalibration method.
- GPM IMERG rainfall with the GLUE technique showed the highest performance.

**Abstract**

Accurate flow prediction is a primary goal of hydrological modeling studies, which can be affected by the use of varying rainfall datasets, autocalibration methods, and performance indices. The combined effect of three satellite precipitation products (SPPs) — Fifth generation of European ReAnalysis (ERA-5), Gridded meteorological data (gridMET), Global Precipitation Measurement Integrated Multi-satellitE Retrievals (GPM IMERG) — and three autocalibration techniques — Dynamically Dimensioned Search (DDS), Generalized Likelihood Uncertainty Estimation (GLUE), Latin Hypercube Sampling (LHS) — on Soil Water Assessment Tool Plus (SWAT+) river flow prediction is measured using three evaluation metrics — Nash Sutcliffe Efficiency (NSE), Kling Gupta Efficiency (KGE) and coefficient of determination ($R^2$) — for two watersheds in North Carolina (Cape Fear, Tar-Pamlico) using the SWAT+ model. Our findings are: (1) Five parameters in the SWAT+ model, cn2, revap_co, flo_min, revap_min, and awc are the most sensitive among others and over chosen watersheds. (2) Rainfall products are found to have a greater role in streamflow variation compared to calibration techniques. (3) GPM IMERG outperforms other SPPs over assessments, followed by ERA-5 and gridMET. (4) NSE is more sensitive to SPPs and calibration techniques than the KGE. (5) SWAT+ underperforms in the prediction of baseflow for the groundwater-driven watershed. Overall, our findings suggest that the GPM IMERG rainfall dataset, combined with the GLUE optimization technique and KGE

performance index, provides the most effective approach for optimal flow simulations. The results from this study will help hydrological modelers choose an optimal combination of rainfall dataset, autocalibration technique, and performance index depending on watershed characteristics.

**Keywords**

Hydrological Modeling; SWAT+; Rainfall Datasets; Autocalibration Techniques; Performance Indices

**Graphical Abstract**

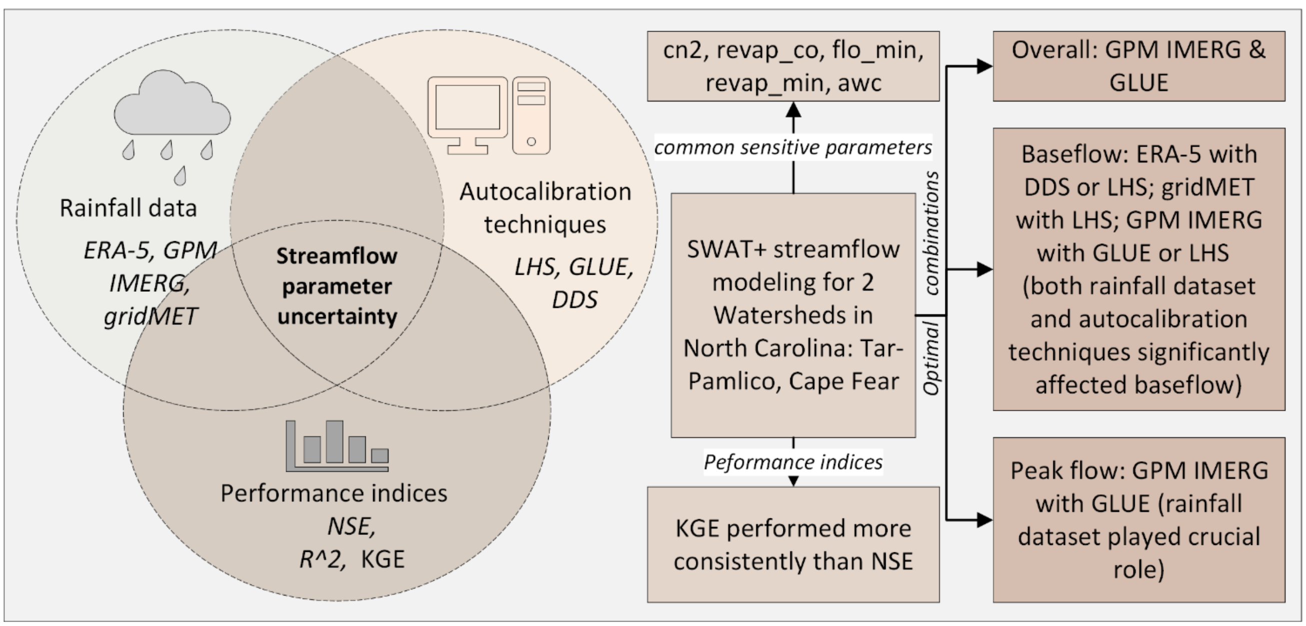

## 1. Introduction

Hydrological models are developed and used to support policies at the watershed and regional scales (Brauman et al., 2022; Aryal et al., 2022). These models are designed using a variety of mathematical equations (e.g., continuity equation, Darcy's law, and Manning's equation) to simulate the complex interactions of hydrological processes (Grimaldi et al., 2021; Herman et al., 2020 ; Ahmed et al., 2020). Policymakers use models' results to evaluate the effectiveness of proposed policies, improve effectiveness of policies, and mitigate unintended side effects when implemented (Maviza & Ahmed, 2021; Pandi et al., 2021; Nguyen et al., 2022; Tran et al., 2021a, 2021b, 2022c; Nuong et al., 2022). These models serve as valuable tools for showing how water quality and quantity may change within a watershed due to alterations in land cover management practices (Brauman et al., 2022; Tran, 2022d; Smigaj et al., 2023). However, the accuracy of these multi-parameterized models has been questioned for informed decision-making (Garibaldi et al., 2019; Grimaldi et al., 2021).

In recent decades, the rapid growth in computational power has enabled the development of more complex models that use a higher number of parameters to accurately represent water movement in a watershed (Adeyeri et al., 2020). However, there are often limited numbers of observations available to assist with model calibration, raising challenges for the accuracy of model predictions (Gupta & Govindaraju, 2019). This mismatch between observed data and multi-parameter simulations increases modeling uncertainty (Beven & Freer, 2001; Wellen et al., 2015). Another type of uncertainty in environmental system models comes from input datasets (Bosshard et al., 2013). These datasets include rainfall, land cover, elevation, and soil information (Chaubey et al., 2005; Cho et al., 2009). Uncertainty in the rainfall dataset comes from low spatiotemporal resolution and assumptions made to average rainfall over the spatial scale used in the model (Fraga et al., 2019; Junqueira et al., 2022).

In recent years, many studies have examined the use of satellite-based rainfall data sets as an alternative to in-situ data, such as Sharifi et al. (2019), Tran et al. (2023b), or Le et al. (2020) evaluating the performance of common satellite-based precipitation products (SSPs) in Austria and Vietnam, respectively. Specifically, Tran et al. (2023b) and Le et al. (2020) conducted experiments that showcased that Global Precipitation Measurement (GPM) Integrated Multi-satellitE Retrievals (IMERG) (Hou et al., 2014) achieved the highest performance across different assessments. However, Tran et al. (2023b) mentioned that SPPs tend to underestimate the total actual amount of rainfall and have issues with rainfall estimates in coastal and arid regions. Thus, one of the main objectives of this study is to evaluate some commonly used precipitation datasets, namely the Fifth Generation of European ReAnalysis (ERA-5) (Muñoz-sabater et al., 2021), IMERG (Hou et al., 2014) and the Gridded Surface Meteorological (gridMET) (Abatzoglou, 2013) to optimize flow simulations in a coastal region.

The Soil and Water Assessment Tool (SWAT), developed by the United States Department of Agriculture (USDA) and Texas A&M AgriLife, is a comprehensive hydrological model designed to predict the impacts of land use, land management, and climate change on sediment transport (Betrie et al., 2011), water quality (Oeurng et al., 2016), and nutrient cycling (Kansara et al., 2021) in river basins. This model has been widely used in previous studies throughout the world: Mekong River Basin (Mohammed et al., 2018b, 2018a; Mondal et al., 2022), Vietnam River Basins (Le et al., 2020; Tran et al., 2022a, 2022b, 2023c), Nepal (Kumar et al., 2017), and United States (Jha et al., 2006; Sehgal et al., 2018; Tapas et al., 2022a, 2022b, Tran et al., 2022e). In recent years, the new version of SWAT, known as SWAT plus (SWAT+), has been released with new features regarding spatial process interactions and visualization (Bieger et al., 2017; Wu et al., 2023). This version allows users to better model the transport and retention of nutrients and sediment in the watershed.

Hydrological models depend on various simplifications, making it extremely challenging to obtain accurate simulations with the initial model setup (Gupta & Govindaraju, 2019; Vieux, 2001). To address this issue and improve the correlation between simulated and observed flow, hydrological modelers perform calibration. Although manual calibration by adjusting individual parameters is possible, the high number of parameter combinations makes this approach impractical (Efstratiadis & Koutsoyiannis, 2010; Sunmin, 2021). Consequently, extensive study has been devoted to developing more accurate hydrological models using automatic optimization techniques (Getirana, 2010; Yen et al., 2019). Arsenault et al. (2014) compared ten stochastic calibration methods and determined that Dynamically Dimensioned Search (DDS) (Tolson & Shoemaker, 2007) outperforms most other techniques, especially with increased model complexity. The Generalized Likelihood Uncertainty Estimation (GLUE) is a widely utilized method among hydrological modelers due to its simplicity (Blasone et al., 2008). Latin Hypercube Sampling (LHS) (Stein, 1987) is another popular method in uncertainty analysis, as it prevents repeated sampling (Yue et al., 2023). However, there is still a lack of comprehensive understanding regarding the application of these calibration methods when using satellite-based precipitation products (SPPs) in the context of enhancing flow simulations at the basin scale.

The performance of hydrological models can be assessed using visual interpretations or statistical indices (Jain & Sudheer, 2008; Wealands et al., 2005). Visual analysis of simulated streamflow can give useful insights into model behavior (Wealands et al., 2005) but needs expert analysis, and is impractical from an automatic calibration point of view (Jain & Sudheer, 2008).

However, performance indices do not require expert opinions and can be optimized using automated calibration techniques (Idrissou et al., 2020; Jain & Sudheer, 2008; Ritter & Munoz-Carpena, 2013). Several performance indices are available to measure the agreement between the observed data and simulated data. Nash Sutcliffe Efficiency (NSE; Nash & Sutcliffe, 1970) is the most widely used performance index for many hydrological models (Tran et al., 2023a, 2023b; Du et al., 2022); however, it is advisable to assess hydrological models using additional performance indices along with NSE (Jain & Sudheer, 2008; Ritter & Munoz-Carpena, 2013; Tran et al., 2023d). Other popular performance indices with hydrological modelers are Kling Gupta Efficiency (KGE) (Gupta et al., 2009) and coefficient of determination ($R^2$) (Adeyeri et al., 2020; Idrissou et al., 2020; Jain & Sudheer, 2008; Chang et al., 2023). NSE, KGE, and $R^2$ are popular as they can be compared with their ideal value of one. All these indices have shortcomings and strengths. For example, NSE does not distinguish between different kinds of errors (Jain & Sudheer, 2008), KGE corrects bias factors from NSE (Gupta et al., 2009), and $R^2$ is not able to measure non-linear relationships among different parameters (Barrett, 1974; Waseem et al., 2017).

The optimal flow prediction and parameter set can vary based on the rainfall dataset, autocalibration techniques, and evaluation metric used. However, there are few studies that provide a comprehensive examination of the relationship between these factors. This study aims to examine the combined effects of these factors on SWAT+ flow simulations. We will perform this analysis on two major watersheds of North Carolina. We will use three different sources of rainfall data (ERA-5, gridMET, GPM IMERG), three automatic calibration methods (DDS, LHS, and GLUE), and three evaluation metrics (NSE, KGE, $R^2$). The objectives of this study are (1) to explore which combinations of three rainfall datasets and three optimization techniques yield better results for flow simulations; (2) to identify how performance indices vary based on the chosen rainfall dataset and optimization technique; and (3) to compare parameter sensitivity and uncertainty analysis for the two watersheds and three rainfall datasets. Our findings will assist hydrological modelers in choosing the most suitable combination of rainfall datasets, optimization techniques, and performance index for stream and river flow simulation.

## 2. Materials and Methods

### 2.1. Study area

This study was conducted in (1) the Tar-Pamlico watershed and (2) the Cape Fear watershed in North Carolina (Figure 1.1). The Cape Fear is the largest river basin in the state (NCDEQ, n.d.-a), while the Tar-Pamlico is the fourth largest (NCDEQ, n.d.-b). These watersheds are two of only four river basins located entirely within North Carolina. The Cape Fear basin discharges into the Atlantic Ocean, while the Tar-Pamlico River flows into the Pamlico Sound. Both watersheds boast diverse ecosystems with a variety of habitats (NCDEQ, n.d.-b, n.d.-a). The Tar-Pamlico watershed contains a larger proportion of agricultural land and wetlands, whereas the Cape Fear watershed has a higher percentage of forested land, pastureland, and urban areas. The Cape Fear watershed also has a higher elevation range compared to the Tar-Pamlico watershed. The major characteristics of both watersheds are summarized in Table 1.1.

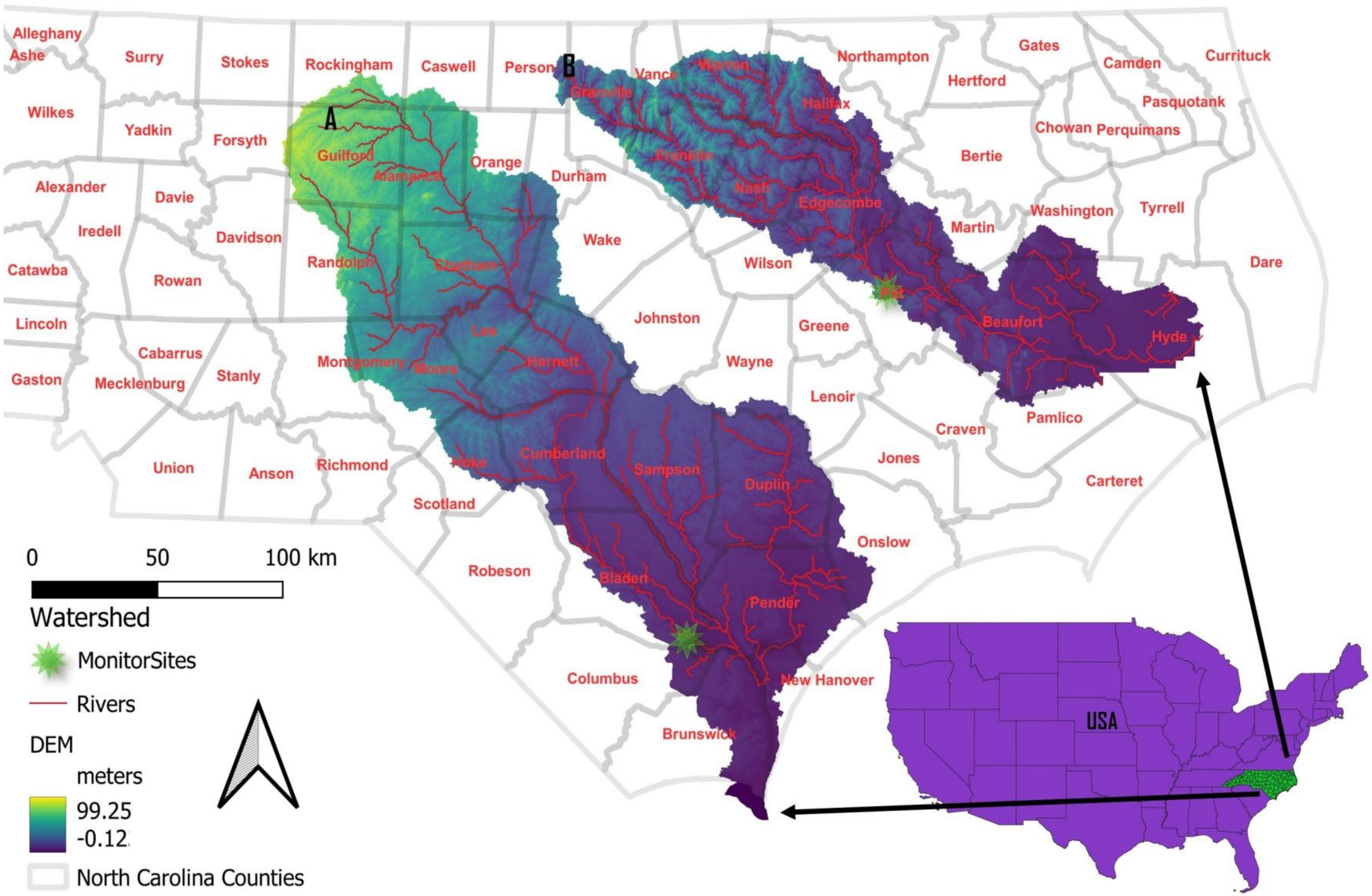


**Figure 1.1** The location of (A) Cape Fear and (B) Tar-Pamlico watersheds.

**Table 1.1** Characteristics of the Tar-Pamlico and Cape Fear watersheds (sources: (NCDEQ, n.d.-b, a, 2023).

| Characteristics | | Tar-Pamlico | Cape-Fear |
|---|---|---|---|
| **Location** | | North Carolina, USA | North Carolina, USA |
| **Area ($mi^2$)** | | 6,400 | 9,164 |
| **Counties** | | 15 | 26 |
| **Population** | | 470,000+ | 2,070,000+ |
| **Land use distribution (%)** | | | |
| **(i)** | **Agriculture** | 27.9 | 18.9 |
| **(ii)** | **Forest land** | 33.9 | 52 |
| **(iii)** | **Wetlands** | 31.9 | 17.9 |
| **(iv)** | **Pasture land** | 3.5 | 6.4 |
| **(v)** | **Rangeland** | 1.3 | 0 |
| **(vi)** | **Urban areas** | 1.4 | 4.7 |

### 2.2. SWAT+ model

SWAT is a semi-distributed hydrological model developed in the early 1990s and is one of the most widely used tools for water quality and quantity simulation (Arnold et al., 1998; Gassman et al., 2022; Guo & Su, 2019; Tran et al., 2024). Technological advancements since the original model was developed have made more detailed hydrological modeling possible, and complexity has been added to the model (Bieger et al., 2017; Efstratiadis & Koutsoyiannis, 2010; Tumsa et al., 2022). SWAT+ is an advanced version of SWAT with respect to data management, data analysis, data visualization, and process interaction at a watershed and sub-watershed level

(SWAT+, 2020). SWAT+ is capable of implementing landscape units as well as flow and pollutant routing over the landscape (SWAT+, 2020). Although the basic equations for calculating flow in SWAT+ have not been changed, significant changes have been made in the code and the formatting of the input files (SWAT+, 2020; White et al., 2022). SWAT+ is also more appealing for spatial and temporal data analysis and data visualization (Bieger et al., 2017). In this study, version 2.2.0 of SWAT+ (released Feb 2023) was used.

## 2.3. Datasets

### 2.3.1. Model set up

We obtained both watershed boundary shapefiles using the United States Geological survey (USGS) StreamStats website (Ries et al., 2017). We used QSWAT+ (Dile et al., 2019) to create streams, sub-basins, and Hydrological Response Units (HRU) using the Digital Elevation Model (DEM), land cover, and soil files. SWAT+ divides the watershed into sub-watersheds, sub-watersheds into landscape units, and landscape units into HRUs. An HRU is the smallest spatial unit in SWAT+, with at least one HRU per sub-basin, incorporating unique land cover, soil, and slope data for their creation (SWAT+, 2020). We used Digital Elevation Model (DEM) data from the United States Geological Survey (USGS), land-use land cover data from the National Land Cover Database (NLCD), and soil data from Soil Survey Geographic Database (SSURGO) at 90 m resolution (Table 1.2) within QSWAT+ (Dile et al., 2019) for initial model setup. We simulated both watersheds with a two-year warm-up period to initiate and stabilize several hydrological processes (Oo et al., 2020).

**Table 1.2.** Data used for HRU creation (TP: Tar-Pamlico watershed, CF: Cape Fear Watershed).

| Product | Spatial resolution | Year | Source |
|---|---|---|---|
| DEM | 90 m | 2011:TP; 2011: CF | USGS |
| Land-use land cover | 90 m | 2008:TP; 2010: CF | NLCD |
| Soil | 90 m | 2015 | SSURGO |

2.3.2. Description of SPPs

2.3.2.1. ERA-5

ERA-5 is the latest climate reanalysis product from the European Centre for Medium-Range Weather Forecasts (ECMWF) and stands as their fifth-generation reanalysis. It provides hourly data encompassing atmospheric, land-surface, and sea-state parameters, complete with uncertainty estimates (C3S, 2017; Hersbach et al., 2020; Muñoz-sabater et al., 2021). The ERA-5 analysis is produced at hourly intervals using an advanced 4Dvar integration approach. This dataset can be found in the Climate Data Store (CDS), structured on regular latitude-longitude grids with a resolution of 0.25° × 0.25°. For our study, we obtained the daily ERA-5 precipitation data by aggregating it from the hourly dataset. The ERA-5 data used in our study is available from the ECMWF website (https://cds.climate.copernicus.eu/).

2.3.2.2. gridMET

gridMET is a 0.04° resolution daily meteorological dataset providing climate data such as temperature, precipitation, wind, humidity, and radiation for the contiguous United States (CONUS). It combines the spatial characteristics of gridded climate data from the Parameter-elevation Regressions on Independent Slopes Model (PRISM) with the favorable temporal features (and additional variables) of the regional reanalysis of North American Land Data Assimilation System Phase 2 (NLDAS-2) through climatically aided interpolation (Abatzoglou, 2013; Abatzoglou & Ficklin, 2017). The gridMET data used in this study can be accessed from the Climatology Lab website (https://www.climatologylab.org/gridmet.html).

2.3.2.3. IMERG

IMERG is a multi-satellite precipitation dataset that provides global precipitation data with high temporal and spatial resolution. It is a product of NASA's GPM mission, which aims to provide accurate and comprehensive precipitation measurements for the entire globe (Li et al., 2021). The GPM IMERG dataset combines data from various sources, including passive microwave sensors, infrared sensors, and radar, to provide precipitation estimates with a spatial resolution of 0.1º and a temporal resolution of 30 minutes (Hou et al., 2014). The IMERG product used in this study can be obtained from the NASA website (https://gpm.nasa.gov/data).

**Table 1.3.** Description of SPP data sets.

| **Product** | **Temporal coverage** | **Spatial resolution** | **Spatial coverage** | **Temporal resolution** | **References** |
|---|---|---|---|---|---|
| ERA-5 | 1940 – present | 0.25º | 90°S – 90°N | 24h | Hersbach et al. (2020) |
| gridMET | 1979 – present | 0.04º | 25°N – 50°N | 24h | Abatzoglou. (2013) |
| IMERG | 2000 – 2021 | 0.1º | 60°N – 60°S | 1/2h | Hou et al. (2014) |

### 2.3.3. In-situ data

For calibration of the SWAT+ model, we used daily observed flow data from USGS. We used the USGS station at the Tar River in Greenville, NC (USGS station id: 02084000) for Tar-Pamlico watershed calibration. The data available at this station is from Oct 1st, 2001, to the present, with data missing from Oct 2006 to Sept 2007 and Oct 2016 to Aug 2019. We used the USGS station at Kelly, NC (USGS station id: 02105769) for calibration of the model for the Cape Fear watershed. The USGS station in Greenville, NC, has some tidal influence and occasionally shows negative flow values. It is important to note that only a small fraction of the readings—specifically, 50 out of 5022, which is less than 1%—exhibited negative flows. As SWAT+ cannot handle backflow (SWAT+, 2020), we converted negative flow values to zeros to ensure the negative flows are captured as low flows and should simulate as low as possible, ideally zero, considering one-dimensional flow limitations. The USGS station for the Cape Fear River calibration does not have any tidal influence. Considering the missing observed flow data and available weather data period, we simulated the Tar-Pamlico watershed from Jan 2001 to Sept 2016 and the Cape Fear watershed from Jan 2003 to Dec 2018 with two years as a warm-up period.

### 2.4. Autocalibration techniques

Calibration is an important step in hydrological modeling in which users try to match simulated data with observed data by changing multiple parameters in the model (Sunmin, 2021; Tolson & Shoemaker, 2007). We used LHS (Stein, 1987), DDS (Tolson & Shoemaker, 2007), and GLUE (Blasone et al., 2008) automatic calibration approaches. LHS is a powerful method of selecting parameter values for a given number of simulations. It divides *n* number of parameters in *m* equal ranges so that each region is targeted. This method tests the combination of parameters in fewer simulations relative to random sampling. We performed a sensitivity analysis using LHS with

2,100 simulations considering the 17 most widely used flow parameters (Table 1.4). We selected diverse parameters from the aquifer, soil, channel, HRU, and basin level to comprehensively model flow (Bailey et al., 2020; Nguyen et al., 2022; Srinivasan et al., 2010; Tan & Yang, 2020). In our preliminary analysis using the GPM IMERG rainfall dataset, we conducted 2,100 simulations and found that the sensitive parameters were consistently identified for both the Tar-Pamlico and Cape Fear watersheds.

The DDS algorithm is a heuristic-artificial intelligence technique to find the best option amongst given options – the algorithm searches for a globally optimal solution at the start and narrows to the optimal local solution towards the end of user-specified iterations (Tolson & Shoemaker, 2007). For the DDS method, we performed parallel processing with 175 iterations on 12 threads with a total of 2,100 simulations. GLUE is a simple and flexible algorithm widely used by environmental system modelers (Beven & Binley, 1992; Tolson & Shoemaker, 2007). In the GLUE method, numerous parameter combinations are randomly selected. Each combination is assigned a likelihood — representing its chance of appearing in multiple model sets — based on the principle of equifinality, which acknowledges that multiple parameter sets can similarly well simulate system behavior despite the differences in the parameter values themselves. (Blasone et al., 2008; Mirzaei et al., 2015). For GLUE and LHS methods, we also used a parallel processing approach with a total of 2,100 simulations.

**Table 1.4.** SWAT+ flow parameters selected for sensitivity analysis and optimization.

| Parameter | Resolution | Description |
|---|---|---|
| alpha | Aquifer | Baseflow recession factor |
| awc | Soil | Available water capacity of the soil layer |
| bf_max | Aquifer | Maximum baseflow rate when the whole area is adding up to the baseflow |
| canmx | HRU | The upper limit of canopy storage |
| chk | Channel | Channel base conductivity |
| cn2 | HRU | SCS curve number for soil moisture condition-2 |
| cn3_swf | HRU | Curve number condition III for soil moisture factor |
| epco | HRU | Plant uptake compensation factor |
| esco | HRU | Soil evaporation compensation factor |
| flo_min | Aquifer | The minimum depth from the surface to the water table required for groundwater flow to occur |
| k | Soil | Hydraulic conductivity |
| ovn | HRU | Manning’s coefficient for overland flow |
| perco | HRU | Percolation coefficient |
| revap_co | Aquifer | Groundwater revap coefficient |
| revap_min | Aquifer | Threshold depth of shallow aquifer for revap to occur |
| surlag | Basin | The coefficient for surface runoff lag |
| evlai | Basin | Leaf area index at zero evaporation from water bodies |

### 2.5. Performance metrics

The goodness-of-fit of model output is measured using performance indicators (Jain & Sudheer, 2008; Wealands et al., 2005). We used the three most widely used performance indicators: NSE (Nash & Sutcliffe, 1970), KGE (Gupta et al., 2009), and $R^2$ (Barrett, 1974; Ozer, 1985). All of them have an ideal value of one for comparison, and each measures different aspects of goodness-of-fit (Ritter & Muñoz-Carpena, 2013). NSE indicates the variation between observed and residual data variance (Nash & Sutcliffe, 1970). KGE is a comprehensive score considering the ratios of means and dispersion, along with the correlation of observed and simulated datasets (Gupta et al., 2009). The $R^2$ explains how well the simulated variable explains the observed variable's variation (Ozer, 1985). Most hydrological models use NSE for testing model performance; however, NSE can be biased depending on data repetition, magnitude, and the number of measurements (Jain & Sudheer, 2008; Ritter & Muñoz-Carpena, 2013). Thus, it is advised to assess the model goodness-of-fit using multiple performance indices (Jain & Sudheer, 2008). In this study, we compared model results using three performance indices. We optimized the model for NSE and found the maximum value from all 2,100 simulations using each autocalibration technique. The formula for calculating NSE, KGE, and $R^2$ are shown in Table 1.5.

**Table 1.5.** Model performance indicators used in this study ($Q_{obs}$ is observed streamflow, $Q_{sim}$ is simulated streamflow, i is $i^{th}$ simulation, and $\bar{Q}$ is the mean value, and n is the total number of values).

| Performance indicator | Metric equation |
|---|---|
| NSE | $\mathrm{NSE} = 1 - \frac{\sum_{i=1}^{n}(Q_{obs} - Q_{sim})^2}{\sum_{i=1}^{n}(Q_{obs} - \overline{Q_{obs}})^2}$ |
| KGE | $\mathrm{KGE} = 1 - \sqrt{(CC-1)^2 + \left(\frac{{Q_{sim}}^d}{{Q_{obs}}^d} - 1\right)^2 + \left(\frac{\overline{Q_{sim}}}{\overline{Q_{obs}}} - 1\right)^2}$ |
| $R^2$ | $R^2 = \frac{\left[\sum_i (Q_{obs,i} - \overline{Q_{obs}})(Q_{sim,i} - \overline{Q_{sim}})\right]^2}{\sum_i (Q_{obs,i} - \overline{Q_{obs}})^2 \sum_i (Q_{sim,i} - \overline{Q_{sim}})^2}$ |

2.6. R-SWAT

Over the last decade, there has been a significant development in autocalibration tools and platforms for hydrological models. The current SWAT+ calibration tools are SWAT+ Toolbox (Celray, 2022; Gassman et al., 2007), SWATplusR (Schuerz, 2022), SWATplus-CUP (WWEE, 2023), R-SWAT (Nguyen et al., 2022), and IPEAT+ (Yen et al., 2019). SWAT+ toolbox is coded in the C language and is not available for the Linux and Mac operating systems. There is no explicit SWAT+ toolbox user portal functional for researchers to discuss modeling challenges. SWATplusR is a package in R that allows users to identify reasonable parameter ranges along with parallel processing. SWATplusR currently does not have a graphical user interface and could be challenging to use for those with no experience using R software. SWATplusCUP has a graphical user interface and can be used by beginners. SWATplusCUP premium features, such as parallel processing, are not open source. IPEAT+ in the current version does not provide uncertainty analysis or a graphical user interface (Nguyen et al., 2022; Yen et al., 2019).

R-SWAT has a graphical user interface within R and provides an open-source parallel processing option for SWAT+. R-SWAT was developed using the Shiny-R-package (Nguyen et al., 2022) and has a user group for researchers to discuss questions. These advantages are why R-SWAT was used in this study. Parameters can be altered in 3 ways in SWAT+: (1) absolute value change, (2) change the value by relative percentage, and (3) change the value by a specified amount. For instance, if the original parameter value in SWAT+ is x, then the new value of a parameter (x') after assigning change (C) under different change types will be absolute value change (x' = x + c), percentage change (x' = x + c*x), replace (x' = c) (Nguyen et al., 2022). The calibration (CAL) file included with SWAT+ shows the absolute minimum and maximum range of the parameters in the model. We used the replace parameter change option for the basin-wide parameters and a few aquifer-level parameters based on previous literature (Table 1.6). We justify using replace options for aquifer-level parameters due to SWAT+ defaulting to assigning uniform values for all aquifers in a given watershed; thus, we have no loss of resolution at the aquifer level. For parameters with a narrow range (range 0 to 1), we used absolute value change, and for the parameters with a wide range, we used the relative change option (Table 1.6). This allowed us to target for large number of parameter combinations with limited simulations.

**Table 1.6.** Type of change and range of parameters used for calibration.

| Parameter | Type of change | Min | Max | Units |
|---|---|---|---|---|
| alpha.aqu | replace | 0.01 | 0.5 | Days |
| awc.sol | absolute | 0.01 | 0.3 | mm_H20/mm |
| bf_max.aqu | absolute | 0 | 1 | mm |
| canmx.hru | relative | -0.25 | 0.25 | mm/H20 |
| chk.rte | relative | -0.25 | 0.25 | mm/hr |
| cn2.hru | relative | -0.3 | 0.2 | Null |
| cn3_swf.hru | absolute | 0 | 0.5 | Null |
| epco.hru | absolute | 0 | 0.5 | Null |
| esco.hru | absolute | 0 | 0.5 | Null |
| flo_min.aqu | relative | -0.25 | 0.5 | m |
| k.sol | relative | -0.25 | 0.25 | mm/hr |
| ovn.hru | absolute | 0 | 10 | Null |
| perco.hru | absolute | 0 | 0.5 | fraction |
| revap_co.aqu | absolute | 0 | 0.1 | Null |
| revap_min.aqu | relative | -0.25 | 0.25 | m |
| surlag.bsn | replace | 0.05 | 24 | Days |
| evlai.bsn | replace | 0 | 10 | Null |

Both watersheds were automatically calibrated using three different methods (LHS, DDS, GLUE) with three rainfall datasets (ERA-5, gridMET, GPM IMERG) in R-SWAT. Based on the literature review and watershed characteristics, we selected the 17 most widely used flow parameters (Table 1.6) for sensitivity analysis and model optimization. We analyzed models with three performance indices (NSE, KGE, $R^2$) and visual interpretation to explore the goodness-of-fit of SWAT+ simulated flow for different scenarios.

Sensitivity analysis was conducted utilizing the Latin Hypercube Sampling (LHS) in parallel mode through R-SWAT. A total of 2,100 simulations were performed using 17 calibration parameters (Table 1.6). An $\alpha$ value of 0.05 was used to determine whether a parameter was considered sensitive - a parameter with a *p-value* less than 0.05 was indicated as sensitive. These sensitive parameters were confirmed with a high t-statistic (t-stat) value.

## 3. Results

### 3.1. Sensitivity analysis

Key parameters affected by the different rainfall datasets were identified using sensitivity analysis for the Tar-Pamlico and Cape Fear watersheds. For Tar-Pamlico watershed for (a) ERA-5 rainfall data we found sensitive parameters are cn2, revap_co, flo_min, revap_min, awc, alpha, perco, and epco; (b) gridMET dataset the sensitive parameters are cn2, revap_co, flo_min, revap_min, awc, epco and cn3_swf; (c) GPM IMERG dataset we found sensitive parameters are cn2, revap_co, flo_min, revap_min, awc, alpha, and esco (Figure 1.2).

In the case of the Cape Fear river basin (a) ERA-5 rainfall data we found sensitive parameters are cn2, revap_co, flo_min, revap_min, awc, alpha, perco, and epco; (b) gridMET dataset the sensitive parameters are cn2, revap_co, flo_min, revap_min, awc, alpha, perco, epco and cn3_swf; (c) GPM IMERG dataset we found sensitive parameters are cn2, revap_co, flo_min, revap_min, awc, alpha, perco, and cn3_swf (Figure 1.2).

Five common sensitive parameters were identified, including cn2, revap_co, flo_min, revap_min, and awc, for different rainfall datasets for Cape Fear and Tar-Pamlico watersheds (Figure 1.2). Flow was sensitive to the alpha parameter (representing baseflow) for all rainfall datasets and both watersheds, with the exception of the Tar-Pamlico watershed model utilizing the gridMET rainfall dataset. The percolation coefficient (perco) parameter was found to be sensitive under all rainfall datasets in the Cape Fear watershed and the ERA-5 dataset for the Tar-Pamlico watershed. For gridMET, flow simulations for both watersheds were found to be sensitive to epco (plant uptake compensation factor) and cn3_swf (soil water factor for cn3 parameter). In this work, the chosen watersheds showed their unique characteristics due to complex interactions between land and water processes, especially under tidal influences which significantly impact the baseflow and peaks. Our findings can serve as a reference for using these chosen parameters, tested across various SPPs and calibration techniques. Additionally, they highlight the challenges and considerations necessary when modeling coastal watershed dynamics.

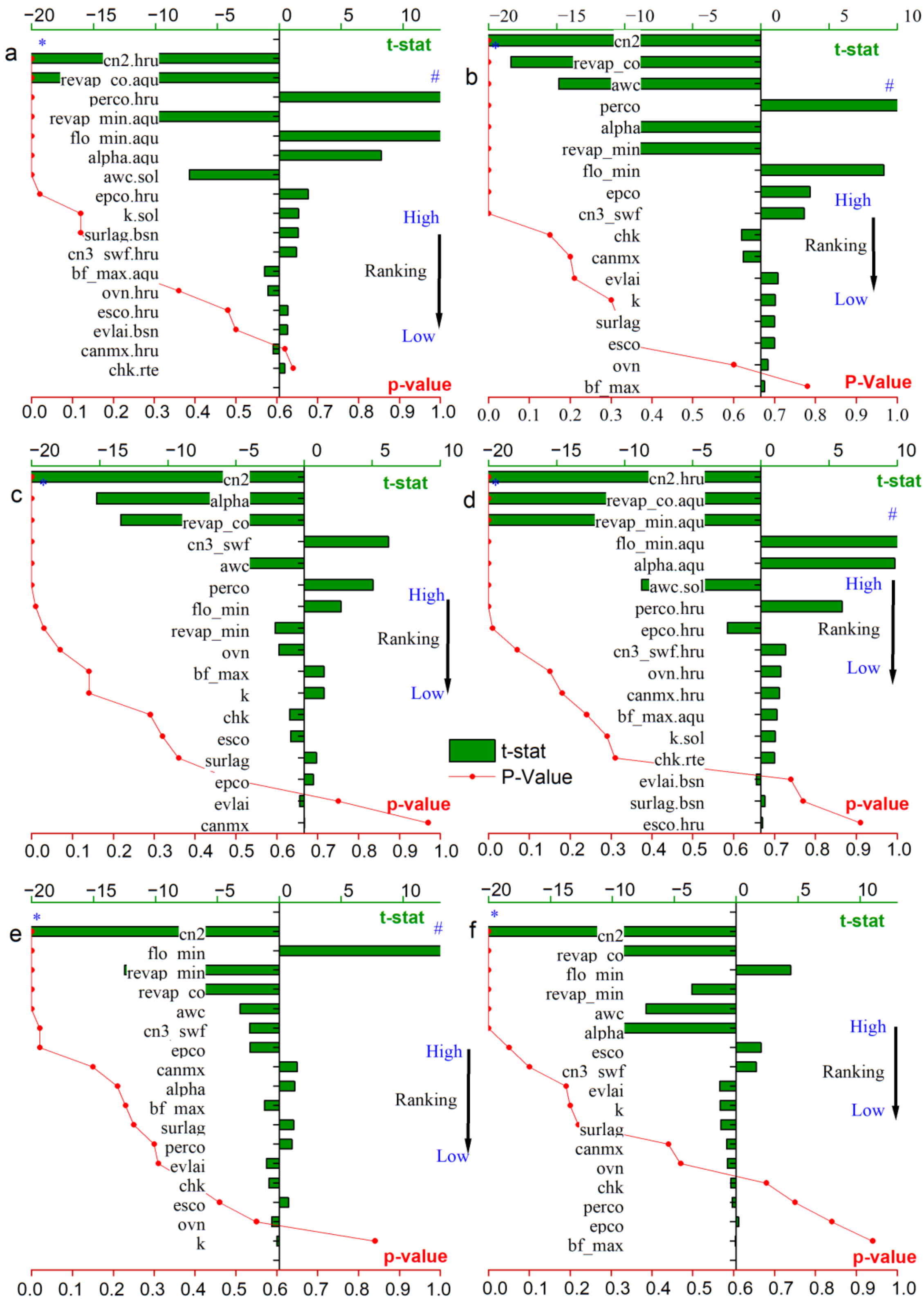


**Figure 1.2** Parameter sensitivity analysis (a: CF_ERA-5, b: CF_gridMET, c: CF_GPM IMERG, d: TP_ERA-5, e:TP_gridMET, f:TP_GPM IMERG; * indicates t_stat<20; # indicates t_stat>10).

3.2. Analysis of simulated streamflow

We tested nine different simulated flow scenarios with the combination of three rainfall datasets and three autocalibration techniques using SWAT+ for each watershed. One method of assessing model accuracy is visually comparing the simulated and observed flow. As shown in Figure 1.3 for the Tar-Pamlico watershed, the high observed flow in 2011 (above 250 $m^3s^{-1}$) occurred around late August and early September (Figure 1.3). This increased flow was due to Hurricane Irene - a category one hurricane - hitting eastern North Carolina. The high flows were measured at USGS Greenville station from August 28th, 2011, to September 5th, 2011, with the highest observed daily flow on August 31st, 2011, of 345 $m^3s^{-1}$ (Figure 1.3). We simulated the flow for Tar-Pamlico from 2001 to 2016, but to get more insights into SWAT+ peak flow and baseflow predictions, we have shown the predictions for the year 2011 in Figure 1.3 for the Tar-Pamlico watershed. This section helps us understand the combined effects of rainfall datasets and optimization techniques on simulated storm flows. SWAT+ fell short of capturing peak flow duration for all scenarios by three days. The calibrations using the GPM IMERG rainfall product did the best job predicting the magnitude of peak flow, whereas gridMET did the worst. Simulated flows using all three rainfall products under all optimization techniques underestimated the time to peak flow and subsequent baseflow recession times.

SWAT+ model performed well in predicting flow magnitude with GPM IMERG rainfall dataset followed by ERA-5 and gridMET dataset. For GPM IMERG data, the GLUE optimization technique (358 $m^3s^{-1}$) performed better than LHS (426 $m^3s^{-1}$) and DDS (309 $m^3s^{-1}$) for simulating the peak flow during Hurricane Irene. For ERA-5 data, LHS (311 $m^3s^{-1}$) and GLUE (372 $m^3s^{-1}$) optimization procedures performed better than DDS (595 $m^3s^{-1}$), for simulating the peak flow. For gridMET data, the LHS (243 $m^3s^{-1}$) optimization method performed much better than both GLUE

(974 $m^3s^{-1}$) and DDS (1013 $m^3s^{-1}$) for simulating the peak flow during Hurricane Irene, as DDS and GLUE provided unreasonably high flows.

Similar data is shown in Figure 1.4 for the Cape Fear basin. The results in the Cape Fear basin for each calibration method and rainfall dataset were similar to the results in the Tar-Pamlico basin. Figures 1.3 and 1.4 include periods of baseflow and storm flow simulation using different rainfall data sets. We found that the combinations of the ERA-5 dataset with LHS or GLUE, gridMET dataset with LHS, and GPM IMERG dataset with either GLUE or LHS give better baseflow magnitude prediction results. In the Cape Fear watershed, we observed high baseflows (greater than 40 $m^3$ $s^{-1}$). LHS performed better than DDS and GLUE in most cases, implying that the LHS technique should be used over DDS and GLUE for groundwater-driven watersheds (Figure 1.4).

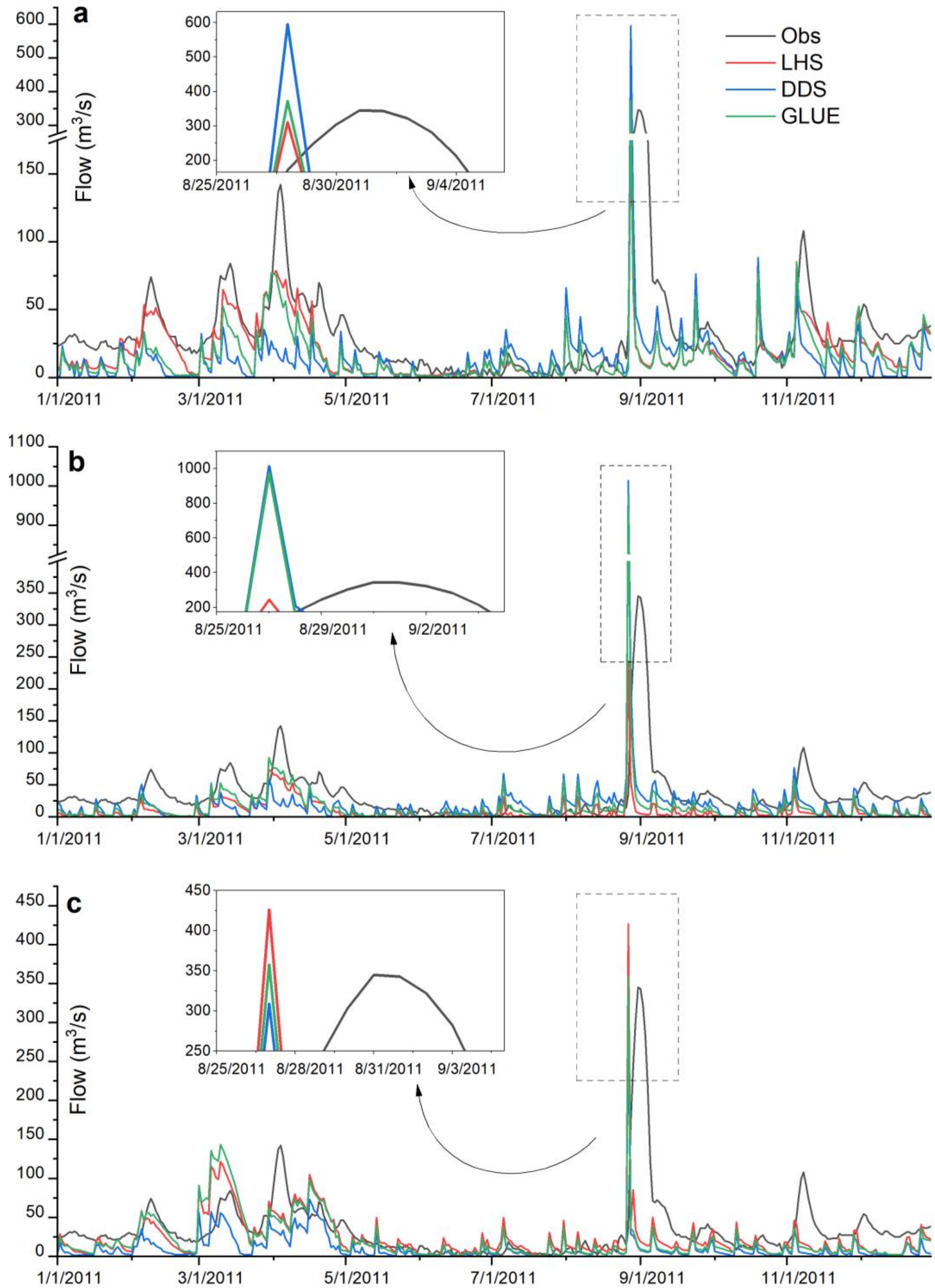


**Figure 1.3** Tar-Pamlico flow simulation for 2011 under different scenarios (a: ERA-5, b: gridMET, c: GPM IMERG).

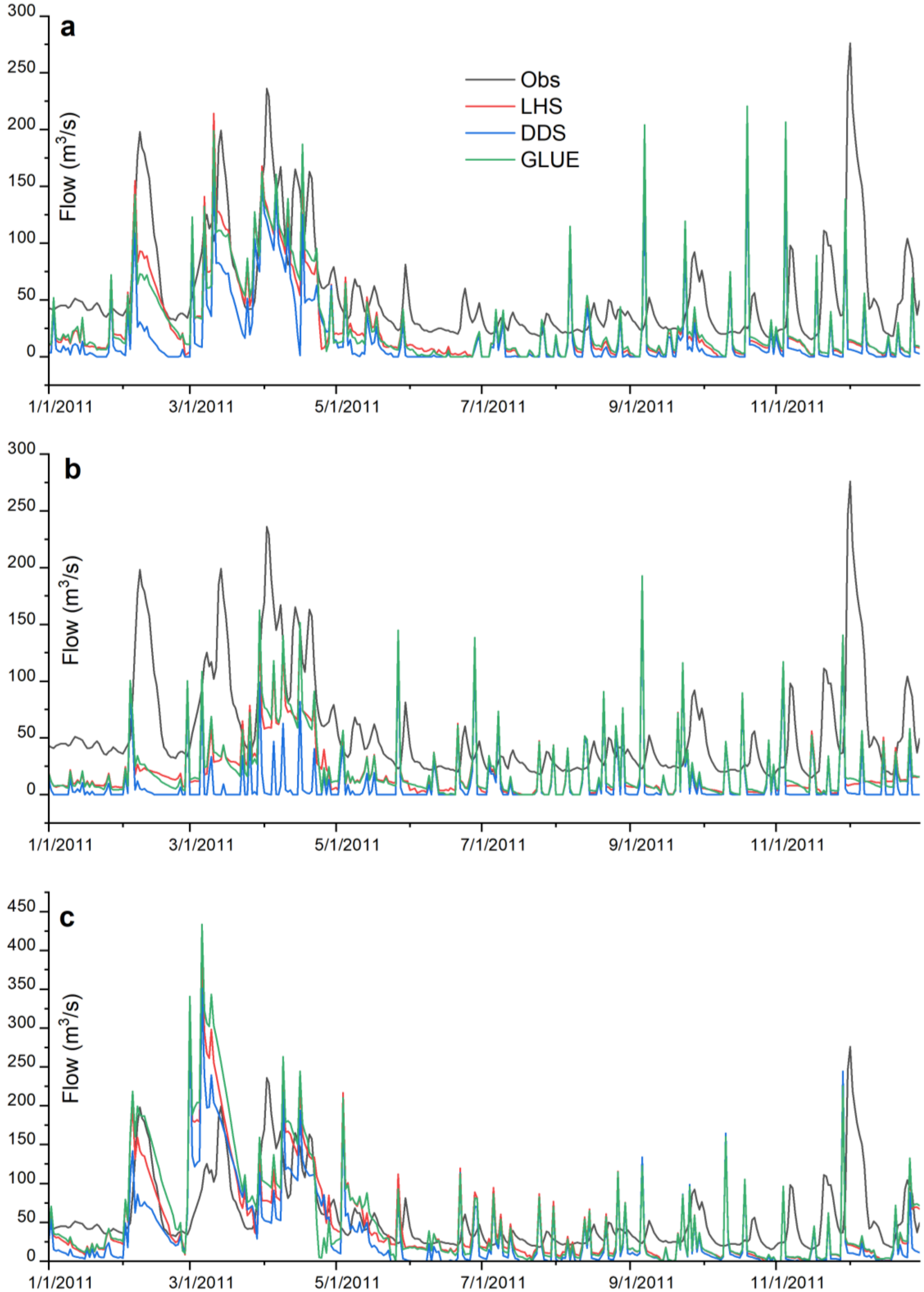


**Figure 1.4** Cape Fear flow simulation for 2011 under different scenarios (a: ERA-5, b: gridMET, c: GPM IMERG).

### 3.3. SWAT+ calibration results evaluation

In this study, we systematically calibrated flow parameters to maximize the Nash-Sutcliffe Efficiency (NSE) utilizing three distinct rainfall datasets and three optimization techniques within two different watersheds. KGE and $R^2$ were evaluated based on all 2,100 simulations for a watershed with a specific set of rainfall data. Figure 1.5 depicts the maximum value of the particular performance metric amongst all simulations for the given scenario.

GPM IMERG data produced optimal flow for both watersheds under LHS and GLUE methods. For the Tar-Pamlico watershed, we found the best KGE (0.424) and $R^2$ (0.501) for the ERA-5 dataset with the LHS method and the best NSE (0.323) with the GLUE method. The gridMET dataset gave the best KGE (0.188) and $R^2$ (0.439) with the LHS method and the best NSE (0.059) with the GLUE method. The GPM IMERG rainfall data produced the best KGE (0.619) with the LHS method and the best NSE (0.412) and $R^2$ (0.498) with the GLUE method (Figure 1.5).

For the Cape Fear River basin, we found the best NSE (0.449), KGE (0.522), and $R^2$ (0.559) for ERA-5 data with the LHS method. The gridMET dataset gave the best NSE (0.341) and $R^2$ (0.498) with the GLUE method and the best KGE (0.426) with the LHS method. For the GPM IMERG dataset, we found the best NSE (0.498) and KGE (0.676) with the GLUE method and the best $R^2$ (0.532) with the LHS method (Figure 1.5).

The ERA-5 and GPM IMERG datasets performed better than the gridMET rainfall dataset when evaluated using KGE and NSE indices (Figure 1.5). On the other hand, $R^2$ performed better than NSE and KGE for the gridMET dataset (Figure 1.5). We found the worst performance index values for gridMET rainfall data when optimized with the DDS technique (NSE, KGE, $R^2$ — Tar-Pamlico: -0.236, 0.057, 0.212 —Cape Fear: 0.029, 0.148, 0.304).

We found that KGE varied less among different scenarios than NSE (Figure 1.5). In most cases, we found higher performance indices for ERA-5 and GMP IMERG rainfall datasets with the GLUE optimization technique (Figure 1.5). We found comparatively better results for the gridMET dataset with the LHS optimization technique (NSE, KGE, $R^2$ — Tar-Pamlico: 0.041, 0.188, 0.439 — Cape Fear: 0.314, 0.426, 0.489). NSE gave lower values than KGE and $R^2$ under all scenarios (Figure 1.5). Maximum values of KGE and $R^2$ varied based on the rainfall dataset and optimization technique. We found $R^2$ to give consistently higher values than KGE and NSE for the gridMET rainfall dataset (Figure 1.5). Overall, our findings suggest that the GPM IMERG rainfall dataset, combined with the GLUE optimization technique and KGE performance index, provides the most effective approach for optimal flow simulations (Figure 1.5).

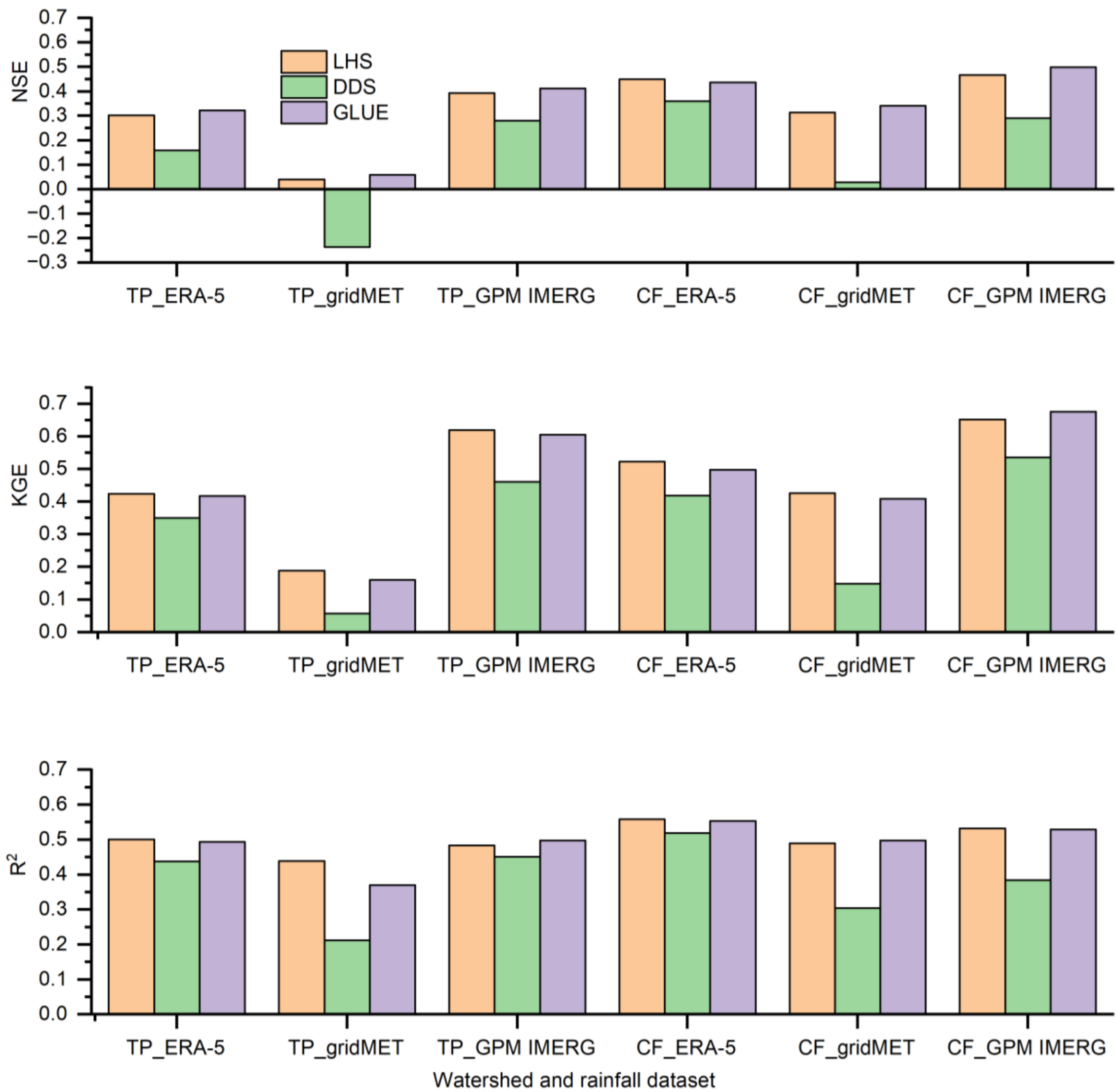


**Figure 1.5** Performance indices for different SPP and optimization technique scenarios (TP: Tar-Pamlico, CF: Cape Fear).

3.4. Parameter uncertainty analysis

We conducted a parameter uncertainty analysis to assess the variability and reliability of the parameters used in predicting streamflow. This analysis encompassed the nine scenarios, involving three rainfall datasets and three optimization techniques, applied across both watersheds, as depicted in Figure 1.6. We compared the optimal values variation of the sensitive parameters under the best NSE for a given scenario. Figure 1.6 shows the box plot of the five common sensitive parameters (cn2, revap_co, awc, flo_min, and revap_min) for both watersheds. We used relative change (cn2, flo_min, revap_min) and absolute value change (awc, revap_co) for these parameters (Table 1.6).

We assumed that the uncertainty in the prediction of these parameters is only from the rainfall dataset and optimization technique used, as we kept all other data (soil map, land cover, observed data, and other SWAT+ input data) constant while building the model. We found the largest variation in the flo_min (Tar-Pamlico: 0.03 to 0.48; Cape Fear: -0.11 to 0.49) and revap_min (Tar-Pamlico: -0.25 to 0.21; Cape Fear: -0.22 to 0.18) parameters between both watersheds, which implies those are more uncertain than the other three parameters. We found comparatively less variation amongst other sensitive parameters for awc (Tar-Pamlico: 0.01 to 0.29; Cape Fear: 0.01to 0.26), cn2 (Tar-Pamlico: -0.29 to 0; Cape Fear: -0.29 to -0.06), and revap_co (Tar-Pamlico: 0 to 0.09; Cape Fear: 0 to 0.08).

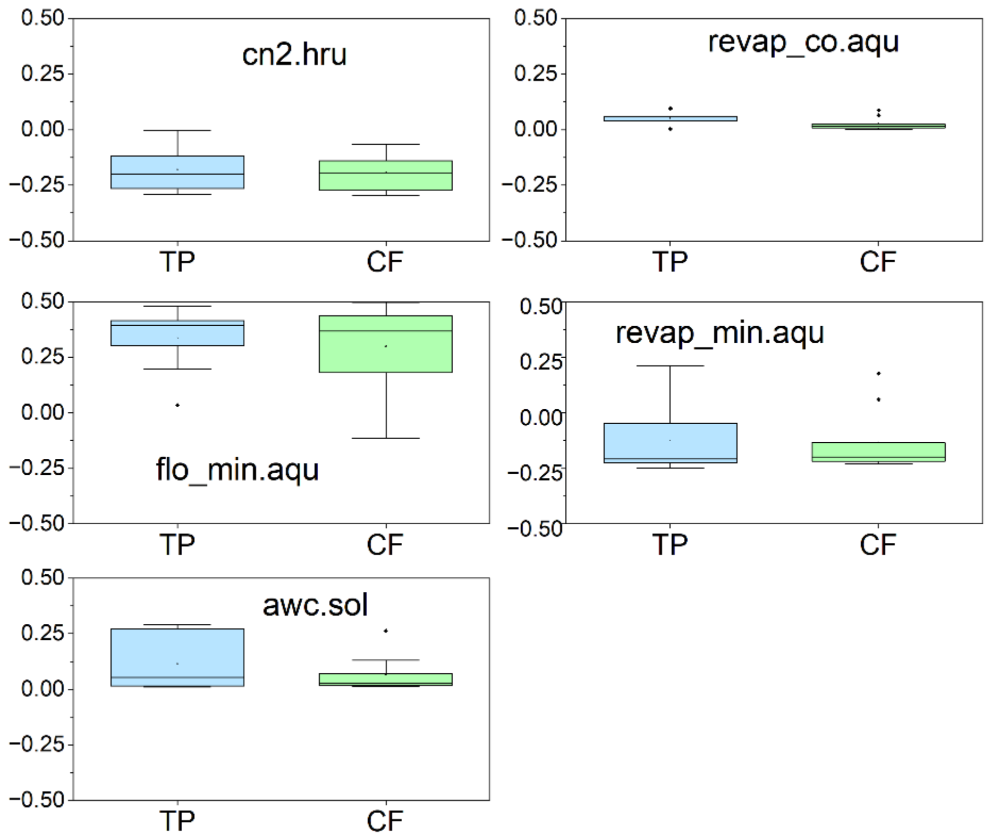


**Figure 1.6** Variation of the common sensitive flow parameters for model combinations and both watersheds: Tar-Pamlico (TP), Cape Fear (CF).

## 4. Discussion

### 4.1. Sensitivity analysis under different rainfall datasets

In the analysis of both Tar-Pamlico and Cape Fear watersheds under each of the three distinct rainfall datasets, five common sensitive parameters consistently emerged: cn2, revap_co, flo_min, revap_min, and awc. This uniformity underscores the significant reliance of flow on these factors that control surface runoff and infiltration partitioning, evapotranspiration, and groundwater discharge to streams. The consistent appearance of these parameters across different scenarios emphasizes their critical role in influencing and regulating watershed responses to different rainfall inputs, reinforcing their importance in SWAT+ modeling and understanding of watershed biogeochemical processes. Our results align with previous literature where they found these parameters sensitive for streamflow simulation (Wagner et al., 2022; Reza & Salmani 2023; Yen et al., 2019)

The high sensitivity of alpha parameter for most scenarios showed the significance of groundwater flow response to recharge changes in flow simulation for ERA-5 and GPM IMERG rainfall datasets and its dependency on the watershed under the gridMET rainfall dataset. In SWAT+, the perco parameter plays a critical role in streamflow simulation, demonstrating sensitivity across most scenarios. This parameter is derived using the Green-Ampt equation for infiltration, as detailed by Rawls et al. (1983), which significantly influences the model's hydrological response. This parameter represents the groundwater infiltration rate as a function of soil hydraulic properties, such as soil texture, structure, and pore size distribution, as well as soil water content and other factors that affect the soil's ability to transmit water (SWAT+, 2020).

The epco parameter specifically addresses simulation of plant water uptake in SWAT+. It is a dimensionless factor that adjusts the plant's root water uptake to account for the reduction in potential evapotranspiration (PET) due to water stress. Sensitivity to the epco parameter can be anticipated in regions with high evapotranspiration rates, such as the Cape Fear and Tar-Pamlico watersheds. These two watersheds exhibit a humid subtropical climate, resulting in high precipitation rates that produce elevated evapotranspiration rates, making the epco parameter critical in evapotranspiration as it adjusts plant root water uptake under water stress conditions.

The newly added parameter, cn3_swf, in SWAT+ enables the simulation of infiltration and ponding on land surfaces before runoff commences following a dry period (Wagner et al., 2022). Studies by Eini et al. (2023), Tumsa et al. (2022), Wagner et al. (2022), and White et al. (2022)

introduced a general view of cn3_swf parameter which accounts for soil water content to adjust the daily curve number. However, we are lacking complete documentation about the use of cn3_swf for SWAT+'s calibration. We found that Cape Fear River's flow is sensitive to cn3_swf under gridMET and GPM IMERG rainfall datasets which could be explained due to its characteristics as having humid subtropical climate, resulting in a high amount of rainfall recorded annually.

In addition, this watershed's soils are highly porous with permeable sediments that could increase the total amount of rainfall recharging to groundwater. Besides, the Tar-Pamlico watershed exhibited high sensitivity to esco (soil evaporation compensation factor) with the GPM IMERG dataset, contributing to SWAT+'s capability to capture the watershed's characteristics as a humid subtropical climatic region with GPM IMERG.

Many SWAT and a few SWAT+ studies mentioned the impacts of watershed characteristics on the performance of rainfall products (Pulighe et al., 2021; Cho et al., 2009). In this study, we also found that the sensitivity of calibration parameters is related to the characteristics of the watershed. Our findings aligned with the studies of Fereidoon et al. (2019) and Guo & Su. (2019) in Tar-Pamlico and Cape Fear, in which curve number (cn2) was found to be the most sensitive parameter with all chosen rainfall datasets and watershed characteristics. In addition, our results aligned with previous works (Migliaccio & Chaubey, 2008; G. Wang et al., 2014; Zhao et al., 2018) that identified revap_co, flo_min, revap_min, awc, alpha, perco, epco, cn3_swf, and esco as significant parameters affecting river flow.

### 4.2. Flow simulation, rainfall dataset and optimization technique

In this study, we analyzed the performance of three rainfall datasets and three optimization techniques on streamflow prediction. We found GPM IMERG rainfall dataset when used with

GLUE optimization technique generally yields better results for flow simulations. Our findings partially address the research gaps identified by Yuan et al. (2019), who called for an evaluation of the compatibility between the GPM IERG dataset and the GLUE optimization technique for optimal flow simulations. Mousavi et al., 2023 reported high values of KGE (0.88) for IMERG-Terra model when used with the GLUE optimization technique.

We have found that the selection of a rainfall dataset can play a vital role in flow simulations. This observation aligns with previous literature on SWAT modeling, where multiple rainfall datasets were used to assess their impact on optimal flow simulations (Cho et al., 2009; Dos et al., 2022). We found a couple of different combinations for optimal flow simulations based on the specific modeling objective. As mentioned earlier, for achieving optimal overall and peak flow simulation, the combination of GPM IMERG rainfall data with the GLUE optimization technique has proven to be more effective. For optimal base flow simulation, the combinations of the ERA-5 rainfall dataset with either DDS or LHS optimization techniques, or the GPM IMERG rainfall dataset with either GLUE or LHS optimization techniques have been found to work better.

The GPM IMERG rainfall dataset showed the best simulation in terms of peak flow magnitude compared to other rainfall datasets. Our results align with previous literature, wherein Tran et al. (2023) indicated that GPM IMERG outperformed five other different satellite precipitation products for flood peak simulations over eleven Vietnam River Basins using SWAT model. This product was rated highly in this assessment due to its design utilizing multiple microwave and infrared sensors, and post-calibration using gauge-based products (Hou et al., 2014).

In general, SWAT+ performance varied greatly for peak flow magnitude simulation, with the GPM IMERG rainfall dataset and GLUE optimization technique combination yielding the best results. SWAT+ underperformed in capturing peak flow duration across various scenarios. Both SWAT and SWAT+ are designed primarily for long-term continuous predictions and have limitations when it comes to capturing instantaneous peak flows (Yu et al., 2018). When simulating flows with all three rainfall products and optimization methods, we consistently experienced an issue of timing peak flow and the subsequent baseflow recession occurring too early. This underscores the significant influence of the curve number (cn2) on hydrograph dynamics during events equivalent to hurricane intensity (Caviedes-Voullième et al., 2012; Lyon et al., 2004). The accuracy of streamflow simulations displayed notable differences depending on the rainfall datasets used. This reinforces the observation that in humid climates, SWAT+ flow simulations exhibit sensitivity to the specific rainfall data (Tan & Yang, 2020).

The Cape Fear watershed is predominantly characterized by sandy soils, conducive to infiltration, is considered as groundwater-driven watershed (Ewen et al., 2011; Valley, 1988), leading to pronounced baseflows sourced from a combination of deep, confined, and shallow aquifers (Ewen et al., 2011; Valley, 1988). However, for the crucial output of baseflow, SWAT+ underperformed in this specific watershed. The model did not accurately predict the magnitude of baseflow. This could be explained by the model's simplified groundwater flow equations. These equations potentially underperform to fully capture the intricacies of baseflow in a watershed that's so heavily influenced by groundwater, as indicated by Bailey et al. (2020).

Our findings indicate that there's no single combination of rainfall dataset and optimization technique is universally superior to other which aligns with previous literature (Dos Santos et al,. 2022; Mararakanye et al., 2020). The combination should be selected based on data availability, computational power availability, watershed location, and watershed characteristics. GPM IMERG (Hou et al., 2014) and ERA-5 (Muñoz-sabater et al., 2021) data are available worldwide, whereas gridMET data is available only for the contiguous United States (Abatzoglou, 2013). There are not regional limitations for choosing optimization techniques; all of them can be accessed worldwide through various open-source applications. We compared these techniques using an equal number of simulations to demonstrate how they perform with similar computational power.

4.3. Effects of rainfall dataset and optimization technique on performance indices

Performance metrics (NSE, KGE, and $R^2$) are formed differently to measure the goodness-of-fit of the simulation and could be biased based on data magnitude, outliers, repetition, and other factors (Ritter & Muñoz-Carpena, 2013). In this study, ERA-5 and GPM IMERG datasets performed better than the gridMET rainfall dataset when evaluated using KGE and NSE indices (Figure 1.5). The worst performance index values for gridMET rainfall data was indicated when using with the DDS technique (NSE, KGE, $R^2$ — Tar-Pamlico: -0.236, 0.057, 0.212 — Cape Fear: 0.029, 0.148, 0.304). Our findings contrast with findings from Tolson and Shoemaker (2007), which determined that DDS was superior in efficiency compared to GLUE. For DDS, our experiment was performed with 175 iterations across 12 threads, yielding a total of 2,100 simulations. We hypothesize that the chosen 175 iterations or the 12-thread configuration might not be adequate to encompass the extensive variety of parameter combinations when employing the DDS's second parallel approach, as mentioned by Nguyen et al. (2022). The method, which involves parallel processing by assigning parameter values to subsequent cores, remains an area where further validation is needed (Nguyen et al., 2022).

Our findings, as shown in Figure 1.5, revealed that KGE exhibited more consistent variations across different scenarios, while NSE values showed abrupt fluctuations when assessing the performance of three rainfall datasets and three optimization techniques in both watersheds.

The robust performance of KGE, especially when compared to NSE, can be attributed to its complex assessment of hydrological model outputs. Specifically, KGE incorporates three different components: correlation (r), variability (alpha), and bias (beta) (Knoben et al., 2019). In contrast, NSE is calculated using the mean squared error between the simulated and observed flows (Moriasi et al., 2007). KGE showed a better performance in identifying model deficiencies and improvements (Pool et al., 2018). This more thorough assessment typically translates to hydrological simulations that are both more precise and dependable (Gupta et al., 2009; Moriasi et al., 2007). It is worth noting that had we adjusted the model specifically for KGE and $R^2$, similar to our optimization for NSE, their performance metrics likely would have been higher.

### 4.4. SWAT+ parameter uncertainty

In this study, we performed experiments with the assumption that the only sources of uncertainty in predicting these parameters stemmed from the rainfall dataset and the optimization techniques used. Thus, scenarios are performed with the same set of input (e.g., soil map, land cover, and observed data) during the modeling process. Our analysis revealed considerable variations, especially in the flo_min parameters for both Tar-Pamlico (ranging from 0.03 to 0.48) and Cape Fear (-0.11 to 0.49) as well as in the revap_min parameters for Tar-Pamlico (-0.25 to 0.21) and Cape Fear (-0.22 to 0.18). The observed variations suggest higher uncertainties in these parameters compared to the other three that were sensitive in all scenarios, emphasizing the need for cautious consideration and potential refinement.

The optimization methods for SWAT+ that we examined were successful in parameterizing cn2 parameter across various HRUs. In SWAT+, groundwater flow parameters, namely revap_co, and revap_min, are delineated at the aquifer level, allowing for a precise parameterization (SWAT+, 2020). The minimal variation observed in the awc parameter highlights SWAT+'s effectiveness in accurately modeling both the flow movement through landscapes and its absorption by vegetation. It has implications for predictions related to runoff and evapotranspiration. The minor discrepancy in the cn2 values across the two watersheds might be attributed to similarities in either land slope or land cover across these regions. Supporting this, Chordia et al. (2022) identified a lesser degree of variation in cn2 in comparison to eight other different parameters over four watersheds. In conclusion, SWAT+ parameterizes key components, such as cn2, the groundwater revap coefficient, and the threshold depth of shallow aquifers where revap takes place, underscoring its effectiveness in SWAT+ modeling.

This study's limitation lies in its use of a broad calibration approach across two watersheds without extensively detailing model inputs or fine-tuning parameters for localized hydrological processes, which could impact the precision of flow predictions in specific scenarios. Additionally, its focus on comparative analysis restricts the ability to fully optimize the model for any single dataset or calibration technique.

## 5. Conclusion

The aim of this study was to comprehensively investigate how the selection of rainfall datasets and autocalibration techniques affect hydrological model flow simulations. We implemented our experiments on two major watersheds located in North Carolina and evaluated them using three performance indices. We found five common sensitive flow parameters — cn2, revap_co, flo_min, revap_min, awc — under all scenarios, with cn2 being the most sensitive parameter. The newly added SWAT+ parameter cn3_swf was found to be sensitive in the groundwater-driven watershed. The sensitivity of the cn3_swf parameter in the groundwater-driven watershed emphasizes the interconnectedness of surface and subsurface hydrological processes within SWAT+, even when groundwater dynamics predominate. Significant variation in the simulated flow under different scenarios of the rainfall dataset and optimization techniques was observed. In most cases, we found overall better flow predictions for ERA-5 and GMP IMERG rainfall datasets with the GLUE optimization technique. We found comparatively better results for the gridMET dataset with the LHS optimization technique.

Autocalibration techniques play an essential role in simulating SWAT+ baseflow accurately compared to storm flows. The rainfall dataset plays a crucial role in both storm flows and baseflow predictions. Overall, SWAT+ does better in capturing baseflow magnitude than peak flow magnitude. GPM IMERG rainfall dataset did a better job than ERA-5 and gridMET in predicting peak flow magnitude. We suggest the combination of the ERA-5 dataset with DDS or LHS, the gridMET dataset with LHS, and the GPM IMERG dataset with either GLUE or LHS to improve baseflow predictions. SWAT+ fell short in predicting baseflow magnitude in the groundwater-driven watershed. SWAT+ has limited capacity to predict extreme runoff events. We were not able to adequately simulate the peak runoff duration caused by Hurricane Irene (North Carolina, Aug 27, 2011) with SWAT+ using any combination of rainfall datasets and optimization techniques. However, GPM IMERG did a better job in capturing peak runoff magnitude with the GLUE method than any other combination.

We found some common trends in performance indices among different scenarios, with NSE giving lower values than KGE and $R^2$ in all cases. Depending on the rainfall dataset and optimization technique used, either KGE or $R^2$ produced the highest values. We found $R^2$ to provide consistently higher values than KGE and NSE for the gridMET rainfall dataset. Overall, we found the GPM IMERG data along with the GLUE optimization technique and KGE performance index for optimal flow modeling. This study will be helpful for hydrological modelers to wisely select the rainfall dataset, calibration method, and performance index combination to predict the more accurate simulated flow. Future studies should explore the effect of the different number of iterations on flow prediction under different rainfall datasets. A better technique for estimating minimum aquifer storage to allow return flow is needed in groundwater-driven watersheds in SWAT+.

**Acknowledgments**

This research was supported by the Center for Sustainable Energy and Environmental Engineering and Water Resources Center at East Carolina University. This work was funded by the National Science Foundation [Funder ID: 2009185 and 2052889] and the Environmental Protection Agency [Funder ID: R840181]. We are grateful to Drs. Ariane Peralta, Meg Blome, Nancy Sammons, Julie Miller, and Zeke Holloman for their insightful feedback on this work. We also thank the editors, Drs. Momcilo Markus and Ying Ouyang, along with the anonymous reviewers, for their constructive comments.

**Data availability**

In accordance with the FAIR (Findable, Accessible, Interoperable, and Reusable) principles, we will make all data, results, and code from our study publicly available in the GitHub repository https://github.com/EtheridgeLab/Tar_Pam_SWAT following the publication of our findings, ensuring transparency and accessibility.. The majority of the data utilized in our research is sourced from open databases.

**ORCID**

Mahesh R Tapas (https://orcid.org/0000-0001-8833-5531)

**References**

Abatzoglou, J. T. (2013). Development of gridded surface meteorological data for ecological applications and modelling. International Journal of Climatology, 33(1), 121–131. https://doi.org/10.1002/joc.3413

Abatzoglou, J. T., & Ficklin, D. L. (2017). Climatic and physiographic controls of spatial variability in surface water balance over the contiguous United States using the Budyko relationship. Water Resources Research, 53(9), 7630–7643.

Adeyeri, O. E., Laux, P., Arnault, J., Lawin, A. E., & Kunstmann, H. (2020). Conceptual hydrological model calibration using multi-objective optimization techniques over the transboundary Komadugu-Yobe basin, Lake Chad Area, West Africa. Journal of Hydrology: Regional Studies, 27, 100655.

Ahmed, Z., Tran, T. N. D., & Nguyen, Q. B. (2020). Applying semi distribution hydrological model SWAT to assess hydrological regime in Lai Giang catchment, Binh Dinh Province, Vietnam. Proceedings of the 2nd Conference on Sustainability in Civil Engineering (CSCE'20), Capital University of Science and Technology, Islamabad, Pakistan, 8. https://csce.cust.edu.pk/archive/20-404.pdf

Anaba, L. A., Banadda, N., Kiggundu, N., Wanyama, J., Engel, B., & Moriasi, D. (2017). Application of SWAT to Assess the Effects of Land Use Change in the Murchison Bay

Catchment in Uganda. Computational Water, Energy, and Environmental Engineering, 06(01), 24–40. https://doi.org/10.4236/cweee.2017.61003

Arnold JG, Srinivasan R, Muttiah RS, Williams Jr. 1998. Large area hydrologic modeling and assessment part I: model development. Journal of the American Water Resources Association 34(1): 73–89

Aryal, A., Tran, T. N. D., Kim, K. Y., Rajaram, H., & Lakshmi, V. (Venkat). (2022). Climate and Land Use/Land Cover Change Impacts on Hydrological Processes in the Mountain Watershed of Gandaki River Basin, Nepal. AGU Fall Meeting Abstracts, 2022, H52L-0615.

Bailey, R. T., Park, S., Bieger, K., Arnold, J. G., & Allen, P. M. (2020). Enhancing SWAT+ simulation of groundwater flow and groundwater-surface water interactions using MODFLOW routines. Environmental Modelling & Software, 126, 104660.

Barrett, J. P. (1974). The coefficient of determination—some limitations. The American Statistician, 28(1), 19–20.

Betrie, G. D., Mohamed, Y. A., van Griensven, A., & Srinivasan, R. (2011). Sediment management modelling in the Blue Nile Basin using SWAT model. Hydrology and Earth System Sciences, 15(3), 807–818.

Beven, K., & Binley, A. (1992). The future of distributed models: model calibration and uncertainty prediction. Hydrological Processes, 6(3), 279–298.

Beven, K., & Freer, J. (2001). Equifinality, data assimilation, and uncertainty estimation in mechanistic modelling of complex environmental systems using the GLUE methodology. Journal of Hydrology, 249(1–4), 11–29.

Bieger, K., Arnold, J. G., Rathjens, H., White, M. J., Bosch, D. D., Allen, P. M., Volk, M., & Srinivasan, R. (2017). Introduction to SWAT+, a completely restructured version of the soil and water assessment tool. JAWRA Journal of the American Water Resources Association, 53(1), 115–130.

Blasone, R.-S., Vrugt, J. A., Madsen, H., Rosbjerg, D., Robinson, B. A., & Zyvoloski, G. A. (2008). Generalized likelihood uncertainty estimation (GLUE) using adaptive Markov Chain Monte Carlo sampling. Advances in Water Resources, 31(4), 630–648.

Brauman, K. A., Bremer, L. L., Hamel, P., Ochoa-Tocachi, B. F., Roman-Dañobeytia, F., Bonnesoeur, V., Arapa, E., & Gammie, G. (2022). Producing valuable information from hydrologic models of nature-based solutions for water. Integrated Environmental Assessment and Management, 18(1), 135–147.

C3S. (2017). ERA5: Fifth generation of ECMWF atmospheric reanalyses of the global climate. European Centre for Medium-Range Weather Forecasts. https://cds.climate.copernicus.eu/cdsapp#!/home

Caviedes-Voullième, D., García-Navarro, P., & Murillo, J. (2012). Influence of mesh structure on 2D full shallow water equations and SCS Curve Number simulation of rainfall/runoff events. Journal of Hydrology, 448, 39–59.

Celray, J. (2022). SWAT+ Toolbox - Home.

Chaplot, V. (2014). Impact of spatial input data resolution on hydrological and erosion modeling: Recommendations from a global assessment. Physics and Chemistry of the Earth, Parts A/B/C, 67, 23–35.

Chordia, J., Panikkar, U. R., Srivastav, R., & Shaik, R. U. (2022). Uncertainties in Prediction of Streamflows Using SWAT Model—Role of Remote Sensing and Precipitation Sources. Remote Sensing, 14(21), 5385.

Pulighe, G., Lupia, F., Chen, H., & Yin, H. (2021). Modeling climate change impacts on water balance of a Mediterranean watershed using SWAT+. Hydrology, 8(4), 157.

Cho, J., Bosch, D., Lowrance, R., Strickland, T., & Vellidis, G. (2009). Effect of spatial distribution of rainfall on temporal and spatial uncertainty of SWAT output. Transactions of the ASABE, 52(5), 1545-1556.

Cooper, V. A. (2007). Calibration of conceptual rainfall – runoff models using global optimisation methods with hydrologic process-based parameter constraints. Journal of Hydrology, 334, 455–466. https://doi.org/10.1016/j.jhydrol.2006.10.036

Chang, C., Lee, H., Do, S. K., Du, T. L. T., Markert, K., Hossain, F., Khalique, S., Piman, T., Meechaiya, C., Bui, D. D., Bolten, J. D., Hwang, E., & Chul, H. (2023). Operational forecasting inundation extents using REOF analysis (FIER) over lower Mekong and its potential economic impact on agriculture. Environmental Modelling and Software, 162(August 2022), 105643. https://doi.org/10.1016/j.envsoft.2023.105643

Dile, Y., Srinivasan, R., & George, C. (2019). QGIS Interface for SWAT+(QSWAT+), version 1.2. 2. Texas AM University.

Dos Santos, V., Oliveira, R. J., Datok, P., Sauvage, S., Paris, A., Gosset, M., & Sánchez-Pérez, J. M. (2022). Evaluating the performance of multiple satellite-based precipitation products in the Congo River Basin using the SWAT model. Journal of Hydrology: Regional Studies, 42, 101168.

Du, T. L. T., Lee, H., Bui, D. D., Graham, L. P., Darby, S. D., Pechlivanidis, I. G., Leyland, J., Biswas, N. K., Choi, G., Batelaan, O., Bui, T. T. P., Do, S. K., Tran, T. V., Nguyen, H. T., & Hwang, E. (2022). Streamflow Prediction in Highly Regulated, Transboundary Watersheds Using Multi-Basin Modeling and Remote Sensing Imagery. Water Resources Research, 58(3), 1–25. https://doi.org/10.1029/2021WR031191

Efstratiadis, A., & Koutsoyiannis, D. (2010). One decade of multi-objective calibration approaches in hydrological modelling: a review. Hydrological Sciences Journal–Journal Des Sciences Hydrologiques, 55(1), 58–78.

Eini, M. R., Massari, C., & Piniewski, M. (2023). Satellite-based soil moisture enhances the reliability of agro-hydrological modeling in large transboundary river basins. Science of the Total Environment, 873, 162396.

Ewen, C. R., Whyte, T. R., & Davis Jr, R. P. S. (2011). The Archaeology of North Carolina: Three Archaeological Symposia. Carolina Archaeological Council Publication.

Fereidoon, M., Koch, M., & Brocca, L. (2019). Predicting rainfall and runoff through satellite soil moisture data and SWAT modelling for a poorly gauged basin in Iran. Water, 11(3), 594.

Gassman, P. W., Jeong, J., Boulange, J., Narasimhan, B., Kato, T., Somura, H., Watanabe, H., Eguchi, S., Cui, Y., & Sakaguchi, A. (2022). Simulation of rice paddy systems in SWAT: A review of previous applications and proposed SWAT+ rice paddy module. International Journal of Agricultural and Biological Engineering, 15(1), 1–24.

Gassman, P. W., Jeong, J., Boulange, J., Narasimhan, B., Kato, T., Somura, H., Watanabe, H., Eguchi, S., Cui, Y., Sakaguchi, A., Tu, L. H., Jiang, R., Kim, M. K., Arnold, J. G., Ouyang, W., Waidler, D., White, M. J. M., Steglich, E., Wang, S., … Tar-Pamlico Basin Oversight

Committee. (2007). 済無No Title No Title No Title. Water Resources Research, 43(6), 1–16. https://doi.org/10.1016/B978-0-12-818597-1.50012-6

Getirana, A. C. V. (2010). Integrating spatial altimetry data into the automatic calibration of hydrological models. Journal of Hydrology, 387(3–4), 244–255.

Grimaldi, S., Nardi, F., Piscopia, R., Petroselli, A., & Apollonio, C. (2021). Continuous hydrologic modelling for design simulation in small and ungauged basins: A step forward and some tests for its practical use. Journal of Hydrology, 595, 125664.

Guo, J., & Su, X. (2019). Parameter sensitivity analysis of SWAT model for streamflow simulation with multisource precipitation datasets. Hydrology Research, 50(3), 861–877.

Gupta, A., & Govindaraju, R. S. (2019). Propagation of structural uncertainty in watershed hydrologic models. Journal of Hydrology, 575, 66–81.

Gupta, H. V., Kling, H., Yilmaz, K. K., & Martinez, G. F. (2009). Decomposition of the mean squared error and NSE performance criteria: Implications for improving hydrological modelling. Journal of Hydrology, 377(1–2), 80–91. https://doi.org/10.1016/j.jhydrol.2009.08.003

Ha, L. T., & Bastiaanssen, W. G. M. (2018). Calibration of Spatially Distributed Hydrological Processes and Model Parameters in SWAT Using Remote Sensing Data and an Auto-Calibration Procedure: A Case Study in a Vietnamese River Basin. Water (Switzerland), 10(2). https://doi.org/10.3390/w10020212

Herman, J. D., Quinn, J. D., Steinschneider, S., Giuliani, M., & Fletcher, S. (2020). Climate adaptation as a control problem: Review and perspectives on dynamic water resources planning under uncertainty. Water Resources Research, 56(2), e24389.

Hersbach, H., Bell, B., Berrisford, P., Hirahara, S., Horányi, A., Nicolas, J., Peubey, C., Radu, R., Balsamo, G., Bonavita, M., Dee, D., Dragani, R., Flemming, J., Forbes, R., Geer, A., Hogan, R. J., Janisková, H. M., Keeley, S., Laloyaux, P., … Thépaut, J. (2020). The ERA5 global reanalysis. Quarterly Journal of the Royal Meteorological Society, 146(June), 1999–2049. https://doi.org/10.1002/qj.3803

Hou, A. Y., Kakar, R. K., Neeck, S., Azarbarzin, A. A., Kummerow, C. D., Kojima, M., Oki, R., Nakamura, K., & Iguchi, T. (2014). The global precipitation measurement mission. Bulletin of the American Meteorological Society, 95(5), 701–722. https://doi.org/10.1175/BAMS-D-13-00164.1

Jain, S. K., & Sudheer, K. P. (2008). Fitting of hydrologic models: a close look at the Nash–Sutcliffe index. Journal of Hydrologic Engineering, 13(10), 981–986.

Jha, M., Arnold, J. G., Gassman, P. W., Giorgi, F., & Gu, R. R. (2006). Climate change sensitivity assessment on Upper Mississippi River Basin streamflows using SWAT. Journal of the American Water Resources Association, 42(4), 997–1015. https://doi.org/10.1111/j.1752-1688.2006.tb04510.x

Kansara, P., Sen, I., & Lakshmi, V. V. (2021). Application of the SWAT model for nutrient modelling of the Narmada River basin. AGU Fall Meeting Abstracts, 2021, H15E-1086.

Knoben, W. J. M., Freer, J. E., & Woods, R. A. (2019). Inherent benchmark or not? Comparing Nash–Sutcliffe and Kling–Gupta efficiency scores. Hydrology and Earth System Sciences, 23(10), 4323–4331.

Kumar, B., Lakshmi, V., & Patra, K. C. (2017). Evaluating the Uncertainties in the SWAT Model Outputs due to DEM Grid Size and Resampling Techniques in a Large Himalayan River Basin. Journal of Hydrologic Engineering, 22(9), 04017039. https://doi.org/10.1061/(asce)he.1943-5584.0001569

Le, M. H., Lakshmi, V., Bolten, J., & Bui, D. Du. (2020). Adequacy of Satellite-derived Precipitation Estimate for Hydrological Modeling in Vietnam Basins. Journal of Hydrology, 586(March), 124820. https://doi.org/10.1016/j.jhydrol.2020.124820

Lee, J., Kim, J., Jang, W. S., Lim, K. J., & Engel, B. A. (2018). Assessment of baseflow estimates considering recession characteristics in SWAT. Water, 10(4), 371.

Levy, M. C., Cohn, A., Lopes, A. V., & Thompson, S. E. (2017). Addressing rainfall data selection uncertainty using connections between rainfall and streamflow. Scientific Reports, 7(1), 1–12.

Li, X., Chen, Y., Deng, X., Zhang, Y., & Chen, L. (2021). Evaluation and hydrological utility of the GPM IMERG precipitation products over the Xinfengjiang River Reservoir basin, China. Remote Sensing, 13(5), 866.

Lovett, E. N. N. R. N. J. C. (2018). Effect of single and multi-site calibration techniques on hydrological model performance , parameter estimation and predictive uncertainty: a case study in the Logone catchment, Lake Chad basin. Stochastic Environmental Research and Risk Assessment, 32(6), 1665–1682. https://doi.org/10.1007/s00477-017-1466-0

Luo, Y., Arnold, J., Allen, P., & Chen, X. (2012). Baseflow simulation using SWAT model in an inland river basin in Tianshan Mountains, Northwest China. Hydrology and Earth System Sciences, 16(4), 1259–1267.

Lyon, S. W., Walter, M. T., Gérard-Marchant, P., & Steenhuis, T. S. (2004). Using a topographic index to distribute variable source area runoff predicted with the SCS curve-number equation. Hydrological Processes, 18(15), 2757–2771.

Maviza, A., & Ahmed, F. (2021). Climate change/variability and hydrological modelling studies in Zimbabwe: a review of progress and knowledge gaps. SN Applied Sciences, 3(5), 549.

Mararakanye, N., Le Roux, J. J., & Franke, A. C. (2020). Using satellite-based weather data as input to SWAT in a data poor catchment. Physics and Chemistry of the Earth, Parts A/B/C, 117, 102871.

Migliaccio, K. W., & Chaubey, I. (2008). Spatial distributions and stochastic parameter influences on SWAT flow and sediment predictions. Journal of Hydrologic Engineering, 13(4), 258–269.

Mirzaei, M., Huang, Y. F., El-Shafie, A., & Shatirah, A. (2015). Application of the generalized likelihood uncertainty estimation (GLUE) approach for assessing uncertainty in hydrological models: a review. Stochastic Environmental Research and Risk Assessment, 29, 1265–1273.

Mohammed, I. N., Bolten, J. D., Srinivasan, R., & Lakshmi, V. (2018a). Improved hydrological decision support system for the Lower Mekong River Basin using satellite-based earth observations. Remote Sensing, 10(6). https://doi.org/10.3390/rs10060885

Mohammed, I. N., Bolten, J. D., Srinivasan, R., & Lakshmi, V. (2018b). Satellite observations and modeling to understand the Lower Mekong River Basin streamflow variability. Journal of Hydrology, 564(January), 559–573. https://doi.org/10.1016/j.jhydrol.2018.07.030

Mondal, A., Le, M. H., & Lakshmi, V. (2022). Land use, climate, and water change in the Vietnamese Mekong Delta (VMD) using earth observation and hydrological modeling. Journal of Hydrology: Regional Studies, 42(June), 101132. https://doi.org/10.1016/j.ejrh.2022.101132

Moriasi, D. N., Arnold, J. G., Van Liew, M. W., Bingner, R. L., Harmel, R. D., & Veith, T. L. (2007). Model evaluation guidelines for systematic quantification of accuracy in watershed simulations. Transactions of the ASABE, 50(3), 885–900.

Mousavi, R., Nasseri, M., Abbasi, S., Taheri, M., & Shamsi Anboohi, M. (2023). Global gridded products efficiency in closing water balance models: various modeling scenarios for behavioral assessments. Acta Geophysica, 71(5), 2401-2422.

Muñoz-sabater, J., Dutra, E., Agustí-panareda, A., Albergel, C., Hersbach, H., Martens, B., Miralles, D. G., Piles, M., & Rodríguez-fernández, N. J. (2021). ERA5-Land: a state-of-the-art global reanalysis dataset for land applications. Earth System Science Data, January 2020, 4349–4383.

Nash, J. E., & Sutcliffe, J. V. (1970). River flow forecasting through conceptual models part I— A discussion of principles. Journal of Hydrology, 10(3), 282–290.

NCDEQ. (n.d.-a). Cape Fear River Basin | NC DEQ.

NCDEQ. (n.d.-b). Tar-Pamlico River Basin Documents | NC DEQ.

NCDEQ. (2023). Tar-Pamlico River Basin | NC DEQ GIS Data.

Nguyen, T. V., Dietrich, J., Dang, T. D., Tran, D. A., Van Doan, B., Sarrazin, F. J., Abbaspour, K., & Srinivasan, R. (2022). An interactive graphical interface tool for parameter calibration, sensitivity analysis, uncertainty analysis, and visualization for the Soil and Water Assessment Tool. Environmental Modelling and Software, 156(August). https://doi.org/10.1016/j.envsoft.2022.105497

Nguyen, B. Q., Tran, T., Łukaszewska, M. G.-, Sinicyn, G., & Lakshmi, V. (2022). Assessment of Urbanization-Induced Land-Use Change and Its Impact on Temperature, Evaporation, and Humidity in Central Vietnam. 14(21), 3367. https://doi.org/10.3390/w14213367

Nuong, B. T., Linh, B. K., Trang, V. Q., Huyen, P. T., Thi, B., Thao, P., Ngoc, N. T., & Duong, B. Du. (2022). Applying Fuzzy Analytical Hierarchy Process to Establish Environmental Sustainability Indicators for Water Resources Srepok River Basin, Vietnam. VNU Journal of Science: Earth and Environmental Sciences, 38(4), 63–74. https://doi.org/10.25073/2588-1094/vnuees.4877

Oeurng, C., Cochrane, T. A., Arias, M. E., Shrestha, B., & Piman, T. (2016). Assessment of changes in riverine nitrate in the Sesan, Srepok and Sekong tributaries of the Lower Mekong River Basin. Journal of Hydrology: Regional Studies, 8, 95–111. https://doi.org/10.1016/j.ejrh.2016.07.004

Oo, H. T., Zin, W. W., & Kyi, C. C. T. (2020). Analysis of streamflow response to changing climate conditions using SWAT model. Civil Engineering Journal, 6(2), 194–209.

Ozer, D. J. (1985). Correlation and the coefficient of determination. Psychological Bulletin, 97(2), 307.

Pandi, D., Kothandaraman, S., & Kuppusamy, M. (2021). Hydrological models: a review. International Journal of Hydrology Science and Technology, 12(3), 223–242.

Pool, S., Vis, M., & Seibert, J. (2018). Evaluating model performance: towards a non-parametric variant of the Kling-Gupta efficiency. Hydrological Sciences Journal, 63(13–14), 1941–1953.

Rawls, W. J., Brakensiek, D. L., & Miller, N. (1983). Green-Ampt infiltration parameters from soils data. Journal of Hydraulic Engineering, 109(1), 62–70.

Ries, K. G., Newson, J. K., Smith, M. J., Guthrie, J. D., Steeves, P. A., Haluska, T. L., Kolb, K. R., Thompson, R. F., Santoro, R. D., & Vraga, H. W. (2017). StreamStats. In Version 4: US Geological Survey Fact Sheet USGS Numbered Series (Vol. 2017).

Ritter, A., & Muñoz-Carpena, R. (2013). Performance evaluation of hydrological models: Statistical significance for reducing subjectivity in goodness-of-fit assessments. Journal of Hydrology, 480, 33–45. https://doi.org/10.1016/j.jhydrol.2012.12.004

Schuerz, C. (2022). Getting started with SWATplusR • SWATplusR.

Sehgal, V., Sridhar, V., Juran, L., & Ogejo, J. A. (2018). Integrating climate forecasts with the soil and water assessment tool (SWAT) for high-Resolution hydrologic simulations and forecasts in the Southeastern US. Sustainability, 10(9), 3079.

Sharifi, E., Eitzinger, J., & Dorigo, W. (2019). Performance of the state-of-the-art gridded precipitation products over mountainous terrain: A regional study over Austria. Remote Sensing, 11(17), 1–20. https://doi.org/10.3390/rs11172018

Smigaj, M., Hackney, C. R., Kieu, P., Dang, V. P., Ngoc, N. T., Du, D., Darby, S. E., & Leyland, J. (2023). Science of the Total Environment Monitoring riverine traffic from space: The untapped potential of remote sensing for measuring human footprint on inland waterways. Science of the Total Environment, 860(September 2022), 160363. https://doi.org/10.1016/j.scitotenv.2022.160363

Srinivasan, R., Zhang, X., & Arnold, J. (2010). SWAT ungauged: hydrological budget and crop yield predictions in the Upper Mississippi River Basin. Transactions of the ASABE, 53(5), 1533–1546.

Stein, M. (1987). Large sample properties of simulations using Latin hypercube sampling. Technometrics, 29(2), 143–151.

Sunmin, K. (2021). Real-time flood forecasting with weather radar and distributed hydrological model. In Water Engineering Modeling and Mathematic Tools (pp. 369–380). Elsevier.

SWAT+. (2020). I/O documentation for SWAT+. Retrieved from https://swatplus.gitbook.io/io-docs

Tan, M. L., & Yang, X. (2020). Effect of rainfall station density, distribution and missing values on SWAT outputs in tropical region. Journal of Hydrology, 584, 124660.

Tapas, M., Etheridge, J. R., Howard, G., Lakshmi, V. V., & Tran, T. N. D. (2022a). Development of a Socio-Hydrological Model for a Coastal Watershed: Using Stakeholders' Perceptions. AGU Fall Meeting Abstracts, 2022, H22O--0996.

Tapas, M., Etheridge, R., Miller Julie. Hinckley Brian, H. Z., & Samantha, F. (2022b). Hydrological Modeling to Forecast Changes in Eastern North Carolina: Implications for Agriculture, Climate Change, and Fisheries. North Carolina Water Resources Research Institute Annual Conference, 1(Lightning talk).

Tran, T. N. D., Nguyen, Q. B., & Zeeshan, A. (2021a). Application of Plaxis for Calculating the Construction Stability and Soft Embankment in Protecting Ha Thanh. 2nd Conference on Sustainability in Civil Engineering (CSCE) 2020, 202–210. https://csce.cust.edu.pk/archive/20-613.pdf

Tran, T. N. D., Zeeshan, A., & Vo, N. D. (2021b). APPLICATION OF HYDRODYNAMIC MODELLING TO ASSESS THE EFFICIENCY OF HURRICANE PROTECTION MEASURE AT XOM RO DIKE, PHU YEN PROVINCE, VIETNAM. 2nd Conference on Sustainability in Civil Engineering (CSCE) 2020, 406. https://csce.cust.edu.pk/archive/20-406.pdf

Tolson, B. A., & Shoemaker, C. A. (2007). Dynamically dimensioned search algorithm for computationally efficient watershed model calibration. Water Resources Research, 43(1).

Tran, T. N. D., Nguyen, B. Q., Le, M.-H., Lakshmi, V. (Venkat), Bolten, J. D., & Aryal, A. (2022a). Robustness of Gridded Precipitation Products in Hydrological Assessment for Vietnam River basins. AGU Fall Meeting Abstracts, 2022, H22M-07.

Tran, T. N. D., Nguyen, Q. B., Vo, N. D., Marshall, R., & Gourbesville, P. (2022b). Assessment of Terrain Scenario Impacts on Hydrological Simulation with SWAT Model. Application to Lai Giang Catchment, Vietnam. In Advances in Hydroinformatics (Issue 2022, pp. 1205–1222). https://doi.org/10.1007/978-981-19-1600-7_77

Tran, T. N. D., Nguyen, Q. B., Nguyen, T. T., Vo, N. D., Nguyen, C. P., & Gourbesville, P. (2022c). Operational Methodology for the Assessment of Typhoon Waves Characteristics. Application to Ninh Thuan Province, Vietnam. In Advances in Hydroinformatics (Issue 2022, pp. 887–902). https://doi.org/10.1007/978-981-19-1600-7_55

Tran, T. N. D, Nguyen, Q. B., Tam, D., Le, L., Nguyen, T. D., Vo, N. D., & Gourbesville, P. (2022d). Evaluate the Influence of Groynes System on the Hydraulic Regime in the Ha Thanh River, Binh Dinh Province, Vietnam. In Advances in Hydroinformatics (pp. 241–254). https://doi.org/https://doi.org/10.1007/978-981-19-1600-7_15

Tran, T.-N.-D., & Lakshmi, V. (2022e). The land use changes impacts on socio-economic drivers and simulation of surface and groundwater in the Eastern Shore of Virginia, the United States. AGU Fall Meeting Abstracts, 2022, H42D-1270.

Tran, T.-N.-D., Le, M.-H., Zhang, R., Nguyen, B. Q., Bolten, J. D., & Lakshmi, V. (2023a). Robustness of gridded precipitation products for vietnam basins using the comprehensive assessment framework of rainfall. Atmospheric Research, 293(15), 106923. https://doi.org/https://doi.org/10.1016/j.atmosres.2023.106923

Tran, T.-N.-D., Le, M.-H., Zhang, R., Nguyen, B. Q., Bolten, J. D., & Lakshmi, V. (2023b). Corrigendum to "Robustness of gridded precipitation products for Vietnam basins using the comprehensive assessment framework of rainfall." Atmospheric Research, 294, 106945. https://doi.org/10.1016/j.atmosres.2023.106945

Tran, T.-N.-D., Nguyen, Q. B., Zhang, R., Aryal, A., Łukaszewska, M.-G., Sinicyn, G., & Lakshmi, V. (2023c). Quantification of Gridded Precipitation Products for the Streamflow Simulation on the Mekong River Basin Using Rainfall Assessment Framework: A Case Study for the Srepok River Subbasin, Central Highland Vietnam. Remote Sensing, 15(4), 1–27. https://doi.org/10.3390/rs15041030

Tran, T. N. D., Nguyen, Q. B., Vo, N. D., Le, M. H., Nguyen, Q. D., Lakshmi, V., & Bolten, J. (2023d). Quantification of global Digital Elevation Model (DEM) – A case study of the newly released NASADEM for a river basin in Central Vietnam. Journal of Hydrology: Regional Studies, 45(October 2022), 101282. https://doi.org/10.1016/j.ejrh.2022.101282

Tran, T.-N.-D., Do, S. K., Nguyen, B. Q., Tran, V. N., Grodzka-Lukaszewska, M., Sinicyn, G., & Lakshmi, V. (2024). Investigating the Future Flood and Drought Shifts in the Transboundary Srepok River basin Using CMIP6 Projections. IEEE Journal of Selected Topics in Applied Earth Observations and Remote Sensing, 17, 7516–7529. https://doi.org/10.1109/JSTARS.2024.3380514

Tumsa, B. C., Kenea, G., & Tola, B. (2022). The Application of SWAT+ model to quantify the impacts of Sensitive LULC changes on water balance in Guder catchment, Oromia, Ethiopia. Heliyon, e12569.

Valley, L. C. F. R. (1988). Geology and tectonic history of the lower Cape Fear River valley, southeastern North Carolina.

Wagner, P. D., Bieger, K., Arnold, J. G., & Fohrer, N. (2022). Representation of hydrological processes in a rural lowland catchment in Northern Germany using SWAT and SWAT+. Hydrological Processes, 36(5), e14589.

Wang, G., Barber, M. E., Chen, S., & Wu, J. Q. (2014). SWAT modeling with uncertainty and cluster analyses of tillage impacts on hydrological processes. Stochastic Environmental Research and Risk Assessment, 28, 225–238.

Wang, Y., Jiang, R., Xie, J., Zhao, Y., Yan, D., & Yang, S. (2019). Soil and water assessment tool (SWAT) model: A systemic review. Journal of Coastal Research, 93(SI), 22–30.

Wealands, S. R., Grayson, R. B., & Walker, J. P. (2005). Quantitative comparison of spatial fields for hydrological model assessment—some promising approaches. Advances in Water Resources, 28(1), 15–32.

Wei, C., Dong, X., Ma, Y., Gou, J., Li, L., Bo, H., Yu, D., & Su, B. (2023). Applicability comparison of various precipitation products of long-term hydrological simulations and their impact on parameter sensitivity. Journal of Hydrology, 618, 129187.

Wellen, C., Kamran-Disfani, A.-R., & Arhonditsis, G. B. (2015). Evaluation of the current state of distributed watershed nutrient water quality modeling. Environmental Science & Technology, 49(6), 3278–3290.

White, M. J., Arnold, J. G., Bieger, K., Allen, P. M., Gao, J., Čerkasova, N., Gambone, M., Park, S., Bosch, D. D., & Yen, H. (2022). Development of a Field Scale SWAT+ Modeling Framework for the Contiguous US. JAWRA Journal of the American Water Resources Association.

Wu, T., Zhu, L.-J., Shen, S., Zhu, A.-X., Shi, M., & Qin, C.-Z. (2023). Identification of watershed priority management areas based on landscape positions: An implementation using SWAT+. Journal of Hydrology, 619, 129281.

WWEE. (2023). SWATplus-CUP.

Yen, H., Park, S., Arnold, J. G., Srinivasan, R., Chawanda, C. J., Wang, R., Feng, Q., Wu, J., Miao, C., & Bieger, K. (2019). IPEAT+: A built-in optimization and automatic calibration tool of SWAT+. Water, 11(8), 1681.

Yu, D., Xie, P., Dong, X., Hu, X., Liu, J., Li, Y., Peng, T., Ma, H., Wang, K., & Xu, S. (2018). Improvement of the SWAT model for event-based flood simulation on a sub-daily timescale. Hydrology and Earth System Sciences, 22(9), 5001–5019.

Yuan, F., Zhang, L., Soe, K. M. W., Ren, L., Zhao, C., Zhu, Y., ... & Liu, Y. (2019). Applications of TRMM-and GPM-era multiple-satellite precipitation products for flood simulations at sub-daily scales in a sparsely gauged watershed in Myanmar. Remote Sensing, 11(2), 140.

Yue, W., Yao, Y., Su, M., Rong, Q., & Xu, C. (2023). Identifying distributions of urban ecosystem health based on Latin-hypercube sampling and multi-criteria decision analysis framework. Ecological Indicators, 147, 109957.

Zhang, A., Li, T., Si, Y., Liu, R., Shi, H., Li, X., Li, J., & Wu, X. (2016). Double-layer parallelization for hydrological model calibration on HPC systems. Journal of Hydrology, 535, 737–747. https://doi.org/10.1016/j.jhydrol.2016.01.024

Zhao, F., Wu, Y., Qiu, L., Sun, Y., Sun, L., Li, Q., Niu, J., & Wang, G. (2018). Parameter uncertainty analysis of the SWAT model in a mountain-loess transitional watershed on the Chinese Loess Plateau. Water, 10(6), 690.

# Chapter 2: Simulating the Effects of Sea Level Rise on Nitrogen Export Using the SWAT+ Model: A Case Study of the Tar-Pamlico River Basin, NC, USA

Mahesh R Tapas[a*], Randall Etheridge[b], Thanh-Nhan-Duc Tran[c], Colin Finlay[d], Ariane Peralta[d], Natasha Bell[e], Yicheng Xu[a], Venkataraman Lakshmi[c]

[a] Integrated Coastal Program, East Carolina University, Greenville, NC 27858, USA

[b] Department of Engineering, Center for Sustainable Energy and Environmental Engineering, East Carolina University, Greenville, NC 27858, USA

[c] Department of Civil & Environment Engineering, University of Virginia, Charlottesville, VA 22904, USA

[d] Department of Biology, East Carolina University, NC 27858, USA

[e] Department of Biological Systems Engineering, Virginia Tech, Blacksburg, VA 24061, USA

*Corresponding author: tapasm21@students.ecu.edu (Mahesh R Tapas).

ORCID: 0000-0001-8833-5531

**Abstract:**

This study addresses the urgent need to understand the impacts of climate change on coastal ecosystems by using the SWAT+ model to assess how sea level rise (SLR) affects nitrate export in a coastal watershed. Our framework for incorporating SLR in the SWAT+ model includes: (1) reclassifying current land uses to water for areas with elevations below 0.3 meters based on projections for mid-century; (2) creating new SLR-influenced land use, SLR-influenced crop database, and hydrological response units for areas with elevations below 2.4 meters; and (3) adjusting SWAT+ parameters for the SLR-influenced areas to simulate the effects of saltwater intrusion on processes such as plant yield and denitrification rates.

We demonstrate this approach in the Tar-Pamlico River basin, a coastal watershed in eastern North Carolina. We calibrated the model for nitrate load at Washington, achieving a Nash-Sutcliffe Efficiency (NSE) of 0.61. Our findings show SLR significantly alters nitrate delivery to the estuary through enhanced nitrate mobility throughout the year. We observed an increase in mean annual nitrate loads from 155,000 kg N under baseline conditions to 157,000 kg N under SLR scenarios, a change confirmed by a statistically significant paired t-test ($p = 2.16\times10^{-10}$). This pioneering framework sets the stage for more sophisticated and accurate modeling of SLR impacts in diverse hydrological scenarios, offering a vital tool for hydrological modelers.

**Study region:**

Tar-Pamlico River basin, Eastern North Carolina, United States.

**Keywords:**

SWAT+; Water quality; Nitrate; Coastal Watershed; Sea Level Rise.

**Highlights:**

1. The study enhances the SWAT+ model to assess how sea level rise impacts nitrate dynamics in the Tar-Pamlico River basin, NC, USA.

2. The research alters SWAT+ hydrological parameters and inputs to model the primary and secondary impacts of sea level rise by integrating new SLR-influenced land use, HRUs, and crop databases.

3. Results show a significant increase in nitrate loads due to sea level rise, emphasizing the importance of integrating climate change into water quality planning.

**Graphical Abstract:**

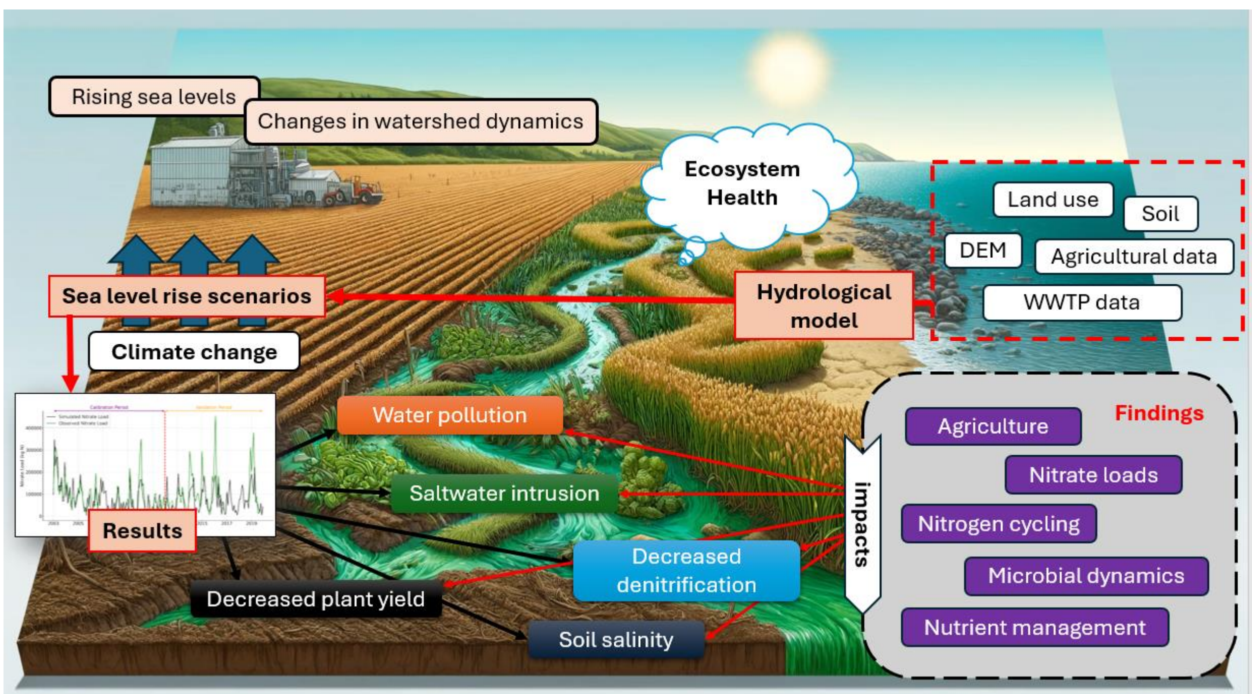

**1. Introduction**

Water quality is an important aspect of water resources management (Abbaspour et al., 2007). Since the 20th century, elevated nitrate levels in water bodies have posed significant threats to coastal watersheds (Pringle 2001; Vilmin et al., 2018). While the invention of nitrogen-based fertilizers was tremendously advantageous for mass food production, it poses a significant risk to our coastal ecosystems (Galloway et al., 2013; Fixen & West, 2002). To be specific, high nitrate levels in water can create an excessive growth of algae and certain aquatic plants. These algal blooms can hinder sunlight from reaching the bottom of rivers, streams, lakes, or estuaries; leading to the inhibition of benthic aquatic plant growth (Wurtsbaugh et al., 2019). Eventually, as these plants and algae die, they are broken down by microbes that consume oxygen (Jewell & McCarty, 1971; Cui et al., 2021), leading to the creation of low-oxygen zones where few organisms can survive (Gerloff & Krombholz, 1966; Seibel, 2011). Addressing elevated nitrate levels in coastal watersheds—a global issue—costs billions annually, particularly straining developing countries and threatening economic stability and aquatic ecosystem health (Sekhon, 1995; Bernhardt et al., 2005; Craswell 2021; Rasiah et al., 2005; Mathewson et al., 2020). This raises global concern and should be a major part of a country's plan for conserving or restoring healthy aquatic ecosystems. In this study, ecosystem health is defined as the ability of a coastal watershed to sustain biological productivity (Sherman 1994), maintain ecological processes (O'Brien et al., 2016), support biodiversity (Qian et al., 2023), and meet societal needs (Christensen et al., 1996). Nitrate loading to the estuary was used as an indicator of ecosystem health.

Nitrogen gas ($N_2$) makes up the majority of Earth's atmosphere, representing 78 percent of its total composition (Hart 1978). Although nitrogen is abundant in the atmosphere, it needs to be converted to ammonia/ammonium ($NH_3^+$/$NH_4^+$) through fixation before plants and animals can use it (Postgate 1998). Bacteria that fix nitrogen are essential as they transform atmospheric nitrogen gas into forms like ammonium ($NH_4^+$) or ammonia ($NH_3$) (Postgate 1998). Animals obtain nitrogen through eating plants (Temperton et al., 2007), integrating it into the broader food web (Meunier et al., 2016). When plants and animals die, the organic nitrogen they contain is broken down by microbes, turning it back into $NH_4^+$ (mineralization) and eventually nitrate ($NO_3^-$) via nitrification (Abatenh et al., 2018; Gupta et al., 2017). In addition, denitrifying microbes assist in converting nitrate back into nitrogen gas or nitrous oxide ($N_2O$) (Vilar-Sanz et al., 2013).

Climate change and anthropogenic activities greatly affect the nitrogen cycle (Aryal et al., 2022; Bennett et al., 2014; Vitousek et al., 1997), altering the rates of nitrogen fixation (Galloway, 1998), mineralization, and denitrification (Zhu et al., 2015). The alterations in the nitrogen cycle and nutrient availability impact coastal watersheds, especially where nitrogen is the primary limiting nutrient, leading to challenges for the health of aquatic ecosystems (Rabalais, 2002). The nitrogen cycle, carbon cycle, and climate are anticipated to be further altered due to human effects on the planet (Bernal et al., 2012). Sea levels are rising due to multiple influences of rising temperatures. (Karl et al., 2009; Cazenave & Cozannet, 2014). Coastal communities are more susceptible to the effects of climate change (Oliver-Smith, 2009). Specifically, SLR can cause flooding in low-lying areas, saltwater intrusion, and pose significant threats to aquatic ecosystems (Knighton et al., 1991). Sea level rise can alter nitrogen dynamics in watersheds by influencing both the release of ammonium from sediments and the microbial processes of nitrification and denitrification, impacting nitrogen uptake by plants and overall nutrient retention. Increased salinity due to SLR can enhance the bioavailability of ammonium, altering plant-microbe interactions and the nitrogen cycle (Ardón et al., 2013; Kirwan & Megonigal, 2013; Waldron et al., 1997). For farmers in coastal regions, saltwater intrusion is a pronounced concern due to its threat to crop growth. The boundary between saltwater and freshwater shifts as the inflow and outflow rates vary, with an increase in saltwater causing this interface to move further upstream (Michael et al., 2005). This progression leads to saltwater intrusion, resulting in elevated soil salinity, which disturbs the equilibrium of the agroecosystem, including crop growth and nitrogen cycle. This increased salinity, in turn, inhibits the activities of nitrogen-fixing bacteria and interferes with the conversion of organic nitrogen compounds into forms that plants can easily assimilate (Etesami & Adl, 2021; Kirova & Kocheva, 2021). Consequently, this disruption in the nitrogen cycle ultimately reduces nutrient availability for crops (specifically for soybean, which is a major crop type in the Tar-Pamlico basin), thereby affecting their overall health and yield. Additionally, high soil salinity can reduce growth or kill crops despite abundant nitrogen availability (Van et al., 1999), leading to an accumulation of unused nitrogen in soils where fertilizers are applied. SLR compromises the fertility of the soil in coastal agricultural watersheds by disrupting nutrient dynamics (Weissman & Tully, 2020). The effects of SLR are not limited to agriculture, as a higher SLR rate could lead to the drowning of wetlands, reducing their nitrogen removal potential (Kirwan & Megonigal, 2013). It also would increase the flood frequency, in which urban areas tend to have higher runoff, resulting from the increase of anthropogenic nutrients (Macías-Tapia et al., 2021).

Hydrological models are frequently used to assess the potential impacts of climate change and other anthropogenic influences on nitrogen transport and retention in watersheds (Hattermann et al., 2006). The Soil and Water Assessment Tool (SWAT) is one of the most widely used models for this purpose. Developed in the early 1990s, it is a semi-distributed hydrological model extensively used for water quality (Abbaspour et al., 2007) and quantity analyses (Zhang et al., 2011). SWAT has proven effective in modeling nitrate loads in diverse watersheds, with applications in places such as the Vamanapuram River Basin, India (Saravanan et al., 2023), Brittany, France (Conan et al., 2023), the Lower Seyhan Plain, Turkey (Donmez et al., 2020), and the Des Moines River, United States (Schilling and Wolter 2009). In recent years, the release of SWAT+, an enhanced version of SWAT, has gathered attention for its advancements in understanding interactions within watersheds and sub-watersheds, as well as its improved data management, analysis, and visualization capabilities (SWAT+, 2020). However, there is a gap in examining the integration of SLR with the SWAT+ model, possibly due to the model's limited ability to manage the bidirectional flow (Bieger et al., 2017).

In this study, our primary objective is to develop a method for simulating the effects of SLR on nitrogen processing within coastal watersheds using the SWAT+ model. We achieved this by identifying key parameters and input changes in the model, which enabled simulation of changes in nitrate transport and retention based on current literature. Additionally, we investigated how SLR influences nitrate loads in the downstream boundaries of a watershed. The Tar-Pamlico River Basin, located in eastern North Carolina, is used as a case study, given its historical challenges with both SLR and elevated nitrate levels over recent decades (Helmers et al., 2022; Ury et al., 2021). Through this work, we aim to improve the traditional coastal hydrological modeling framework by partially integrating the complex interactions and changes that arise from shifting nitrogen cycle due to SLR.

### 1.1 Objectives

The objectives of this study are to: 1) Develop and optimize a nitrate model for the Tar-Pamlico watershed using the SWAT+ hydrological model. 2) Conduct a literature search on the effects of salinity on watershed processes, with a focus on agricultural land use. 3) Develop a novel approach to incorporating SLR-influenced land use, plant database, and HRUs in SWAT+. 4) Investigate the effects of SLR on ecosystem health, specifically focusing on changes in nitrate load to the Pamlico Estuary under baseline and SLR scenarios.

## 2. Materials and methods

### 2.1 Study area

This study focuses on the Tar-Pamlico River basin, a coastal watershed in North Carolina, USA (Figure 2.1). As the fourth-largest watershed in the state, the Tar-Pamlico River basin stands out as one of just four entirely contained within North Carolina, alongside the Cape Fear, Neuse, and White Oak River basins (NCDEQ, 2023). With its waters ultimately flowing into the Pamlico Sound, this watershed has a rich diversity of ecosystems and varied habitats (North Carolina Department of Environmental Quality (NCDEQ, 2023). The Tar-Pamlico covers an expansive 6,400 square miles and spans 15 counties. It is home to a population exceeding 470,000 residents. The Tar-Pamlico watershed is divided into five major sub-watersheds, including the Upper Tar River, Fishing Creek, Lower Tar River, Pamlico River, and Pamlico Sound. The land use within this watershed is divided among agriculture (27.9%), forests (33.9%), wetlands (31.9%), pastureland (3.5%), rangeland (1.3%), and urban areas (1.4%) (Claggett et al., 2015). The freshwater streams and rivers within the basin originate in the Piedmont region in north-central North Carolina. These waterways flow southeastward and, upon nearing tidal zones, transform into the expansive (Figure 2.1), tidally influenced estuary (Keith, 2014), enhancing its ecological complexity and economic productivity (NC DEQ, 2009, 1994).

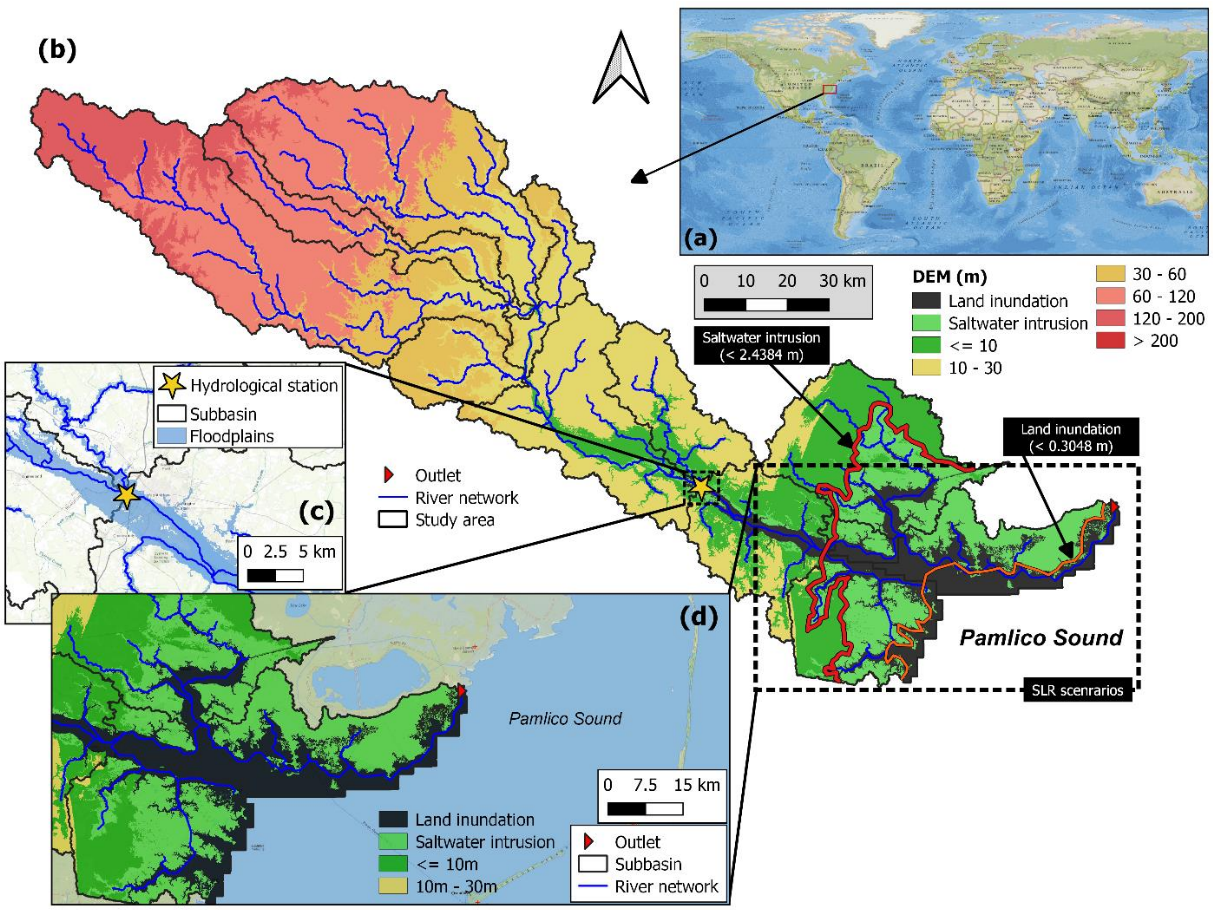


**Figure 2.1** (a) Location of the Tar-Pamlico River basin within the United States, (b) Digital elevation model and geographical characteristics of the Tar-Pamlico watershed, (c) Hydrological monitoring station in Washington used for model calibration, (d) Tar-Pamlico's coastal region where we incorporated the effects of SLR

## 2.2. SWAT+ model setup

In this study, we implemented the SWAT+ model (SWAT+ IO Document, 2020) to simulate hydrological processes throughout the river basin. This tool excels at assessing dynamics within both watersheds and sub-watersheds. SWAT+ enables the evaluation of how various hydrological parameters influence watershed dynamics, affecting water quality, agricultural yields, and nitrogen cycle processes (SWAT+ IO Document, 2020). It allows for detailed simulation of environmental interactions, aiding the creation of policies and strategies especially aimed at mitigating issues related to water quality, water availability, and flood risks (SWAT+ IO Document, 2020).

For setting up the SWAT+ model, a variety of data sources were used to accurately depict watershed characteristics. We obtained watershed boundary data from the United States Geological Survey (USGS) StreamStats service and incorporated elevation, land use, and soil type data from the USGS for 2011, the National Land Cover Database (NLCD) for 2008, and the Soil Survey Geographic Database (SSURGO) for 2015, all at a 90m resolution. These inputs were processed using QSWAT+ to delineate drainage networks, sub-basins, and Hydrological Response Units (HRUs), crucial for modeling the intricate hydrological behaviors within the watershed. We used weather data from the Global Precipitation Measurement Integrated Multi-satellite Retrievals. Additionally, we assimilated agricultural data, including crop types and fertilizer application rates, from reports by the North Carolina Department of Environmental Quality (NCDEQ) and the North Carolina Department of Agriculture & Consumer Services (NCDEQ, 2014; NCGAR, 2022), specifically pertaining to the Tar-Pamlico watershed. This information proved essential for more accurate simulations of agricultural runoff and nutrient transport.

We also integrated wastewater treatment data for the 22 discharges (Appendix 1) within the Tar-Pamlico watershed from the National Pollutant Discharge Elimination System (NPDES) and atmospheric deposition data from the National Atmospheric Deposition Program (NADP, 2023). Observed flow data were collected from USGS monitoring stations in Greenville and Washington. Due to incomplete data at the Washington station post-September 2006, we extrapolated the flow data from Greenville using a linear regression model. This model showed a strong correlation ($R^2 = 0.90$), indicating that approximately 90% of the discharge variability at Washington could be reliably predicted from Greenville's data. We used this relationship to compensate for missing flow data at Washington. Nitrate concentration data was obtained from NCDEQ (site 21NC01WQ).

To calculate monthly nitrate load, we first calculated the average daily discharge at Washington for each month. Then, we calculated the average nitrate concentration for each month from the available nitrate concentration data. We multiplied the average discharge for a specific month by the average nitrate concentration for the same month and then multiplied it by the total number of days in that month (Preston et al., 1989). In 2003, there were 357 daily observations, indicating a high-frequency data collection effort at this location (site 21NC01WQ) in Washington, NC. However, this frequency declined sharply over the years. By 2005, the frequency of data collection had decreased, with only 144 daily observations. This trend continued, and by 2010, only 40 daily observations were recorded. Eventually, the data collection frequency shifted to a monthly scale, with only about 10 to 13 observations per year from 2011 onwards. This reduction in data collection frequency over time introduces additional challenges in accurately estimating nitrate loads and concentrations, as fewer data points are available to capture the variability and trends (Birgand et al., 2011).

### 2.3. SWAT+ model optimization

We calibrated the model for nitrate load with observed data from Washington, NC (Figure 2.1). We utilized the SWATrunR package (Schuerz 2019) to calibrate the model. Our calibration efforts targeted 23 parameters identified as crucial for accurately representing hydrological and nitrogen processes, based on sensitivity analysis and literature reviews outlined in Appendix 1. For parameter adjustment, we employed three methods: absolute change ($x' = x + y$), percent change ($x' = y * x / 100$), and absolute value ($x' = y$), where x is the default value, x' the new value, and y the calibrated parameter value (SWAT+ IO Document, 2020). The choice of method was influenced by each parameter's resolution and initial range; for instance, basin-level parameters predominantly used absolute value adjustments. The decision between absolute and percentage changes depended on the magnitude of the parameter's range—absolute changes were preferred for narrow ranges, while percentage changes were favored for wider ranges. This approach allowed for a broad range of parameter adjustments during model calibration, ensuring flexibility across varying resolutions and initial ranges. The detailed optimization table, which includes the parameter name, type of change, parameter description, and its default and calibrated values, is mentioned in Appendix 1. We also soft-calibrated the model for yield and denitrification rate for selected HRUs representing corn, cotton, soybean, and general agricultural crops (Etheridge et al., 2014). In this study, the general agricultural crop type was used for all other crops (e.g. tobacco, sweet potatoes, etc.), and in SWAT+, we simulated that using agricultural_land_row (agrr) crop type. The finalized values of parameter calibration and change type are discussed in Appendix 1.

### 2.4. SLR incorporation:

We aimed to design a framework to simulate the partial effects of SLR in the SWAT+ model with a focus on the nitrogen cycle. We achieved this by systematically adjusting inputs and parameters to reflect the dynamic impacts of SLR. While acknowledging that our base model, SWAT+, primarily functions as a unidirectional rainfall-runoff model and does not typically account for backflow (SWAT+ IO Document, 2020), we focus on altering expected land uses, enhancing the model's capability to simulate critical land processes, such as altered denitrification rates and the reduction of crop yields under SLR conditions.

We utilized mid-century SLR projections from the National Oceanic and Atmospheric Administration (NOAA, 2022), which forecasts an increase of approximately 0.3 m by 2050.

Based on NOAA's projections, we reclassified all landcover with elevations less than 0.3 m to water landcover. To account for the effects of saltwater intrusion, we consider any areas with elevation less than 2.4 m to fall within the risk zone of saltwater intrusion (NOAA, 2022). For areas with elevations under 2.4 m, we used GIS to process the land use changes by developing a new category labeled as saltwater-intruded land use for the respective land uses.

After incorporating these new land use types, we added the saltwater-influenced crops to the SWAT+ plant database (Appendix 1). Subsequently, using the updated land cover map and the revised SWAT+ database, we generated new Hydrological Response Units (HRUs) for areas extending up to 2.4 m above the current mean sea level. For the baseline simulation, we retained the same parameters for the saltwater-intruded crops as their corresponding conventional crops. We confirmed that SWAT+ produced consistent outputs for these new saltwater-intruded crops as for their parent crops when no parameters were altered. The creation of these new saltwater-intruded HRUs allowed us to modify SWAT+ parameters to simulate the impacts of SLR on the nitrogen cycle.

We changed multiple SWAT+ parameters in our initial efforts to simulate the effects of SLR. We conducted a literature review to identify processes and their corresponding SWAT+ parameters potentially affected by saltwater intrusion, such as soil pH (Al-Busaidi & Cookson, 2003) and electrical conductivity (Rhoades & Corwin, 1990). Based on our findings, we adjusted electrical conductivity (ec.sol) and pH (ph.sol) parameters in the model to account for SLR. However, despite significant alterations to these parameters, we observed no impact on the simulated denitrification rate and crop yields. This suggests that these parameters are not directly linked to the outputs we expected them to alter and additional factors within the SWAT+ model would need to be considered to reflect the effects of SLR.

To address this challenge, we opted for an indirect approach to incorporating SLR effects. We introduced new soil nutrient layers in our model to better simulate denitrification rates and plant yield (SWAT+ IO Document, 2020) under SLR. The parameters that were altered were the coefficient for adjusting concentrations based on depth (exp_co) and the fraction of active soil humus (fr_hum_act). In preliminary analysis we found increasing the exp_co parameter decreased denitrification and decreasing fr_hum_act decreased denitrification. Increasing the exp_co parameter likely reduces denitrification by limiting the depth at which there are high concentrations of nitrate, while decreasing fr_hum_act reduces denitrification by lowering the proportion of active humus that supports microbial activity essential for the denitrification process. We developed two new soil nutrient layers: one for saltwater-intruded agricultural crops and another for the rest of the saltwater-intruded land use. The soil nutrient layers were applied at the HRU resolution for the respective land use (SWAT+ IO Document, 2020). The expected decrease in denitrification was simulated along with an excessive decrease in yield, thus we adopted a multiparameter approach to further fine-tune denitrification and plant yield by altering other HRU-specific parameters such as curve number (cn2), plant uptake compensation factor (epco), soil evaporation compensation factor (esco), available water capacity (awc), plant ET curve number coefficient (latq_co), and potential maximum leaf area index (lai_pot). We used SWATrunR (Schuerz et al., 2022) to alter these parameters specifically for saltwater affected HRUs (up to an elevation of 2.4 m) to adjust plant yield and denitrification rate per literature under SLR scenarios, which is further discussed in section 3.2. The values of these parameters under freshwater conditions and saltwater-influenced conditions are discussed in section 3.2. This innovative framework is intended to serve as a pioneering step for hydrological modelers, setting the stage for more sophisticated and accurate modeling of SLR impacts.

## 3. Results and Discussion

### 3.1 Model optimization

In this study, we simulated monthly nitrate load at the Washington, NC station from 2001 to 2019 with 2 years of warm up period. We calibrated the model from 2003 to 2011 and validated it from 2012 to 2019 (Figure 2.2). During the calibration period, the model showed a good level of accuracy within the coastal Tar-Pamlico watershed, achieving Nash-Sutcliffe Efficiency (NSE) of 0.61, Coefficient of Determination ($R^2$) of 0.61, and Kling-Gupta Efficiency (KGE) of 0.77. These metrics suggest a strong agreement between observed and simulated data, indicating that the model is well-calibrated and capable of simulating the dynamics governing nitrate transport and retention. We found lower performance indices values for the validation period; the model's performance metrics declined to a NSE of 0.33, a $R^2$ of 0.33, and a KGE of 0.39, indicating moderate accuracy. This decline likely resulted from uncertainties associated with the change in nitrate concentration sampling frequency post-2010 (Birgand et al., 2011). Despite the lower metrics, the model still demonstrated its capacity to provide reasonable nitrate load predictions under varying conditions (Upadhyay et al., 2022).

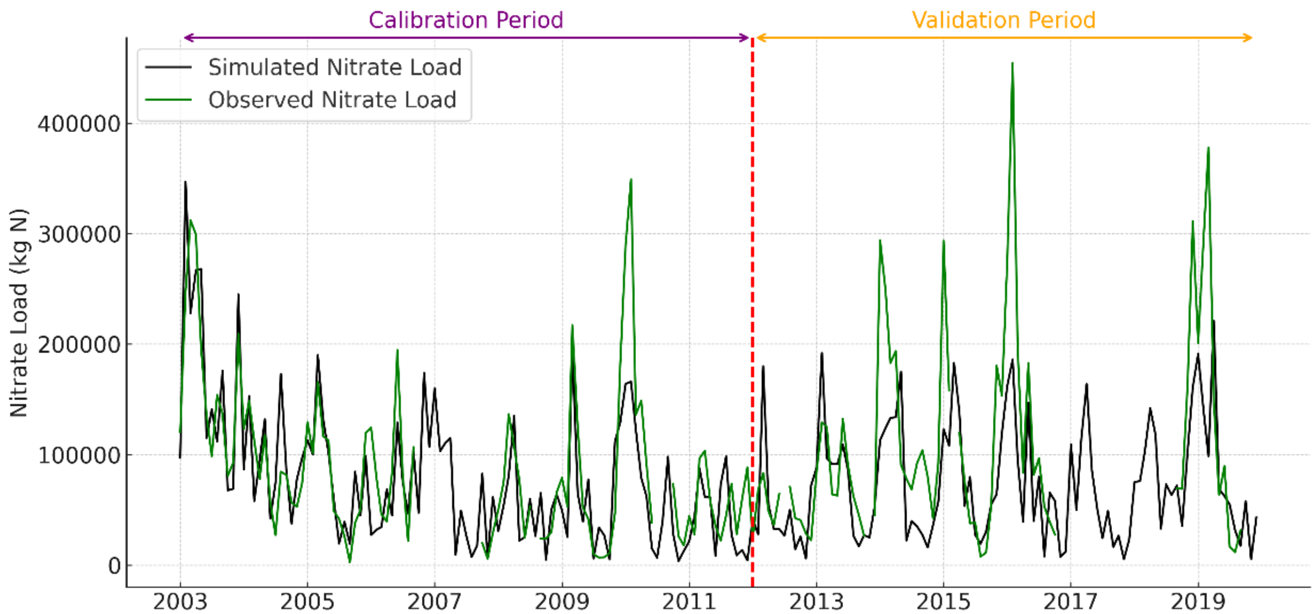


Figure 2.2: Monthly nitrate load optimization results

3.2. Modeling the effects of SLR on nitrogen processes

As mentioned in Section 2.5, simulating the ramifications of SLR on watershed processes, with a particular focus on the adjustment of plant yield and denitrification were not as straightforward as expected. Saltwater intrusion disrupts normal plant physiological processes, impeding nutrient uptake and causing osmotic stress in plants, which is reflected in the reduced yields observed (Okon, 2019; Safdar et al., 2019). Sea level rise can decrease denitrification rates by increasing waterlogged conditions, reducing oxygen availability, and inhibiting microbial activity (Hamonts et al., 2013; Mazhar et al., 2022). SLR reduces potential leaf area (by around 30%) by flooding coastal areas, increasing soil salinity and altering vegetation, leading to sparse foliage (Bond-Lamberty et al., 2023), which we adjusted using the potential maximum leaf area index (lai_pot) parameter in SWAT+. We used previous literature to inform changes made to model parameters (Table 2.1). Even though SWAT+ may not be capable of simulating backflow, the hydrological parameter changes discussed in this section should enable the model to more accurately simulate processes in response to SLR when viewed at the monthly or annual scale. It is highly unlikely to be accurate at the daily time scale. This SLR-calibrated SWAT+ model offers valuable insights into the intricate interplay between SLR and watershed processes governing nitrate export.

Table 2.1: Parameters altered simulate plant yield and denitrification changes under SLR

| **Parameter** | **Potential Parameter Range (Unit)** | **Resolution** | **Type of Change** | **Description** | **Default value** | **Freshwater landuse calibration** | **SLR calibration range** | **SLR-incorporated landuse** |
|---|---|---|---|---|---|---|---|---|
| awc | 0.01, 1.0 (mm H2O $mm^{-1}$) | sol | Absolute Change | The difference in soil water content between field capacity and permanent wilting point | 0.14 | 0.081 | -0.3, 0.08 | -0.021 |
| esco | 0.0, 1.0 (-) | hru | Absolute Change | Soil evaporation compensation factor which allows modification of depth distribution to meet soil evaporative demand, considering capillary action, crusting, and cracks. | 0.95 | -0.069 | -0.3, 0.3 | 0.038 |
| epco | 0.0, 1.0 (-) | hru | Absolute Change | Plant uptake compensation factor which allows adjustment of water uptake depth distribution in | 0.5 | -0.114 | -0.3, 0.3 | -0.042 |

| | | | | | | | | |
|---|---|---|---|---|---|---|---|---|
| | | | | response to plant transpiration demand and soil water availability. | | | | |
| latq_co | 0.0, 1.0 (-) | hru | Absolute Change | Coefficient for the Plant ET curve number | 0.01 | 0.101 | -0.3, 0.3 | 0.279 |
| cn2 | 35.0, 95.0 (-) | hru | Percent Change | Curve number for Condition II runoff potential. | | 12.283 | 13, 20 | 17.834 |
| Lai_pot | 0.5, 10 | Plt | Absolute | Potential maximum leaf area index | | | | |
| | ($m^2$ $m^{-2}$) | | Value | Corn | 6 | 5 | | 3.5 |
| | | | | Cotton | 4 | 2.5 | | 1.75 |
| | | | | Soybean | 5 | 2.027 | | 1.419 |
| | | | | General agricultural crop | 3 | 3 | | 2.1 |

3.2.1. Simulated effects on crop yields:

In this study, we simulated the impacts of SLR on the yields of four distinct crop types—general agricultural, corn, cotton, and soybean—quantified in kilograms per hectare (kg/ha). Figure 2.3 represents an average of a particular crop's average annual yield for SLR-influenced HRUs. Following the adjustments made to the parameters in Table 2.1, our model simulated a reduction in yields for all crops in the ranges found in the literature (Gibson et al., 2021). In our results, general agriculture yields decreased the most by 36%, from 4,700 to 3,000 kg/ha, followed by cotton at 36%, from 2,900 to 1,900 kg/ha, soybean at 33%, from 2,700 to 1,800 kg/ha, and corn at 23%, from 8,900 to 6,800 kg/ha. As expected due to calibration, these findings are consistent with previous literature on the impacts of salinization on crop yields (Gibson et al., 2021).

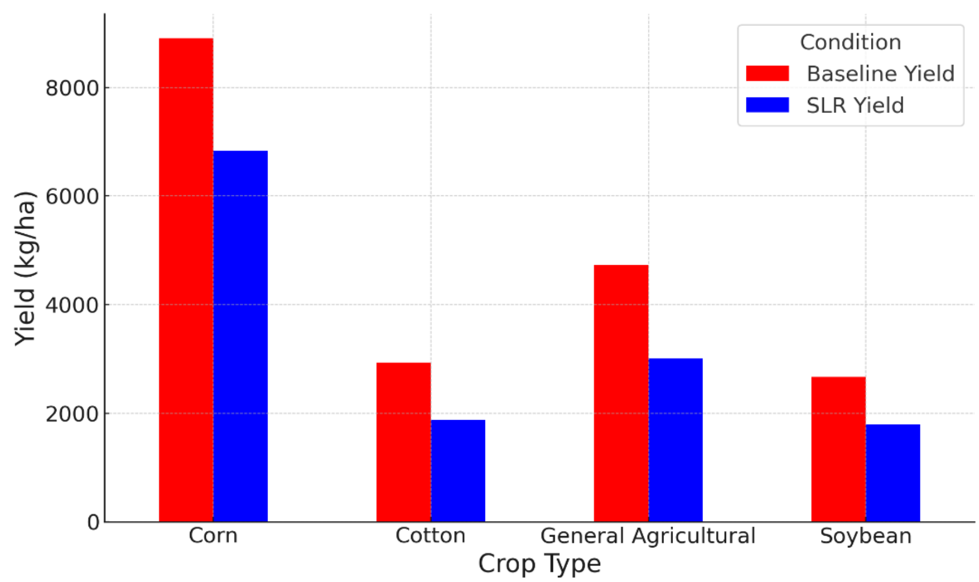


Figure 2.3: Simulated effects of SLR on annual average crop yields

3.2.2. Simulated effects on denitrification rate

Changes made to the SLR-influenced land uses were also aimed at simulating the effects of increased salinity and soil water levels associated with SLR on denitrification. The results of these changes show a significant decline in denitrification across all crop types (Figure 2.4), with reductions ranging from 59% in corn to 72% in soybeans, matching with previous literature (Hofstra & Bouwman, 2005; Qian et al., 1997). The decrease in soil nitrate processing capabilities under SLR conditions, attributed to increased soil salinity inhibiting microbial activity essential for nitrogen cycling, could further complicate microbial community structures and potentially reduce denitrification efficiency (Mazhar et al., 2022; Spivak et al., 2019).

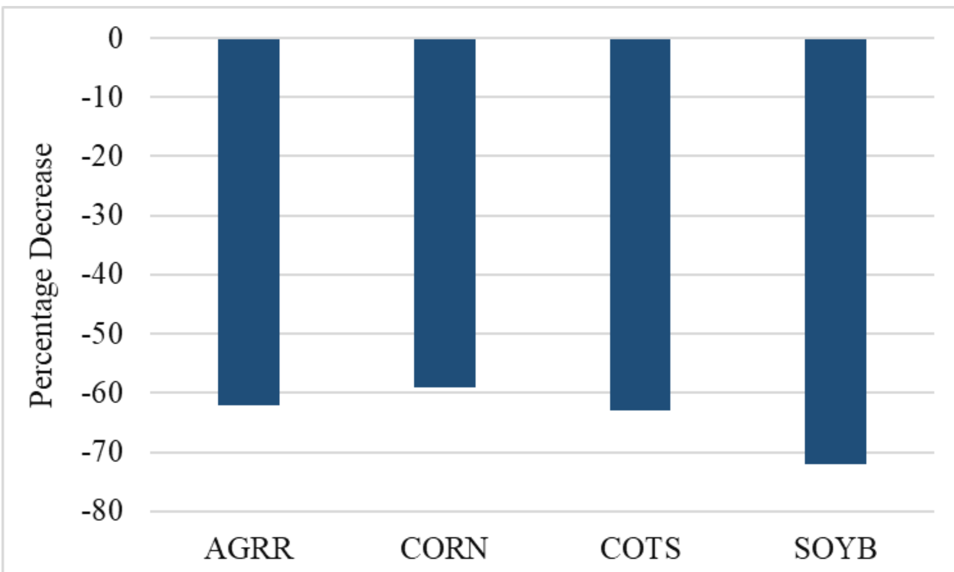


Figure 2.4: Impacts of SLR on annual average denitrification [AGRR: General agricultural crop; COTS: Cotton; SOYB: Soybean]

3.3. Nitrate load to the estuary

We conducted a comprehensive comparison of the monthly nitrate load at the Pamlico Estuary, contrasting conditions under both baseline and SLR scenarios. We compared the model results for both SLR and baseline scenarios from January 2003 to December 2019 (Figure 2.5). This analysis aimed to quantify the variations in nitrate loads across different months, providing a clearer understanding of how rising sea levels could affect nutrient export in this coastal environment. Both datasets exhibit significant variability and peaks over time, but the SLR scenario generally shows a trend of increased nitrate loads compared to the baseline, especially noticeable in the later years depicted (Figure 2.5).

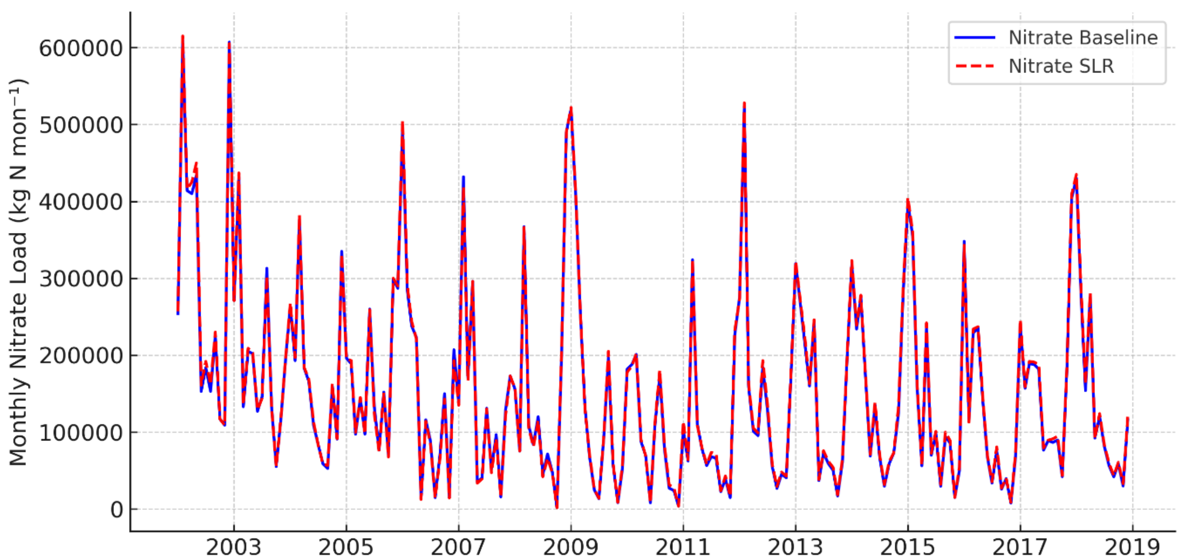


**Figure 2.5** Simulated Nitrate Load For SLR and Baseline Scenarios

The results reveal notable variations in the seasonal nitrate loads when comparing the baseline with the SLR scenarios (Table 2.2). Winter and spring exhibited higher nitrate loads compared to summer and fall. This pattern is likely influenced by increased precipitation during the colder months (Sayemuzzaman & Jha, 2014), which enhances runoff (Moraglia et al., 2022) and nitrate leaching (Oh & Sankarasubramanian, 2012), whereas the growing vegetation in warmer months can assimilate more nutrients (Tian et al., 2014), thereby reducing nitrate levels. The data also showed that nitrate loads consistently increase across all seasons under SLR conditions, with the most substantial increases during winter and spring (Table 2.2). This observation suggests that SLR modifies nitrate availability and transport, particularly during peak precipitation periods (Stuart et al., 2011). The elevation of the sea level can alter the water table (Hay et al., 1990) and increase the inundation of low-lying coastal areas (Mohd et al.,2018), resulting in greater surface runoff (Wang et al., 2011) and potentially higher flows during heavy rains (Rotzoll & Fletcher, 2013). These changes facilitate the more rapid movement of nitrate from terrestrial sources into estuarine and marine environments, underscoring the impact of SLR on nitrate loss (Munksgaard et al., 2019; Voss et al., 2015; Wang et al., 2017).

**Table 2.2** Average seasonal nitrate load from Tar-Pamlico River Basin

| **Season** | **Nitrate Load Baseline (kg $NO_3$-N)** | **Nitrate Load SLR (kg $NO_3$-N)** | **Percentage Change (%)** |
|---|---|---|---|
| Winter | 266,000 | 267,900 | 0.73% |
| Spring | 183,500 | 186,000 | 1.37% |
| Summer | 93,000 | 94,500 | 1.60% |
| Fall | 78,400 | 79,800 | 1.80% |

The percentage change in nitrate loads from the Tar-Pamlico basin into the Pamlico estuary indicates a higher relative increase in nitrate loads during the fall (1.80%) and summer (1.60%)

compared to spring (1.37%) and winter (0.73%), under SLR scenarios (Table 2.2). This heightened increase in nitrate loads during summer and fall under SLR scenarios can be attributed to several interrelated factors (Herbert et al., 2015). Saltwater intrusion due to SLR increases soil salinity (Bayabil et al., 2021), disrupting nitrogen cycling (Nelson & Zavaleta, 2012), and diminishing the nitrate uptake by crops in these growing seasons (He et al., 2018), while simultaneously altering hydrological dynamics that increase nitrate mobility (Donner & Kucharik, 2003). The disruption of microbial denitrification processes by increased salinity may result in more residual nitrates that leach into waterways (Arce et al., 2013). Additionally, seasonal agricultural practices, potentially misaligned with changing environmental conditions, may further contribute to nitrate runoff (Conrad & Marinos, 2024).

Statistical comparison of the nitrate load from the Tar-Pamlico basin under baseline and SLR conditions was conducted using a paired t-test (Table 2.3). The test compared two sets of model output: the mean annual nitrate loads under the baseline condition (mean = 155,200 kg N) and under the SLR condition (mean = 157,100 kg N), with each set comprising 204 observations (Table 2.3). The Pearson Correlation coefficient of 0.9995 indicates a very high degree of linear correlation between the paired samples, which is expected since the measurements under both scenarios pertain to the same time points (Cohen et al., 2009).

**Table 2.3** Statistical summary of paired t-test analysis for monthly nitrate loads under baseline and SLR conditions

| **Statistical Measure** | **Value** |
|---|---|
| Mean Nitrate Load (Baseline) | 155,200 kg $NO_3$-N |
| Mean Nitrate Load (SLR) | 157,100 kg $NO_3$-N |
| Pearson Correlation Coefficient | 0.9995 |
| Degrees of Freedom (df) | 203 |
| t-Statistic | -6.6869 |
| p-Value (Two-tailed) | $2.16\times10^{-10}$ |

The paired t-test, yielded a t-statistic of -6.6869, reflecting a significant difference between the means. The negative t-statistic suggests that the nitrate load under SLR conditions is higher than under baseline conditions. The two-tailed p-value of approximately $2.16\times10^{-10}$ indicates that this difference is highly statistically significant, far below the conventional alpha level of 0.05. The outcome of this t-test provides strong evidence to reject the null hypothesis, which suggested no mean difference between the nitrate loads under the two conditions. Therefore, we can infer with high confidence that SLR has a statistically significant effect on simulated nitrate loads in the Pamlico Estuary. Overall, the interaction between abiotic factors like precipitation and SLR and biotic factors such as microbial activity underscores the complex nature of nitrate dynamics in coastal watersheds (Bouwman et al., 2013). Understanding these interactions is crucial for developing effective management strategies to mitigate the impacts of nutrient loading and protect aquatic ecosystems in the context of ongoing climate change (Hamilton et al., 2016).

## 4. Conclusion

This study presents a novel methodology to simulate the impacts of SLR on nitrate cycling and its effect on ecosystem health, specifically on nitrate export in the Tar-Pamlico River basin, using the SWAT+ model. We attempted to innovatively integrate adjustments for the effects of SLR on hydrological parameters and inputs, significantly enhancing the model's ability to project changes in nitrate loads due to these environmental changes.

To simulate the effects of SLR in the SWAT+ model, we adjusted parameters related to land use, crop databases, and HRUs to incorporate both primary impacts like land inundation and secondary impacts such as saltwater intrusion. Specifically, land uses at elevations below 0.3 meters were reclassified to water, and SWAT+ parameters were adjusted for areas below 2.4 meters to model the effects of increased soil salinity on crop yield and denitrification rates. The findings reveal that SLR significantly influences nitrate loads, with an observed increase in nitrate transport to the Pamlico Estuary, particularly during wetter seasons. The introduction of SLR into the SWAT+ model facilitated a detailed analysis of how altered hydrological dynamics and increased salinity affect agricultural productivity and ecosystem health.

This study acknowledges the limitations of SWAT+, particularly its inability to simulate backflow, and recognizes that our approach to modeling land processes under SLR conditions may not be definitive. However, this research represents a crucial first step toward integrating SLR impacts into the SWAT+ framework, providing a foundation for further refinement and development by hydrological modelers.

**Appendix 1:** https://github.com/EtheridgeLab/Tar_Pam_SWAT/blob/main/Appendix1.docx

**References**

Abatenh, E., Gizaw, B., Tsegaye, Z., & Tefera, G. (2018). Microbial function on climate change-a review. Environment Pollution and Climate Change, 2(1), 1-6.

Abbaspour, K. C., Yang, J., Maximov, I., Siber, R., Bogner, K., Mieleitner, J., ... & Srinivasan, R. (2007). Modelling hydrology and water quality in the pre-alpine/alpine Thur watershed using SWAT. Journal of hydrology, 333(2-4), 413-430.

Al-Busaidi, A. S., & Cookson, P. (2003). Salinity–pH relationships in calcareous soils. Journal of Agricultural and Marine Sciences [JAMS], 8(1), 41-46.

Araújo, W. L., Nunes-Nesi, A., & Fernie, A. R. (2014). On the role of plant mitochondrial metabolism and its impact on photosynthesis in both optimal and sub-optimal growth conditions. Photosynthesis research, 119, 141-156.

Arce, M. I., Gómez, R., Suárez, M. L., & Vidal-Abarca, M. R. (2013). Denitrification rates and controlling factors in two agriculturally influenced temporary Mediterranean saline streams. Hydrobiologia, 700, 169-185.

Ardón, M., Morse, J. L., Colman, B. P., & Bernhardt, E. S. (2013). Drought-induced saltwater incursion leads to increased wetland nitrogen export. Global change biology, 19(10), 2976-2985.

Aryal, B., Gurung, R., Camargo, A. F., Fongaro, G., Treichel, H., Mainali, B., ... & Puadel, S. R. (2022). Nitrous oxide emission in altered nitrogen cycle and implications for climate change. Environmental Pollution, 120272.

Bayabil, H. K., Li, Y., Tong, Z., & Gao, B. (2021). Potential management practices of saltwater intrusion impacts on soil health and water quality: a review. Journal of Water and Climate Change, 12(5), 1327-1343.

Bennett, E., Carpenter, S., Gordon, L., Ramankutty, N., Balvanera, P., Campbell, B., ... & Spierenburg, M. (2014). Toward a more resilient agriculture. Solutions, 5(5), 65-75.

Bernal, S., Hedin, L. O., Likens, G. E., Gerber, S., & Buso, D. C. (2012). Complex response of the forest nitrogen cycle to climate change. Proceedings of the National Academy of Sciences, 109(9), 3406-3411.

Bernhardt, E. S., Palmer, M. A., Allan, J. D., Alexander, G., Barnas, K., Brooks, S., ... & Sudduth, E. (2005). Synthesizing US river restoration efforts. Science, 308(5722), 636-637.

Bhardwaj, A. K., Nagaraja, M. S., Srivastava, S., Singh, A. K., & Arora, S. (2016). A framework for adaptation to climate change effects in salt affected agricultural areas of Indo-Gangetic region. Journal of Soil and Water Conservation, 15(1), 22-30.

Bieger, K., Arnold, J. G., Rathjens, H., White, M. J., Bosch, D. D., Allen, P. M., ... & Srinivasan, R. (2017). Introduction to SWAT+, a completely restructured version of the soil and water assessment tool. JAWRA Journal of the American Water Resources Association, 53(1), 115-130.

Birgand, F., Appelboom, T. W., Chescheir, G. M., & Skaggs, R. W. (2011). Estimating nitrogen, phosphorus, and carbon fluxes in forested and mixed-use watersheds of the lower coastal plain of North Carolina: Uncertainties associated with infrequent sampling. Transactions of the ASABE, 54(6), 2099-2110.

Bond-Lamberty, B., Haddock, L. M., Pennington, S. C., Sezen, U. U., Shue, J., & Megonigal, J. P. (2023). Salinity exposure affects lower-canopy specific leaf area of upland trees in a coastal deciduous forest. Forest Ecology and Management, 548, 121404.

Bouwman, A. F., Bierkens, M. F. P., Griffioen, J., Hefting, M. M., Middelburg, J. J., Middelkoop, H., & Slomp, C. P. (2013). Nutrient dynamics, transfer and retention along the aquatic continuum from land to ocean: towards integration of ecological and biogeochemical models. Biogeosciences, 10(1), 1-22.

Cazenave, A., & Cozannet, G. L. (2014). Sea level rise and its coastal impacts. Earth's Future, 2(2), 15-34.

Christensen, N. L., Bartuska, A. M., Brown, J. H., Carpenter, S., d'Antonio, C., Francis, R., ... & Woodmansee, R. G. (1996). The report of the Ecological Society of America committee on the scientific basis for ecosystem management. Ecological applications, 6(3), 665-691.

Church, J. A., Godfrey, J. S., Jackett, D. R., & McDougall, T. J. (1991). A model of sea level rise caused by ocean thermal expansion. Journal of Climate, 4(4), 438-456.

Cohen, I., Huang, Y., Chen, J., Benesty, J., Benesty, J., Chen, J., ... & Cohen, I. (2009). Pearson correlation coefficient. Noise reduction in speech processing, 1-4.

Conan, C., Bouraoui, F., Turpin, N., de Marsily, G., & Bidoglio, G. (2003). Modeling flow and nitrate fate at catchment scale in Brittany (France). Journal of Environmental Quality, 32(6), 2026-2032.

Conrad, P. E., & Marinos, R. E. (2024). Nitrogen availability and denitrification in urban agriculture and regreened vacant lots. Urban Ecosystems, 1-12.

Craswell, E. (2021). Fertilizers and nitrate pollution of surface and ground water: an increasingly pervasive global problem. SN Applied Sciences, 3(4), 518.

Cui, J., Jin, Z., Wang, Y., Gao, S., Fu, Z., Yang, Y., & Wang, Y. (2021). Mechanism of eutrophication process during algal decomposition at the water/sediment interface. Journal of Cleaner Production, 309, 127175.

Cui, Z., Huang, J., Gao, J., & Han, J. (2022). Characterizing the impacts of macrophyte-dominated ponds on nitrogen sources and sinks by coupling multiscale models. Science of The Total Environment, 811, 152208.

Donmez, C., Sari, O., Berberoglu, S., Cilek, A., Satir, O., & Volk, M. (2020). Improving the applicability of the SWAT model to simulate flow and nitrate dynamics in a flat data-scarce agricultural region in the Mediterranean. Water, 12(12), 3479.

Donner, S. D., & Kucharik, C. J. (2003). Evaluating the impacts of land management and climate variability on crop production and nitrate export across the Upper Mississippi Basin. Global Biogeochemical Cycles, 17(3).

Etesami, H., & Adl, S. M. (2020). Can interaction between silicon and non–rhizobial bacteria help in improving nodulation and nitrogen fixation in salinity–stressed legumes? A review. Rhizosphere, 15, 100229.

Etheridge, Randall J., Lepistö, A., Granlund, K., Rankinen, K., Birgand, F., & Burchell, M. R. (2014). Reducing uncertainty in the calibration and validation of the INCA-N model by using soft data. Hydrology Research, 45(1), 73-88.

Fixen, P. E., & West, F. B. (2002). Nitrogen fertilizers: meeting contemporary challenges. Ambio: a journal of the human environment, 31(2), 169-176.

Galloway, J. N. (1998). The global nitrogen cycle: changes and consequences. Environmental pollution, 102(1), 15-24.

Galloway, J. N., Leach, A. M., Bleeker, A., & Erisman, J. W. (2013). A chronology of human understanding of the nitrogen cycle. Philosophical Transactions of the Royal Society B: Biological Sciences, 368(1621), 20130120.

Gerloff, G. C., & Krombholz, P. H. (1966). Tissue analysis as a measure of nutrient availability for the growth of angiosperm aquatic plants 1. Limnology and Oceanography, 11(4), 529-537.

Gibson, N., McNulty, S., Miller, C., Gavazzi, M., Worley, E., Keesee, D., & Hollinger, D. (2021). Identification, mitigation, and adaptation to salinization on working lands in the US Southeast. Forest Service, US Department of Agriculture, Southern Research Station.

Gupta, A., Gupta, R., & Singh, R. L. (2017). Microbes and environment. Principles and applications of environmental biotechnology for a sustainable future, 43-84.

Hamilton, D. P., Salmaso, N., & Paerl, H. W. (2016). Mitigating harmful cyanobacterial blooms: strategies for control of nitrogen and phosphorus loads. Aquatic Ecology, 50, 351-366.

Hamonts, K., Clough, T. J., Stewart, A., Clinton, P. W., Richardson, A. E., Wakelin, S. A., ... & Condron, L. M. (2013). Effect of nitrogen and waterlogging on denitrifier gene abundance, community structure and activity in the rhizosphere of wheat. FEMS Microbiology Ecology, 83(3), 568-584.

Hart, M. H. (1978). The evolution of the atmosphere of the Earth. Icarus, 33(1), 23-39.

Hattermann, F. F., Krysanova, V., Habeck, A., & Bronstert, A. (2006). Integrating wetlands and riparian zones in river basin modelling. Ecological modelling, 199(4), 379-392.

Hay, W. W., & Leslie, M. A. (1990). Could possible changes in global groundwater reservoir cause eustatic sea-level fluctuations. Sea-level change, 161-170.

He, W., Yang, J. Y., Qian, B., Drury, C. F., Hoogenboom, G., He, P., ... & Zhou, W. (2018). Climate change impacts on crop yield, soil water balance and nitrate leaching in the semiarid and humid regions of Canada. PloS one, 13(11), e0207370.

Helmers, M. J., Abendroth, L., Reinhart, B., Chighladze, G., Pease, L., Bowling, L., ... & Strock, J. (2022). Impact of controlled drainage on subsurface drain flow and nitrate load: A synthesis of studies across the US Midwest and Southeast. Agricultural Water Management, 259, 107265.

Herbert, E. R., Boon, P., Burgin, A. J., Neubauer, S. C., Franklin, R. B., Ardón, M., ... & Gell, P. (2015). A global perspective on wetland salinization: ecological consequences of a growing threat to freshwater wetlands. Ecosphere, 6(10), 1-43.

Hofstra, N., & Bouwman, A. F. (2005). Denitrification in agricultural soils: summarizing published data and estimating global annual rates. Nutrient Cycling in Agroecosystems, 72, 267-278.

Jewell, W. J., & McCarty, P. L. (1971). Aerobic decomposition of algae. Environmental Science & Technology, 5(10), 1023-1031.

Karl, T. R., Melillo, J. M., & Peterson, T. C. (2009). Global climate change impacts in the United States: a state of knowledge report from the US Global Change Research Program. Cambridge University Press.

Kirova, E., & Kocheva, K. (2021). Physiological effects of salinity on nitrogen fixation in legumes–a review. Journal of Plant Nutrition, 44(17), 2653-2662.

Kirwan, M. L., & Megonigal, J. P. (2013). Tidal wetland stability in the face of human impacts and sea-level rise. Nature, 504(7478), 53-60.

Knighton, A. D., Mills, K., & Woodroffe, C. D. (1991). Tidal-creek extension and saltwater intrusion in northern Australia. Geology, 19(8), 831-834.

Kuenzler, E. J., Stanley, D. W., & Koenings, J. R. (1979). Nutrient kinetics of phytoplankton in the Pamlico River, North Carolina. Water Resources Research Institute of the University of North Carolina.

Mathewson, P. D., Evans, S., Byrnes, T., Joos, A., & Naidenko, O. V. (2020). Health and economic impact of nitrate pollution in drinking water: a Wisconsin case study. Environmental Monitoring and Assessment, 192(11), 724.

Mazhar, S., Pellegrini, E., Contin, M., Bravo, C., & De Nobili, M. (2022). Impacts of salinization caused by sea level rise on the biological processes of coastal soils-A review. Frontiers in Environmental Science, 10, 909415.

Mazhar, S., Pellegrini, E., Contin, M., Bravo, C., & De Nobili, M. (2022). Impacts of salinization caused by sea level rise on the biological processes of coastal soils-A review. Frontiers in Environmental Science, 10, 909415.

Mazhar, S., Pellegrini, E., Contin, M., Bravo, C., & De Nobili, M. (2022). Impacts of salinization caused by sea level rise on the biological processes of coastal soils-A review. Frontiers in Environmental Science, 10, 909415.

Melino, V., & Tester, M. (2023). Salt-tolerant crops: time to deliver. Annual Review of Plant Biology, 74, 671-696.

Meunier, C. L., Gundale, M. J., Sánchez, I. S., & Liess, A. (2016). Impact of nitrogen deposition on forest and lake food webs in nitrogen-limited environments. Global Change Biology, 22(1), 164-179.

Mohd, F. A., Maulud, K. A., Karim, O. A., Begum, R. A., Awang, N. A., Hamid, M. A., ... & Abd Razak, A. H. (2018, June). Assessment of coastal inundation of low lying areas due to sea level rise. In IOP Conference Series: Earth and Environmental Science (Vol. 169, No. 1, p. 012046). IOP Publishing.

Moraglia, G., Brattich, E., & Carbone, G. (2022). Precipitation trends in North and South Carolina, USA. Journal of Hydrology: Regional Studies, 44, 101201.

Munksgaard, N. C., Hutley, L. B., Metcalfe, K. N., Padovan, A. C., Palmer, C., & Gibb, K. S. (2019). Environmental challenges in a near-pristine mangrove estuary facing rapid urban and industrial development: Darwin Harbour, Northern Australia. Regional studies in marine science, 25, 100438.

NADP National Atmospheric Deposition Program. (2023). Retrieved December, 2023, from https://nadp.slh.wisc.edu/

National Oceanic and Atmospheric Administration (NOAA). (2022). Sea level rise technical report. Retrieved from https://oceanservice.noaa.gov/hazards/sealevelrise/sealevelrise-tech-report.html#step1

NCAGR North Carolina Department of Agriculture and Consumer Services. (2022). Tar-Pamlico Watershed Initiatives. North Carolina Department of Agriculture and Consumer Services. https://www.ncagr.gov/divisions/soil-water-conservation/programs-initiatives/watershed-initiatives/tar-pamlico#Contact-4304

NCDEQ North Carolina Department of Environmental Quality. (2014). Tar-Pamlico Basin Plan. North Carolina Department of Environmental Quality. https://www.deq.nc.gov/about/divisions/water-resources/water-planning/basin-planning/river-basin-plans/tar-pamlico#2014Tar-PamlicoBasinPlan-4040

Nelson, J. L., & Zavaleta, E. S. (2012). Salt marsh as a coastal filter for the oceans: changes in function with experimental increases in nitrogen loading and sea-level rise.

Oh, J., & Sankarasubramanian, A. (2012). Interannual hydroclimatic variability and its influence on winter nutrient loadings over the Southeast United States. Hydrology and Earth System Sciences, 16(7), 2285-2298.

Okon, O. G. (2019). Effect of salinity on physiological processes in plants. Microorganisms in saline environments: strategies and functions, 237-262.

Oliver-Smith, A. (2009). Sea level rise and the vulnerability of coastal peoples: responding to the local challenges of global climate change in the 21st century. UNU-EHS.

O'Brien, A., Townsend, K., Hale, R., Sharley, D., & Pettigrove, V. (2016). How is ecosystem health defined and measured? A critical review of freshwater and estuarine studies. Ecological Indicators, 69, 722-729.

Postgate, J. (1998). Nitrogen fixation. Cambridge University Press.

Preston, S. D., V. J. Bierman Jr., and S. E. Silliman. 1989. An evaluation of methods for the estimation of tributary mass loads.Water Resour. Res. 25(6): 1379-1389.

Pringle, C. M. (2001). Hydrologic connectivity and the management of biological reserves: a global perspective. Ecological Applications, 11(4), 981-998.

Qian, J. H., Doran, J. W., Weier, K. L., Mosier, A. R., Peterson, T. A., & Power, J. F. (1997). Soil denitrification and nitrous oxide losses under corn irrigated with high-nitrate groundwater (Vol. 26, No. 2, pp. 348-360). American Society of Agronomy, Crop Science Society of America, and Soil Science Society of America.

Qian, L., Wang, F., Cao, W., Ding, S., & Cao, W. (2023). Ecological health assessment and sustainability prediction in coastal area: A case study in Xiamen Bay, China. Ecological Indicators, 148, 110047.

Rabalais, N. N. (2002). Nitrogen in aquatic ecosystems. AMBIO: a Journal of the Human Environment, 31(2), 102-112.

Rasiah, V., Armour, J. D., & Cogle, A. L. (2005). Assessment of variables controlling nitrate dynamics in groundwater: Is it a threat to surface aquatic ecosystems?. Marine pollution bulletin, 51(1-4), 60-69.

Rhoades, J. D., & Corwin, D. L. (1990). Soil electrical conductivity: effects of soil properties and application to soil salinity appraisal. Communications in soil science and plant analysis, 21(11-12), 837-860.

Rotzoll, K., & Fletcher, C. H. (2013). Assessment of groundwater inundation as a consequence of sea-level rise. Nature Climate Change, 3(5), 477-481.

Safdar, H., Amin, A., Shafiq, Y., Ali, A., Yasin, R., Shoukat, A., ... & Sarwar, M. I. (2019). A review: Impact of salinity on plant growth. Nat. Sci, 17(1), 34-40.

Saravanan, S., Singh, L., Sathiyamurthi, S., Sivakumar, V., Velusamy, S., & Shanmugamoorthy, M. (2023). Predicting phosphorus and nitrate loads by using SWAT model in Vamanapuram River Basin, Kerala, India. Environmental Monitoring and Assessment, 195(1), 186.

Sayemuzzaman, M., & Jha, M. K. (2014). Seasonal and annual precipitation time series trend analysis in North Carolina, United States. Atmospheric Research, 137, 183-194.

Schilling, K. E., & Wolter, C. F. (2009). Modeling nitrate-nitrogen load reduction strategies for the Des Moines River, Iowa using SWAT. Environmental management, 44(4), 671-682.

Schuerz, C., Hsieh, N.-H., & Willem. (2022). chrisschuerz/SWATplusR: SWATplusR 0.6 (Version 0.6) . Zenodo. https://doi.org/10.5281/zenodo.6517027

Seibel, B. A. (2011). Critical oxygen levels and metabolic suppression in oceanic oxygen minimum zones. Journal of Experimental Biology, 214(2), 326-336.

Sekhon, G. S. (1995). Fertilizer-N use efficiency and nitrate pollution of groundwater in developing countries. Journal of Contaminant Hydrology, 20(3-4), 167-184.

Sherman, K. (1994). Sustainability, biomass yields, and health of coastal ecosystems: an ecological perspective. Marine ecology progress series. Oldendorf, 112(3), 277-301.

Spivak, A. C., Sanderman, J., Bowen, J. L., Canuel, E. A., & Hopkinson, C. S. (2019). Global-change controls on soil-carbon accumulation and loss in coastal vegetated ecosystems. Nature Geoscience, 12(9), 685-692.

Stuart, M. E., Gooddy, D. C., Bloomfield, J. P., & Williams, A. T. (2011). A review of the impact of climate change on future nitrate concentrations in groundwater of the UK. Science of the Total Environment, 409(15), 2859-2873.

SWAT+ IO Document. (2020). Input/output file documentation, version 2016 modified on November 16, 2020 according to REV 60.5. Retrieved from https://swatplus.gitbook.io/io-docs

Temperton, V. M., Mwangi, P. N., Scherer-Lorenzen, M., Schmid, B., & Buchmann, N. (2007). Positive interactions between nitrogen-fixing legumes and four different neighbouring species in a biodiversity experiment. Oecologia, 151, 190-205.

Tian, L., Zhang, Y., & Zhu, J. (2014). Decreased surface albedo driven by denser vegetation on the Tibetan Plateau. Environmental Research Letters, 9(10), 104001.

Upadhyay, P., Linhoss, A., Kelble, C., Ashby, S., Murphy, N., & Parajuli, P. B. (2022). Applications of the SWAT model for coastal watersheds: review and recommendations. Journal of the ASABE, 65(2), 453-469.

Ury, E. A., Yang, X., Wright, J. P., & Bernhardt, E. S. (2021). Rapid deforestation of a coastal landscape driven by sea-level rise and extreme events. Ecological applications, 31(5), e02339.

Van Wijnen, H. J., & Bakker, J. P. (1999). Nitrogen and phosphorus limitation in a coastal barrier salt marsh: the implications for vegetation succession. Journal of Ecology, 87(2), 265-272.

Vilar-Sanz, A., Puig, S., Garcia-Lledo, A., Trias, R., Balaguer, M. D., Colprim, J., & Baneras, L. (2013). Denitrifying bacterial communities affect current production and nitrous oxide accumulation in a microbial fuel cell. PLoS One, 8(5), e63460.

Vilmin, L., Mogollón, J. M., Beusen, A. H., & Bouwman, A. F. (2018). Forms and subannual variability of nitrogen and phosphorus loading to global river networks over the 20th century. Global and Planetary Change, 163, 67-85.

Vitousek, P. M., Aber, J. D., Howarth, R. W., Likens, G. E., Matson, P. A., Schindler, D. W., ... & Tilman, D. G. (1997). Human alteration of the global nitrogen cycle: sources and consequences. Ecological applications, 7(3), 737-750.

Voss, B. M., Peucker-Ehrenbrink, B., Eglinton, T. I., Spencer, R. G., Bulygina, E., Galy, V., ... & Luymes, R. (2015). Seasonal hydrology drives rapid shifts in the flux and composition of dissolved and particulate organic carbon and major and trace ions in the Fraser River, Canada. Biogeosciences, 12(19), 5597-5618.

Wang, H., Steyer, G. D., Couvillion, B. R., Beck, H. J., Rybczyk, J. M., Rivera-Monroy, V. H., ... & Visser, J. M. (2017). Predicting landscape effects of Mississippi River diversions on soil organic carbon sequestration. Ecosphere, 8(11), e01984.

Wang, J., Yin, H., & Chung, F. (2011). Isolated and integrated effects of sea level rise, seasonal runoff shifts, and annual runoff volume on California's largest water supply. Journal of Hydrology, 405(1-2), 83-92.

Wurtsbaugh, W. A., Paerl, H. W., & Dodds, W. K. (2019). Nutrients, eutrophication and harmful algal blooms along the freshwater to marine continuum. Wiley Interdisciplinary Reviews: Water, 6(5), e1373.

Zhang, Y., Xia, J., Chen, J., & Zhang, M. (2011). Water quantity and quality optimization modeling of dams operation based on SWAT in Wenyu River Catchment, China. Environmental Monitoring and Assessment, 173, 409-430.

Zhu, X., Zhang, W., Chen, H., & Mo, J. (2015). Impacts of nitrogen deposition on soil nitrogen cycle in forest ecosystems: A review. Acta Ecologica Sinica, 35(3), 35-43.

**Chapter 3a: Framework for Stakeholder-Driven Socio-Hydrological Modeling: Conceptual Foundations for Policy Development and Evaluation to Improve Ecosystem Health**

Mahesh R Tapas[a*], Randall Etheridge[b], Gregory Howard[c], Matthew Mair[d]

[a] Integrated Coastal Program, East Carolina University, Greenville, NC 27858, USA

[b] Department of Engineering, Center for Sustainable Energy and Environmental Engineering, East Carolina University, Greenville, NC 27858, USA

[c] Department of Economics, East Carolina University, Greenville, NC 27858, USA

[d] Department of Economics, Appalachian State University, Boone, NC 28608

**Abstract**

In this paper, we propose a concise framework that integrates stakeholder insights, specifically from farmers, into hydrological modeling (Soil and Water Assessment Tool Plus, SWAT+), to enhance the efficacy of potential watershed management policies. By incorporating farmers' behavioral responses to policy changes within the SWAT+ model, we bridge the gap between econometric and hydrological modeling. This interdisciplinary approach captures the dynamic interactions between stakeholders and ecosystem health, offering a novel perspective on environmental management. Our methodology includes surveys to gauge farmers' reactions to policy changes and quantify the adoption of agricultural best management practices, forecasting the impact of policy changes on land management and subsequent impacts on ecosystem health. This integration facilitates a more realistic representation of socio-environmental systems, underscoring the importance of aligning policy interventions with the practical realities faced by those directly affecting and interacting with the ecosystems. Through this framework, we propose a pathway towards more effective and sustainable environmental policies, emphasizing the critical

role of incorporating stakeholder perspectives into model development and decision-making processes.

**Keywords**

Socio-hydrological modeling, Stakeholder engagement, Behavioral econometrics, Policy development, Ecosystem health

## 1 Introduction

### 1.1 Context and challenge

The evolving landscape of environmental challenges underscores a pressing need to incorporate social dynamics into hydrological modeling (Archfield et al., 2015). Traditional models, primarily focused on physical and biological processes (Vereecken et al., 2016), often oversimplify or overlook the complex interplay between human activities and natural systems (Blair & Buytaert, 2016). This oversight is particularly consequential in coastal ecosystems, where the confluence of land and water creates unique environmental settings (Garcia 2003; Kelly et al., 2018). These areas are not only hotspots for biodiversity but also for human settlement (Kong et al., 2021) and economic activities (Marchese 2015), making them especially vulnerable to the impacts of land use changes (Li et al., 2007), pollution (Blanchard & Lerch, 2000), and climate change (Schulze, 1997).

Hydrological modelers attempt to simulate the complex relationship between water systems and land management (McGrane, 2016), where human activities like agriculture (Curk & Glavan, 2021) and urban development (Salvadore et al., 2015) impact water quality (Keller et al., 2023) and ecosystem health, and vice versa (Qiu et al., 2021). Integrating social dynamics into hydrological models without losing scientific accuracy or efficiency poses a significant challenge, as factors like human decision-making, cultural norms, and socioeconomic conditions could introduce variability and unpredictability in model simulations (Xu et al., 2018). Ecosystems, affected by human actions and natural factors (Zhao et al., 2023), should use a new approach to modeling that combines social sciences (Forrester et al., 2014), economics (Bockstael et al., 1995), and traditional hydrology (Walters, 1997) for models that accurately reflect socio-environmental interactions (Lawyer et al., 2023; Tanim et al., 2022).

Incorporating social dynamics into hydrological models improves their relevance for policymaking (Blair & Buytaert, 2016) providing insights into the impact of interventions on both ecosystems (Elsawah et al., 2017) and communities (Givens et al., 2018). This holistic approach helps anticipate the outcomes of management actions (Mostert, 2018), leading to better environmental stewardship (Sivapalan et al., 2012) and sustainable management of coastal land and ecosystems (Kumar et al., 2020). Thus, integrating social factors into modeling is crucial for sustainable land management (De Jonge, 2012).

### 1.2 Objective

This work introduces a conceptual framework for integrating socio-economic aspects into hydrological modeling, aiming to improve model accuracy and policy relevance. By combining social and hydrological sciences, the framework enhances sustainable land management by considering human impact on downstream systems, increasing the likelihood that adopted strategies are environmentally and socio-economically sustainable.

### 1.3 Significance

Integrating socio-hydrological elements into hydrological models can enhance both theoretical understanding and practical application, leading to more accurate and policy-relevant outcomes

(Mostert, 2018; Troy et al., 2015). Such an approach recognizes the interconnectedness of water systems with human actions, improving model realism by accounting for human variability (Schlueter et al., 2012). Practically, successful integration could make water management policies more effective by addressing the root causes of issues (Jønch-Clausen, 2004), predicting human responses (Srinivasan et al., 2017), and supporting sustainable practices (Sivapalan et al., 2014). This approach has the potential to promote scientifically robust (Vogel et al., 2015), socially equitable (Mirza & Mustafa, 2016), and economically viable strategies (Sivapalan, 2015), improving stakeholder engagement and policy success (Xu et al., 2018).

## 2 Theoretical Background of Socio-Hydrological Integration

### 2.1 Socio-hydrology

Socio-hydrology studies the interaction between human societies and water systems, examining how human activities affect hydrology and how water changes influence human life (Sivapalan et al., 2012). It views water as essential for ecosystems, agriculture, and economies, while examining human impacts on the hydrological cycle (Abbott et al., 2019). As global anthropogenic challenges like population growth and climate change intensify water issues, socio-hydrology's holistic approach combines social and hydrological sciences to foster sustainable water management, guiding the creation of policies that meet both human and environmental needs (Levy et al., 2016; Pande & Sivapalan, 2017).

Integrating socio-economic perspectives with hydrology is key to solving complex water issues beyond just technical means, addressing water conflicts, ecosystem degradation, and community resilience to floods and droughts (Everard, 2019; Pande et al., 2020). Socio-hydrology identifies change drivers and promotes adaptive, inclusive water management (Xu et al., 2018). This emphasizes the need for interdisciplinary research and collaborative policymaking to address challenges at the intersection of water and society (Krueger et al., 2016).

### 2.2 Challenges of integration

Combining social science with hydrological modeling faces challenges due to different approaches and scales (Xu et al., 2018). Modeling complex human behavior and integrating it with hydrological process models is difficult because of the inherent unpredictability and non-linearity of social systems. (Blair & Buytaert, 2016). Developing new tools that accommodate both (quantitative and qualitative) social data and quantitative hydrological data is challenging, given the varying temporal and spatial scales of social and hydrological processes (Fischer et al., 2021).

The integration of social variables into hydrological models is hindered by the scarcity, inconsistency, or absence of social data, posing significant challenges for accurate modeling (Brunner et al., 2021; Muñoz-Carpena et al., 2023). Furthermore, effective interdisciplinary collaboration is difficult due to differences in terminology and concepts between fields (Moirano et al., 2020). Validating socio-hydrological models also presents difficulties, as traditional hydrological validation methods do not suit models with social dynamics, necessitating new approaches to ensure model reliability (Iwanaga et al., 2020). Overcoming these challenges demands innovative and interdisciplinary efforts.

## 3 Econometric Modeling in Socio-Hydrological Contexts

### 3.1 Basics

Econometric modeling, the use of statistical methods to analyze economic data (broadly defined), is a key component of the socio-hydrological framework, allowing researchers to understand how economic policies affect water-related human behaviors (Alamanos & Zeng, 2021; Bertassello et al., 2021). Economic data is defined as data on individuals' resource allocation decisions, and as such involves a wide array of financial and non-financial human decision-making. Econometric modeling quantifies the impact of policies on resource use and management, aiding in forecasting policy outcomes (McColl & Aggett, 2007; Daneshi et al., 2021). By examining the effects of economic incentives on water conservation practices and land use changes, econometric modeling helps create realistic models that blend human decision-making into hydrological simulations (Castro & Lechthaler, 2022; Ovando & Brouwer, 2019). This integrated approach is vital for devising effective land management strategies that account for both environmental processes and socio-economic factors.

### 3.2 Advantages

Incorporating econometric insights into hydrological models enhances their utility by improving human behavior predictions, enabling data-driven policy impact assessments, and fostering an interdisciplinary approach to land management (Dinar, 2024; Jarvis et al., 2013). This integration allows for targeted policy design by explaining the socio-economic drivers of land use and evaluating various policy effects on both human behavior and hydrological systems (Conrad, 2016; Ovando & Brouwer, 2019). Such integration bridges the gap between social science and hydrology, leading to a comprehensive understanding of the interaction between ecological processes and socio-economic factors, and thus promoting holistic solutions to water challenges (Anderson et al., 2019; Di Baldassarre et al., 2019). In human-dominated watersheds, a resource management policy's impact on the environment is heavily mediated through the ways in which the policy alters human action. By adding a layer of social realism, econometric modeling turns hydrological models into more dynamic and relevant tools for addressing water management issues (Jarvis et al., 2013; Liu et al., 2019).

## 4 Framework for Integrating Engineering and Economic Models

### 4.1 Methodological overview

Payment for ecosystem services (PES) programs are a recent policy approach designed to incentivize the adoption of agricultural best management practices (BMPs). PES programs offer financial compensation to landowners for the voluntary implementation of BMPs and other ecosystem services (Ma et al., 2012). There have been several PES programs implemented by the USDA designed to reduce agricultural nutrient pollution, such as the Conservation Reserve Enhancement Program (CREP), Conservation Stewardship Program (CSP), and Environmental Quality Incentives Program (EQIP) (Howard et al., 2023).

Survey data is often employed to study how stakeholders (in this example, farmers) would respond to a diverse set of PES alternatives. Discrete choice experiments can be included in surveys for this purpose. Discrete choice experiments require respondents to choose between two or more hypothetical alternatives. Each alternative differs along a variety of attributes. For example, a farmer may be asked to choose between two hypothetical conservation contracts, which present different requirements for the adoption of BMPs and varying levels of compensation, and a third option of rejecting both contracts. This methodology can be applied to a wide range of contexts including other hypothetical policy scenarios.

By thoughtfully and methodically varying the alternatives presented in a discrete choice experiment, the choice data can be used to tease out how each element of a choice (in discrete choice modeling parlance, each attribute) impacts a decision maker's willingness to choose a given alternative. This process, typically done with a logistic regression model, has been replicated several times in the socio-hydrological context of land-owner preferences for adopting BMPs (Beharry-Borg et al., 2013; Howard et al., 2023; Kaczan et al., 2013; Raes et al., 2017).

By far, the most common application of econometric modeling in the socio-hydrological context is through the random utility maximization (RUM) model (Manski, 1977). The RUM framework posits that the utility a decision maker receives from an alternative is a function of a set of observable (to the researcher) characteristics and an unobserved random component. This framework can account for heterogeneity in preferences for observable factors, such as demographics and attitudes, and is particularly useful when the survey sample is diverse. The random utility model utilizes discrete choice experiment data and maximum likelihood (or maximum simulated likelihood) estimation to generate marginal utility estimates for each element of the observable characteristics of a choice. While utility is an abstract concept of well-being or satisfaction, these estimates are valuable for calculating probabilities that an alternative will be selected as well as willingness-to-accept (WTA) values. In the context of PES contracts, the willingness to accept value for a given alternative represents the minimum compensation necessary to induce the decision maker to agree to the PES contract.

Assuming the sample that is used to parameterize one's econometric model is representative of the target population, it is a relatively straightforward exercise to project the number of people who would adopt or reject a hypothetical policy. In the context of environmental subsidies or PES contracts, the people who adopt the policy are those whose estimated WTA values are below the payment offered by a policy. This method is demonstrated by Howard et al., (2023), who examine participation in agricultural conservation programs in Iowa.

The theoretical integration of engineering models (Figure 3a.1), such as SWAT+ (Soil and Water Assessment Tool Plus), with econometric models presents a methodological advancement in socio-hydrological modeling. This integration is designed to capture the complexity of interactions between human behaviors, policy interventions, and hydrological systems. The framework proposed here operates on a modular basis, where each model—engineering and econometric—functions as an independent module that interacts through well-defined interfaces.

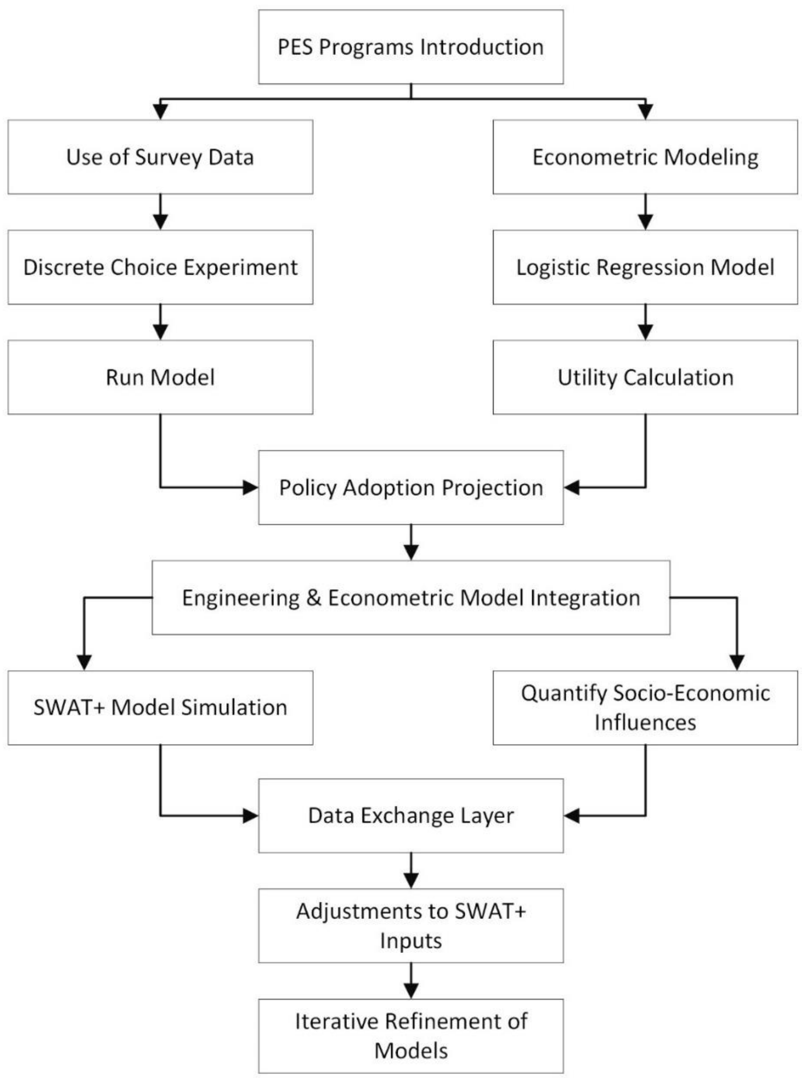


**Figure 3a.1** Framework for Integrating SWAT+ and Econometric Models in Socio-Hydrological Studies

At its core, the SWAT+ model provides a detailed simulation of hydrological processes (Wagner et al., 2022), including water flow, sediment transport, and nutrient cycling across a watershed (Van et al., 2021). While highly effective at these goals, SWAT+ provides little to no insight into how land use and land management practices will change in response to policy stimuli. Econometric models quantify the influence of socio-economic factors on human decisions, including how changes in policy or environmental conditions might affect land use, agricultural practices, and water usage (Zessner et al., 2017). The integration process of these two modeling frameworks involves aligning the outputs of econometric models—essentially predictions of human behavior and land use change—with the input requirements of SWAT+, thereby enabling the hydrological model to simulate the effects of these socio-economic changes on water systems. This methodological integration is facilitated by a data exchange layer, which translates the econometric model's outputs into parameters and variables that are understandable and usable by SWAT+. For instance, changes in crop planting decisions, derived from the econometric model, are input into SWAT+ as changes in land cover, which then influences runoff, evapotranspiration, and nutrient loading in the simulation. Similarly, policy changes affecting water usage or conservation practices are reflected in SWAT+ through adjustments to irrigation practices or the implementation of BMPs. A key advantage of this modular approach is its flexibility; the framework can be adapted or expanded to include additional models or data sources as new information becomes available or as research objectives evolve. Moreover, this integration allows for iterative refinement, where outputs from the combined model can inform further adjustments to the econometric assumptions or SWAT+ parameters, enhancing the overall accuracy and relevance of the socio-hydrological analysis. This methodological overview underscores the framework's potential to provide comprehensive insights into the reciprocal influences of human activities and natural systems, thereby supporting more informed and effective resource management and policy development.

4.2 Potential applications

The integrated framework merging SWAT+ engineering models with econometric models facilitates addressing complex environmental and policy issues through a multidisciplinary lens. This approach enables detailed analysis of the interaction between human activities and water systems, supporting informed water resource management decisions.

*Impact Assessment of Agro-environmental Policies:* Evaluates how agricultural policy changes affect farming practices and their impact on water quality and flow.

*Water Resource Management Under Climate Change:* Assesses the effects of climate change on water availability and demand, supporting the development of adaptive strategies.

*Urbanization and Its Hydrological Impacts:* Examines the hydrological effects of urban expansion, aiding in flood risk mitigation and sustainable urban development.

*Ecosystem Services Valuation:* Quantifies the economic benefits of ecosystem services related to water systems, guiding investments in conservation.

*Stakeholder Engagement in Water Governance:* Simulates participatory governance models to explore consensus-building and collaborative management approaches.

*Evaluation of Water Conservation Measures:* Analyzes individual and societal responses to water conservation policies, essential for managing water scarcity.

### 4.3 Broader Implications

This integrated modeling framework significantly impacts sustainable coastal management and climate adaptation strategies. It can partially evaluate the impacts of saltwater intrusion on farmers' land use and land management. For climate adaptation, it assesses water management strategies under future climate scenarios, considering both environmental sustainability and social equity. By integrating engineering and economic models, this approach enhances policy-making, land use planning, and ecosystem management (Boulanger & Bréchet, 2005). By offering a holistic view of human-nature interactions to inform adaptive, this framework can better inform strategies for environmental change and socio-economic development.

## 5 Conclusion and Future Directions

In summary, our theoretical exploration into Stakeholder-Driven Socio-Hydrological Modeling illuminates the critical importance and vast potential of integrating socio-hydrological models for enhancing land management and policy-making. This integration bridges the gap between hydrological science and social dynamics, thereby enabling policies that are more attuned to the complexities of human-environment interactions. Despite its promise, this approach faces theoretical and practical limitations, including the challenge of accurately modeling human behavior and the need for high-quality, socio-economic data. These hurdles underscore the importance of interdisciplinary collaboration across hydrology, social sciences, and economics to advance our methodological approaches. Future research should focus on refining these integration techniques, improving data acquisition and validation strategies, and exploring innovative ways to incorporate stakeholder insights into hydrological models.

**LLM Statement**

We utilized GPT-4.0 for grammar corrections and to enhance sentence flow. Following the AI's corrections, all materials were carefully reviewed by the authors.

**References**


Abbott, B. W., Bishop, K., Zarnetske, J. P., Minaudo, C., Chapin III, F. S., Krause, S., ... & Pinay, G. (2019). Human domination of the global water cycle absent from depictions and perceptions. Nature Geoscience, 12(7), 533-540.

Alamanos, A., & Zeng, Q. (2021). Managing Scarce water resources for socially acceptable solutions, through hydrological and econometric modeling. Central Asian Journal of Water Research, 7(1), 84-101.

Anderson, E. P., Jackson, S., Tharme, R. E., Douglas, M., Flotemersch, J. E., Zwarteveen, M., ... & Arthington, A. H. (2019). Understanding rivers and their social relations: A critical step to advance environmental water management. Wiley Interdisciplinary Reviews: Water, 6(6), e1381.

Archfield, S. A., Clark, M., Arheimer, B., Hay, L. E., McMillan, H., Kiang, J. E., ... & Over, T. (2015). Accelerating advances in continental domain hydrologic modeling. Water Resources Research, 51(12), 10078-10091.

Vereecken, H., Schnepf, A., Hopmans, J. W., Javaux, M., Or, D., Roose, T., ... & Young, I. M. (2016). Modeling soil processes: Review, key challenges, and new perspectives. Vadose zone journal, 15(5).

Babaeian, F., Delavar, M., Morid, S., & Jamshidi, S. (2023). Designing climate change dynamic adaptive policy pathways for agricultural water management using a socio-hydrological modeling approach. Journal of Hydrology, 627, 130398.

Beharry-Borg, N., Smart, J. C. R., Termansen, M., & Hubacek, K. (2013). Evaluating farmers' likely participation in a payment programme for water quality protection in the UK uplands. *Regional Environmental Change*, *13*(3), 633–647. https://doi.org/10.1007/s10113-012-0282-9

Bertassello, L., Levy, M. C., & Müller, M. F. (2021). Sociohydrology, ecohydrology, and the space-time dynamics of human-altered catchments. Hydrological Sciences Journal, 66(9), 1393-1408.

Blair, P., & Buytaert, W. (2016). Socio-hydrological modelling: a review asking "why, what and how?". Hydrology and Earth System Sciences, 20(1), 443-478.

Blanchard, P. E., & Lerch, R. N. (2000). Watershed vulnerability to losses of agricultural chemicals: Interactions of chemistry, hydrology, and land-use. Environmental science & technology, 34(16), 3315-3322.

Bockstael, N., Costanza, R., Strand, I., Boynton, W., Bell, K., & Wainger, L. (1995). Ecological economic modeling and valuation of ecosystems. Ecological economics, 14(2), 143-159.

Boulanger, P. M., & Bréchet, T. (2005). Models for policy-making in sustainable development: The state of the art and perspectives for research. Ecological economics, 55(3), 337-350.

Brunner, M. I., Slater, L., Tallaksen, L. M., & Clark, M. (2021). Challenges in modeling and predicting floods and droughts: A review. Wiley Interdisciplinary Reviews: Water, 8(3), e1520.

Castro, L. M., & Lechthaler, F. (2022). The contribution of bio-economic assessments to better informed land-use decision making: An overview. Ecological Engineering, 174, 106449.

Conrad, S. A. (2016). The use of discrete choice experiments and a coupled socio-hydrological model to inform water policymaking in the Okanagan region of British Columbia.

Curk, M., & Glavan, M. (2021). Perspectives of hydrologic modeling in agricultural research. In Hydrology. Rijeka, Croatia: IntechOpen.

Daneshi, A., Brouwer, R., Najafinejad, A., Panahi, M., Zarandian, A., & Maghsood, F. F. (2021). Modelling the impacts of climate and land use change on water security in a semi-arid forested watershed using InVEST. Journal of Hydrology, 593, 125621.

De Jonge, V. N., Pinto, R., & Turner, R. K. (2012). Integrating ecological, economic and social aspects to generate useful management information under the EU Directives'‘ecosystem approach’. Ocean & Coastal Management, 68, 169-188.

Di Baldassarre, G., Sivapalan, M., Rusca, M., Cudennec, C., Garcia, M., Kreibich, H., ... & Blöschl, G. (2019). Sociohydrology: scientific challenges in addressing the sustainable development goals. Water Resources Research, 55(8), 6327-6355.

Dinar, A. (2024). Challenges to Water Resource Management: The Role of Economic and Modeling Approaches. Water, 16(4), 610.

Elsawah, S., Pierce, S. A., Hamilton, S. H., Van Delden, H., Haase, D., Elmahdi, A., & Jakeman, A. J. (2017). An overview of the system dynamics process for integrated modelling of socio-ecological systems: Lessons on good modelling practice from five case studies. Environmental Modelling & Software, 93, 127-145.

Everard, M. (2019). A socio-ecological framework supporting catchment-scale water resource stewardship. Environmental science & policy, 91, 50-59.

Fischer, A., Miller, J. A., Nottingham, E., Wiederstein, T., Krueger, L. J., Perez-Quesada, G., ... & Sanderson, M. R. (2021). A systematic review of spatial-temporal scale issues in sociohydrology. Frontiers in Water, 3, 730169.

Forrester, J., Greaves, R., Noble, H., & Taylor, R. (2014). Modeling social-ecological problems in coastal ecosystems: A case study. Complexity, 19(6), 73-82.

Garcia, S. M. (2003). The ecosystem approach to fisheries: issues, terminology, principles, institutional foundations, implementation and outlook (No. 443). Food & Agriculture Org..

Givens, J. E., Padowski, J., Guzman, C. D., Malek, K., Witinok-Huber, R., Cosens, B., ... & Adam, J. (2018). Incorporating social system dynamics in the Columbia River Basin: Food-energy-water resilience and sustainability modeling in the Yakima River Basin. Frontiers in environmental science, 6, 104.

Howard, G., Zhang, W., Valcu-Lisman, A., & Gassman, P. W. (2023). Evaluating the tradeoff between cost effectiveness and participation in agricultural conservation programs. *American Journal of Agricultural Economics*, ajae.12397. https://doi.org/10.1111/ajae.12397

Iwanaga, T., Partington, D., Ticehurst, J., Croke, B. F., & Jakeman, A. J. (2020). A socio-environmental model for exploring sustainable water management futures: Participatory and collaborative modelling in the Lower Campaspe catchment. Journal of Hydrology: Regional Studies, 28, 100669.

Jarvis, D., Stoeckl, N., & Chaiechi, T. (2013). Applying econometric techniques to hydrological problems in a large basin: Quantifying the rainfall–discharge relationship in the Burdekin, Queensland, Australia. Journal of Hydrology, 496, 107-121.

Jarvis, D., Stoeckl, N., & Chaiechi, T. (2013). Applying econometric techniques to hydrological problems in a large basin: Quantifying the rainfall–discharge relationship in the Burdekin, Queensland, Australia. Journal of Hydrology, 496, 107-121.

Jønch-Clausen, T. (2004). Integrated water resources management (IWRM) and water efficiency plans by 2005: Why, what and how. Why, what and how, 5-4.

Kaczan, D., Swallow, B. M., & Adamowicz, W. L. (Vic). (2013). Designing a payments for ecosystem services (PES) program to reduce deforestation in Tanzania: An assessment of payment approaches. *Ecological Economics*, *95*, 20–30. https://doi.org/10.1016/j.ecolecon.2013.07.011

Keller, A. A., Garner, K., Rao, N., Knipping, E., & Thomas, J. (2023). Hydrological models for climate-based assessments at the watershed scale: A critical review of existing hydrologic and water quality models. Science of The Total Environment, 867, 161209.

Kelly, C., Ellis, G., & Flannery, W. (2018). Conceptualising change in marine governance: learning from transition management. Marine Policy, 95, 24-35.

Kong, X., Zhou, Z., & Jiao, L. (2021). Hotspots of land-use change in global biodiversity hotspots. Resources, Conservation and Recycling, 174, 105770.

Krueger, T., Maynard, C., Carr, G., Bruns, A., Mueller, E. N., & Lane, S. (2016). A transdisciplinary account of water research. Wiley Interdisciplinary Reviews: Water, 3(3), 369-389.

Kumar, P., Avtar, R., Dasgupta, R., Johnson, B. A., Mukherjee, A., Ahsan, M. N., ... & Mishra, B. K. (2020). Socio-hydrology: A key approach for adaptation to water scarcity and achieving human well-being in large riverine islands. Progress in Disaster Science, 8, 100134.

Lawyer, C., An, L., & Goharian, E. (2023). A Review of Climate Adaptation Impacts and Strategies in Coastal Communities: From Agent-Based Modeling towards a System of Systems Approach. Water, 15(14), 2635.

Levy, M. C., Garcia, M., Blair, P., Chen, X., Gomes, S. L., Gower, D. B., ... & Zeng, R. (2016). Wicked but worth it: student perspectives on socio-hydrology. Hydrol. Process, 30(9), 1467-1472.

Li, K. Y., Coe, M. T., Ramankutty, N., & De Jong, R. (2007). Modeling the hydrological impact of land-use change in West Africa. Journal of hydrology, 337(3-4), 258-268.

Liu, H., Gopalakrishnan, S., Browning, D., & Sivandran, G. (2019). Valuing water quality change using a coupled economic-hydrological model. Ecological Economics, 161, 32-40.

Ma, S., Swinton, S. M., Lupi, F., & Jolejole-Foreman, C. (2012). Farmers' willingness to participate in payment-for-environmental-services programmes. *Journal of Agricultural Economics*, *63*(3), 604–626. https://doi.org/10.1111/j.1477-9552.2012.00358.x

Manski, C. (1977, July 1). *The Structure of Random Utility Models*. https://www.proquest.com/openview/7acf07ef00e4d7b837b4de87994aed40/1?cbl=1818302&pq-origsite=gscholar

Mao, F., Clark, J., Karpouzoglou, T., Dewulf, A., Buytaert, W., & Hannah, D. (2017). HESS Opinions: A conceptual framework for assessing socio-hydrological resilience under change. Hydrology and Earth System Sciences, 21(7), 3655-3670.

Marchese, C. (2015). Biodiversity hotspots: A shortcut for a more complicated concept. Global Ecology and Conservation, 3, 297-309.

McColl, C., & Aggett, G. (2007). Land-use forecasting and hydrologic model integration for improved land-use decision support. Journal of environmental management, 84(4), 494-512.

McGrane, S. J. (2016). Impacts of urbanisation on hydrological and water quality dynamics, and urban water management: a review. Hydrological Sciences Journal, 61(13), 2295-2311.

Melsen, L. A., Vos, J., & Boelens, R. (2018). What is the role of the model in socio-hydrology? Discussion of "Prediction in a socio-hydrological world". Hydrological Sciences Journal, 63(9), 1435-1443.

Mijic, A., Liu, L., O'Keeffe, J., Dobson, B., & Chun, K. P. (2024). A meta-model of socio-hydrological phenomena for sustainable water management. Nature Sustainability, 7(1), 7-14.

Mirza, M. U., & Mustafa, D. (2016). Access, equity and hazards: highlighting a socially just and ecologically resilient perspective on water resources. Sustainable Development and Disaster Risk Reduction, 143-159.

Moirano, R., Sánchez, M. A., & Štěpánek, L. (2020). Creative interdisciplinary collaboration: A systematic literature review. Thinking Skills and Creativity, 35, 100626.

Mostert, E. (2018). An alternative approach for socio-hydrology: case study research. Hydrology and Earth System Sciences, 22(1), 317-329.

Mostert, E. (2018). An alternative approach for socio-hydrology: case study research. Hydrology and Earth System Sciences, 22(1), 317-329.

Muñoz-Carpena, R., Carmona-Cabrero, A., Yu, Z., Fox, G., & Batelaan, O. (2023). Convergence of mechanistic modeling and artificial intelligence in hydrologic science and engineering. PLOS Water, 2(8), e0000059.

Ovando, P., & Brouwer, R. (2019). A review of economic approaches modeling the complex interactions between forest management and watershed services. Forest Policy and Economics, 100, 164-176.

Ovando, P., & Brouwer, R. (2019). A review of economic approaches modeling the complex interactions between forest management and watershed services. Forest Policy and Economics, 100, 164-176.

Pande, S., & Sivapalan, M. (2017). Progress in socio-hydrology: A meta-analysis of challenges and opportunities. Wiley Interdisciplinary Reviews: Water, 4(4), e1193.

Pande, S., Roobavannan, M., Kandasamy, J., Sivapalan, M., Hombing, D., Lyu, H., & Rietveld, L. (2020). A socio-hydrological perspective on the economics of water resources development and management. In Oxford Research Encyclopedia of Environmental Science.

Qiu, H., Qi, J., Lee, S., Moglen, G. E., McCarty, G. W., Chen, M., & Zhang, X. (2021). Effects of temporal resolution of river routing on hydrologic modeling and aquatic ecosystem health assessment with the SWAT model. Environmental Modelling & Software, 146, 105232.

Raes, L., Speelman, S., & Aguirre, N. (2017). Farmers' Preferences for PES Contracts to Adopt Silvopastoral Systems in Southern Ecuador, Revealed Through a Choice Experiment. *Environmental Management*, *60*(2), 200–215. https://doi.org/10.1007/s00267-017-0876-6

Salvadore, E., Bronders, J., & Batelaan, O. (2015). Hydrological modelling of urbanized catchments: A review and future directions. Journal of hydrology, 529, 62-81.

Schlueter, M., Mcallister, R. R., Arlinghaus, R., Bunnefeld, N., Eisenack, K., Hoelker, F., ... & Stöven, M. (2012). New horizons for managing the environment: A review of coupled social-ecological systems modeling. Natural Resource Modeling, 25(1), 219-272.

Schulze, R. E. (1997). Impacts of global climate change in a hydrologically vulnerable region: challenges to South African hydrologists. Progress in physical geography, 21(1), 113-136.

Sivapalan, M. (2015). Debates—Perspectives on socio-hydrology: Changing water systems and the "tyranny of small problems"—Socio-hydrology. Water Resources Research, 51(6), 4795-4805.

Sivapalan, M., Konar, M., Srinivasan, V., Chhatre, A., Wutich, A., Scott, C. A., ... & Rodríguez-Iturbe, I. (2014). Socio-hydrology: Use-inspired water sustainability science for the Anthropocene. Earth's Future, 2(4), 225-230.

Sivapalan, M., Savenije, H. H., & Blöschl, G. (2012). Socio-hydrology: A new science of people and water. Hydrol. Process, 26(8), 1270-1276.

Sivapalan, M., Savenije, H. H., & Blöschl, G. (2012). Socio-hydrology: A new science of people and water. Hydrol. Process, 26(8), 1270-1276.

Srinivasan, V., Sanderson, M., Garcia, M., Konar, M., Blöschl, G., & Sivapalan, M. (2017). Prediction in a socio-hydrological world. Hydrological Sciences Journal, 62(3), 338-345.

Tanim, A. H., Goharian, E., & Moradkhani, H. (2022). Integrated socio-environmental vulnerability assessment of coastal hazards using data-driven and multi-criteria analysis approaches. Scientific Reports, 12(1), 11625.

Troy, T. J., Pavao-Zuckerman, M., & Evans, T. P. (2015). Debates—Perspectives on socio-hydrology: Socio-hydrologic modeling: Tradeoffs, hypothesis testing, and validation. Water Resources Research, 51(6), 4806-4814.

van Tol, J., Bieger, K., & Arnold, J. G. (2021). A hydropedological approach to simulate streamflow and soil water contents with SWAT+. Hydrological Processes, 35(6), e14242.

Vogel, R. M., Lall, U., Cai, X., Rajagopalan, B., Weiskel, P. K., Hooper, R. P., & Matalas, N. C. (2015). Hydrology: The interdisciplinary science of water. Water Resources Research, 51(6), 4409-4430.

Wagner, P. D., Bieger, K., Arnold, J. G., & Fohrer, N. (2022). Representation of hydrological processes in a rural lowland catchment in Northern Germany using SWAT and SWAT+. Hydrological Processes, 36(5), e14589.

Walters, C. (1997). Challenges in adaptive management of riparian and coastal ecosystems. Conservation ecology, 1(2).

Xu, L., Gober, P., Wheater, H. S., & Kajikawa, Y. (2018). Reframing socio-hydrological research to include a social science perspective. Journal of hydrology, 563, 76-83.

Xu, L., Gober, P., Wheater, H. S., & Kajikawa, Y. (2018). Reframing socio-hydrological research to include a social science perspective. Journal of hydrology, 563, 76-83.

Zessner, M., Schönhart, M., Parajka, J., Trautvetter, H., Mitter, H., Kirchner, M., ... & Schmid, E. (2017). A novel integrated modelling framework to assess the impacts of climate and socio-economic drivers on land use and water quality. Science of The Total Environment, 579, 1137-1151.

Zhao, Q., Chen, Y., Gone, K. P., Wells, E., Margeson, K., & Sherren, K. (2023). Modelling cultural ecosystem services in agricultural dykelands and tidal wetlands to inform coastal infrastructure decisions: A social media data approach. Marine Policy, 150, 105533.

**Chapter 3b: A Socio-Hydrological Framework for Incorporating Farmers' Behavioral Model into the SWAT+ Model and Implications for Improving Ecosystem Health**

Mahesh R Tapas[a*], Randall Etheridge[b], Gregory Howard[c], Matthew Mair[d]

[a] Integrated Coastal Program, East Carolina University, Greenville, NC 27858, USA

[b]Department of Engineering, Center for Sustainable Energy and Environmental Engineering, East Carolina University, Greenville, NC 27858, USA

[c] Department of Economics, East Carolina University, Greenville, NC 27858, USA

[d] Department of Economics, Appalachian State University, Greenville, NC 28608

*Corresponding author: tapasm21@students.ecu.edu (Mahesh R Tapas).

ORCID: 0000-0001-8833-5531

**Abstract:**

Eutrophication poses a significant threat to ecosystems, necessitating effective policies to mitigate nutrient excess. This study adopts an interdisciplinary approach, merging concepts from econometric and engineering frameworks to develop a socio-hydrological model. Integrating a farmers' behavioral model into the hydrological model, the study surveyed around 279 farmers in the Tar-Pamlico River Basin to gauge their responses to policy changes of cover crop adoption and reduced fertilizer use. Analysis revealed that the majority of farmers are hesitant to adopt these practices based on farmers' Willingness To Accept (WTA). Further, simulations using the Soil and Water Assessment Tool Plus (SWAT+) software showed no significant reduction in nitrate loading to the Pamlico Estuary from the widespread adoption of these practices, with both cover crops and reduced fertilizer application failing to produce noticeable changes, underscoring the limitations of the modeled Best Management Practices (BMPs) at the watershed scale.

The study highlights the complexity of nutrient transport in coastal watersheds and suggests exploring combined BMPs and integrating socio-hydrological modeling for more accurate predictions of agricultural policy impacts. It emphasizes the need to consider alternative nitrate sources and scale-up interventions to effectively address eutrophication. By bridging econometric and engineering frameworks, this research provides insights into the challenges of implementing sustainable agricultural practices and underscores the importance of interdisciplinary approaches in tackling environmental issues.

**Study Area:**

Tar-Pamlico Watershed, North Carolina, United States.

**Keywords:**

Socio-hydrological modeling; Best Management Practices (BMPs); Farmers' behavioral model; SWAT+; Eutrophication; Ecosystem health; Nitrate load.

**Highlights:**

1. Integrating hydrological and economic models reveals complex dynamics in nutrient management, emphasizing the need for interdisciplinary policy frameworks.
2. Despite incentives, farmers show limited willingness to adopt strict nitrogen limits, highlighting economic and behavioral barriers in sustainable agriculture.
3. Hydrological models overestimate nitrogen reduction benefits by 15 times, underscoring the need for models that incorporate socio-economic factors for accuracy.

**Graphical Abstract:**

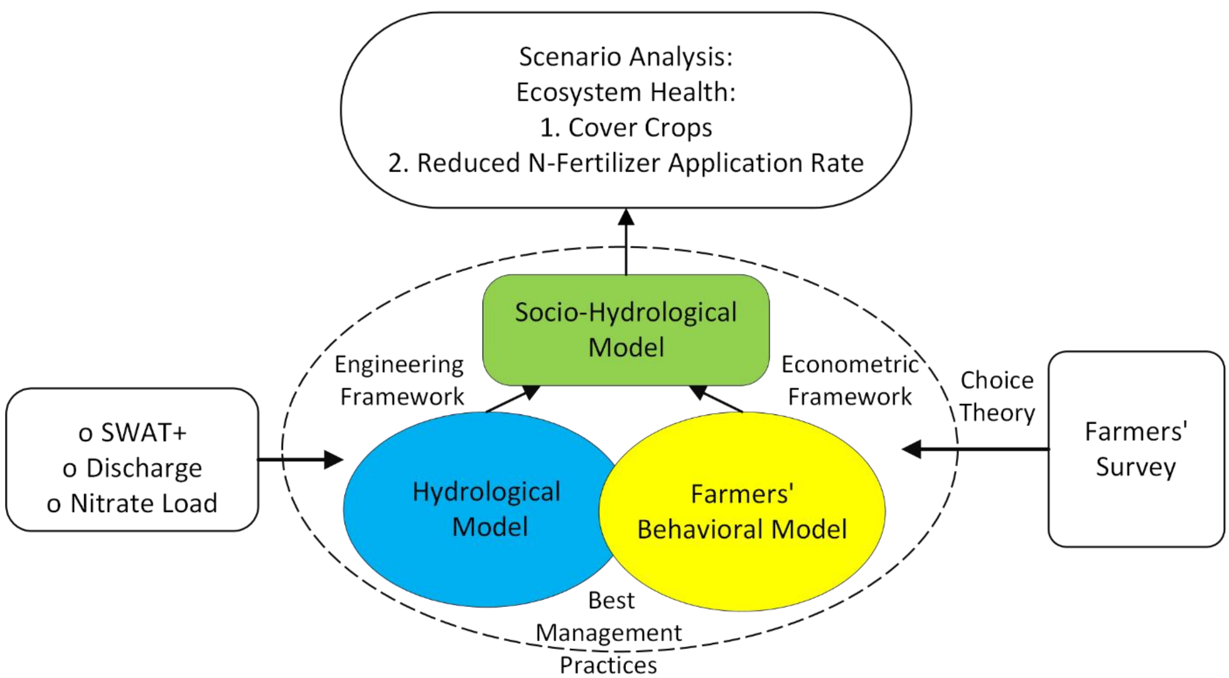

**1. Introduction:**

In recent decades, anthropogenic climate change — climate change induced by human activities — has substantially altered watershed dynamics worldwide (Chang et al., 2015; Palmer et al., 2008). This change is due to human activities such as burning fossil fuels (Höök et al., 2013), excessive use of fertilizers (Celikkol et al., 2017), development of water diversion networks (Bai et al., 2023), and intensive agriculture (Lal 2013). Rising temperatures (Luo et al., 2013), shifting precipitation patterns (Coopersmith et al., 2014), and the increasing frequency and intensity of extreme weather events (Hettiarachchi et al., 2018), such as hurricanes (Ouyang et al., 2022) and droughts (Peterson et al., 2021), are influencing watershed hydrology by altering river flow regimes (Gibson et al., 2005), groundwater recharge rates (Nolan et al., 2007), and soil moisture content (Hawley et al., 1983). These hydrological changes can intensify the issues of excessive nutrients in water bodies (Petry et al., 2002), primarily from agricultural runoff (Cherry et al., 2008) and urban development (Reckhow et al., 1999). Higher temperatures can enhance the biological demand for oxygen in water bodies, exacerbating the effects of nutrient pollution, such as accelerated eutrophication (Cross & Summerfelt 1986). This process can lead to harmful algal blooms (Wurtsbaugh et al., 2019), hypoxia (Howarth et al., 2011), and loss of biodiversity (Hautier et al., 2009), undermining the health of aquatic ecosystems and affecting water quality for recreation and wildlife (Kapsalis & Kalavrouziotis, 2021).

Implementing agricultural Best Management Practices (BMPs), such as the strategic use of cover crops and the reduction of chemical nitrogen (N) fertilization rates, offers a targeted approach to mitigating the threat of excess nutrient loads in watersheds (Howard et al., 2024). Cover crops, planted during times when the soil might otherwise be bare, play a crucial role in improving soil structure, enhancing water infiltration, and increasing soil organic matter (Dabney et al., 2001). This leads to reduced runoff and erosion, thereby limiting the flow of nutrients into adjacent water bodies. Moreover, certain cover crop species have the ability to capture residual nitrogen from previous crop fertilization. This can effectively reduce nitrate leaching into groundwater and surface waters (Wendling et al., 2016). Reducing the application rate of nitrogen fertilizers directly addresses a source of nutrient pollution (Shibu et al., 2010). This practice not only reduces the risk of nitrate runoff into aquatic ecosystems but also encourages more efficient use of fertilizers, resulting in economic benefits for farmers (Howard et al., 2024). Together, these BMPs have the potential to contribute significantly to reducing excessive nutrients in agriculturally dominated watersheds, thus improving water quality and supporting the health of aquatic ecosystems as we adapt to the impacts of climate change (Dabney et al., 2001; Shibu et al., 2010).

Hydrological modeling, particularly using advanced tools like Soil and Water Assessment Tool Plus (SWAT+), plays a pivotal role in evaluating the efficiencies of agricultural BMPs. By simulating complex watershed processes, SWAT+ can assess how different BMP scenarios impact water quantity and quality across various spatial and temporal scales (Singh et al., 2023). This includes the ability to model the effectiveness of cover crops in reducing runoff and enhancing infiltration, as well as quantifying the impact of reduced nitrogen application rates on nitrate leaching into water bodies. SWAT+ allows for the exploration of BMP placement and timing under varying climatic and land use conditions, offering insights into how these practices can be best implemented to achieve maximum environmental benefits (Naganur et al., 2024). The model's capacity to predict environmental outcomes of specific agricultural practices provides a valuable decision-support tool for policymakers, land managers, and farmers aiming to mitigate nutrient pollution and improve watershed health in a changing climate (Naganur et al., 2024; Singh et al., 2023).

Incorporating stakeholders' perspectives into hydrological modeling is essential to ensure that model outputs align with real-world conditions and stakeholder needs (Veisi et al., 2022). While tools like SWAT+ have been proven to simulate physical processes, they often fall short of fully capturing the socioeconomic factors that influence the adoption of BMPs by land managers (Howard et al., 2024). Through the integration of stakeholder engagement and econometric modeling, particularly farmer behavioral models, model simulations can be grounded in practical realities and enhance the accuracy of model predictions. This methodology facilitates the identification of socially acceptable and economically viable BMPs, leveraging statistical methods to quantify how economic, environmental, and policy factors affect farmers' decision-making. Ultimately, this has the potential to spur wider adoption of sustainable practices and more effective watershed management strategies, bridging the gap between physical process simulation and the socio-economic dynamics of agricultural practice adoption (Behboudian et al., 2023; De Bruijn et al., 2023).

In response to the outlined challenges, this study will undertake a multifaceted approach that combines nitrate modeling with an evaluation of the effectiveness of cover crops and reduced nitrogen application rates in mitigating downstream nutrient loading. Recognizing the importance of socio-economic factors in the adoption and success of BMPs, this research will also integrate stakeholder views through farmers' behavioral models. This will ensure that the modeling not only reflects physical and biological processes but also incorporates the decision-making behaviors of land managers. Finally, by comparing the outcomes of traditional hydrological modeling with those informed by a farmer behavioral model, this study aims to highlight the added value of embedding social dynamics into hydrological models. Such an integrative approach should enhance the accuracy of model predictions and provide actionable insights for policymakers, ultimately contributing to more effective and sustainable watershed management strategies in the face of ongoing climate change.

### 1.1. Study objectives:

The objectives of this study are: 1) To develop and optimize a hydrological model for the Tar-Pamlico watershed in coastal North Carolina using SWAT+; 2) To implement cover crops and reduced N-fertilizer application rate and find their impact on nitrate loading at Pamlico estuary using the hydrological model; 3) To survey farmers in the watershed to identify their responses to policy changes; 4) To develop a farmers' behavioral model to identify their willingness to accept cover crops and reduced N-fertilizer application under the current EQIP rate; 5) To integrate the hydrological model (engineering framework) and the farmers' behavioral model (econometric framework) to develop a socio-hydrological model; 6) To test the impacts of different policies on ecosystem health using this socio-hydrological model.

## 2. Materials & Methodology:

### 2.1 Study Area

In this study, we applied our socio-hydrological modeling framework to the Tar-Pamlico watershed (Figure 3b.1), a coastal area in eastern North Carolina covering 16,576 km$^2$. This watershed, characterized by its diverse land use including agriculture (27.9%), forests (33.9%), and wetlands (31.9%), supports a variety of crops with soybeans (40%), corn (19%), and cotton (19%) the predominate agricultural crops. With a population of 470,000, the Tar-Pamlico watershed plays a significant role in discharges to the Pamlico estuary, an area currently facing challenges with algae blooms attributed to excessive nitrate levels. By implementing our methodology in this watershed, we aim to explore the ability of different BMPs to address the critical issue of elevated nutrient loads, thereby contributing to the overall health of the ecosystem and mitigating the adverse effects on the Pamlico estuary.

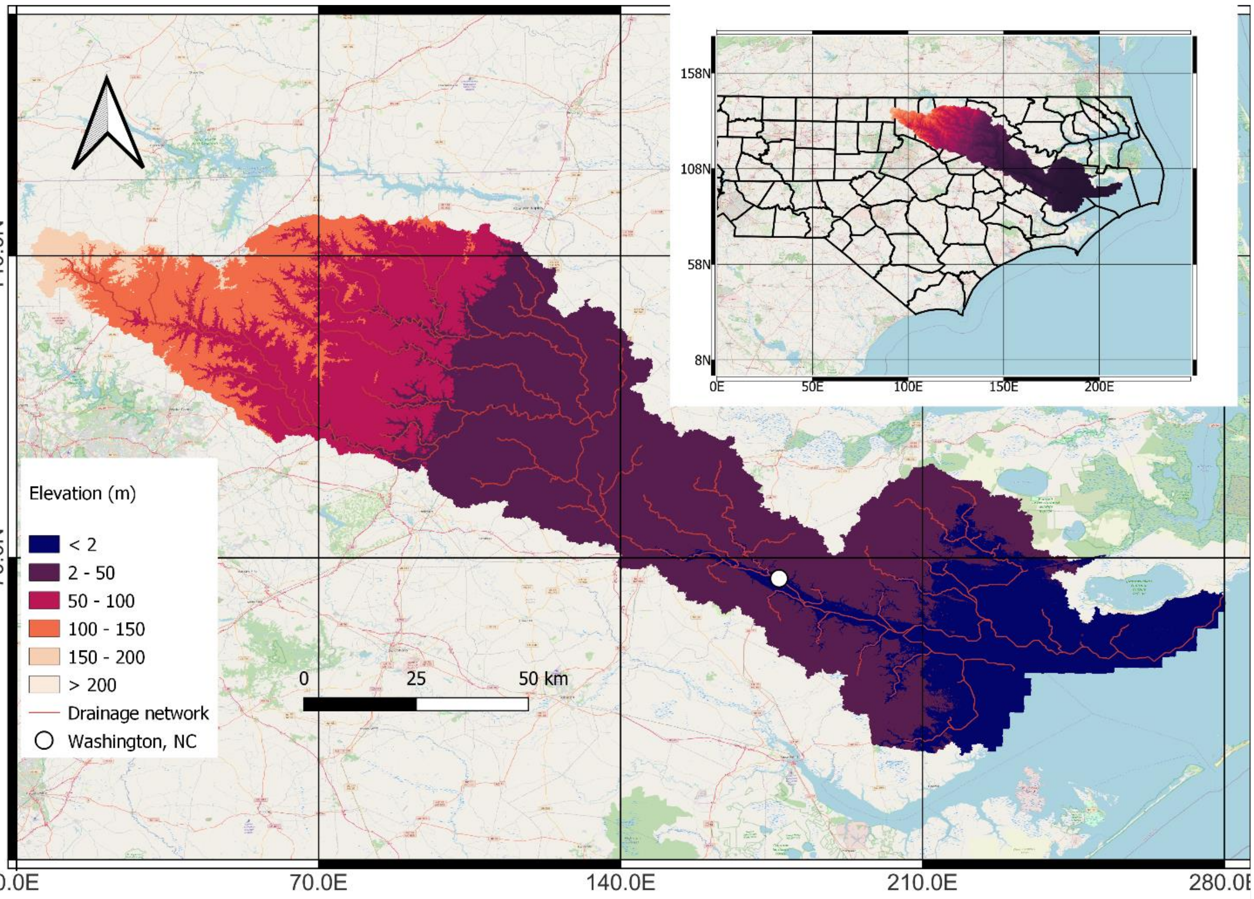


**Figure 3b.1** Study Area (Tar-Pamlico watershed)

2.2 Hydrological model: Engineering Framework

We used the SWAT+ tool for hydrological modeling. SWAT+ is designed to provide comprehensive modeling of watershed and sub-watershed dynamics (SWAT+ IO Document, 2020). It serves as a critical tool for decision-making in water resource management, agricultural planning, and environmental conservation, offering insights into the effects of land management practices on water quality and agricultural productivity (Bieger et al., 2017; Wu et al., 2023). By enabling the simulation of complex environmental processes, SWAT+ supports policy development and planning. SWAT+ uses a semi-distributed hydrological framework and enhanced spatial flexibility compared to SWAT (SWAT+ IO Document, 2020). Particularly noteworthy is its capability to simulate flow and nutrient dynamics, including detailed analyses of plant yield, denitrification rates, and nitrate loss in groundwater, surface water, and lateral flows. This precision allows for the evaluation of the impacts of climate change and land use changes on water resources, making SWAT+ a great tool for future resource planning and environmental protection efforts (SWAT+ IO Document, 2020).

For SWAT+ model setup, we utilized various data sources to represent watershed characteristics accurately. Watershed boundary shapefiles were obtained from the United States Geological Survey (USGS) StreamStats website. The model was initialized using Digital Elevation Model (DEM) data (year: 2011), land-use and land-cover data from the National Land Cover Database (NLCD) (year: 2008), and soil data from the Soil Survey Geographic Database (SSURGO) (year: 2015), all at a 90m resolution. These datasets were integrated into QSWAT+ to delineate streams, sub-basins, and Hydrological Response Units (HRUs), essential for simulating the complex hydrological processes within the watershed. We included atmospheric deposition data from the National Atmospheric Deposition Program (NADP, 2023). We integrated crop data and fertilizer application rates into the SWAT+ model setup based on Tar-Pamlico watershed reports from the North Carolina Department of Environmental Quality (NCDEQ) and the North Carolina Department of Agriculture & Consumer Services (NCDEQ, 2014; NCGAR, 2022). These datasets provided detailed information on agricultural practices within the watersheds, including types of crops grown, the extent of winter cover crop adoption, and specific fertilizer usage rates.

Incorporating this information was crucial for more accurately simulating agricultural runoff and nutrient loading, allowing for a more comprehensive assessment of the watershed's hydrology and nutrient dynamics. The Tar-Pamlico watershed contains a total of 22 Wastewater Treatment Plants that were included in the model. We retrieved flow and nitrate data for each Wastewater Treatment Plant from National Pollutant Discharge Elimination System (NPDES) (National Pollutant Discharge Elimination System (NPDES) | US EPA). All these details were added to increase the accuracy of flow and nitrate simulations.

We obtained observed flow data from USGS stations at Greenville (02084000) and at Washington (02084472). Flow data at Washington station is available only before September 2006. As our nitrate data is available in Washington, we extrapolated our flow data at the Washington station based on flow at the Greenville station because there was a strong linear correlation. The linear regression equation (Flow at Washington = 1.0176 × flow at Greenville + 27.5774) with an $R^2$ of 0.90 indicate that approximately 90% of Washington's discharge variability can be estimated from Greenville's data, offering a reliable method for compensating the data scarcity at Washington. Nitrate concentration data were obtained from the North Carolina Department of Environmental Quality (NCDEQ). We calculated monthly nitrate load at Washington using nitrate concentrations and extrapolated flows (Appendix 1). Because SWAT+ cannot handle the bidirectional flow (SWAT+ IO Document, 2020), we converted any negative flows (0.39%) from our observed flow data file to zero. This ensured that we simulated flow as low as possible during the days of backflow.

2.2.1. SWAT+ model calibration

We used the SWATrunR package (Schuerz 2019) to calibrate the SWAT+ model, with a focus on simulating flow and nitrate load at the Washington station. Our calibration efforts focused on a set of 21 parameters crucial for accurately representing hydrological processes based on sensitivity analysis (Appendix 1) and the existing literature. These parameters were distributed across the basin, soil, HRU, and aquifer levels, with 6 basin parameters, 4 soil parameters, 10 HRU parameters, 2 plant parameters, and 1 aquifer level parameter as shown in Table 3b.1. We customized an R script, using the SWATrunR package as a foundation (Appendix 1).

We employed the parameter adjustment methods of absolute change ($x' = x + y$), percent change ($x' = y * x / 100$), and absolute value ($x' = y$), where x represents the default value, x' denotes the new value, and y signifies the calibrated parameter value. The selection of these adjustment types depended on both the parameter's resolution and its initial range. For instance, when dealing with basin-level parameters, we predominantly utilized absolute value adjustments. Additionally, the choice between absolute and percentage changes was determined by the magnitude of the parameter's range: for narrow ranges, absolute changes were preferred, while percentage changes were favored for wider ranges. This approach facilitated targeting a broad range of parameter combinations during model calibration, ensuring flexibility to adjust parameters effectively across varying resolutions and initial ranges (Table 3b.1).

**Table 3b.1** SWAT+ model optimization parameters details [bsn: Basin, sol: Soil, hru: Hydrological Response Unit, plt: Plant]

| Parameter | Parameter Range (Unit) | Resolution | Type of Change | Description | Initial range used for model calibration (min, max) | Calibrated parameter value |
|---|---|---|---|---|---|---|
| surlag | 0.05, 24.0 (days) | bsn | Absolute Value | Surlag Controls delay in surface runoff release | 0.05, 24 | 3.574 |
| cmn | 0.001, 0.003 (-) | bsn | Absolute Value | Rate factor for humus mineralization of organic nutrients | 0.001, 0.003 | 0.0018 |
| cdn | 0.0, 3.0 (-) | bsn | Absolute Value | Denitrification rate control | 0, 3 | 2.261 |
| sdnco | 0.0, 1.0 (-) | bsn | Absolute Value | Denitrification threshold water content | 0, 1 | 0.559 |
| nperco | 0.0, 1.0 (-) | bsn | Absolute Value | Nitrate percolation coefficient | 0.01, 1 | 0.080 |
| n_updis | 0.0, 100.0 (-) | bsn | Absolute Value | Nitrogen uptake distribution parameter controlling depth distribution of nitrogen uptake in soil | 0, 100 | 49.233 |
| awc | 0.01, 1.0 (mm $H2O$ $mm^{-1}$) | sol | Absolute Change | The difference in soil water content between field capacity and permanent wilting point | -0.3, 0.3 | 0.081 |
| bd | 0.9, 2.5 (g $cm^{-3}$) | sol | Absolute Change | Moist bulk density, representing soil's mass-to-volume ratio at or near field capacity. | -0.4, 0.8 | 0.271 |
| k | 0.0001, 2000.0 (mm $hr^{-1}$) | sol | Percent Change | Saturated hydraulic conductivity, indicating the ease of water movement through soil | -30, 30 | -4.024 |
| z | 0.0, 3500.0 (mm) | sol | Percent Change | Depth from soil surface to bottom of layer | -30, 30 | 1.469 |
| esco | 0.0, 1.0 (-) | hru | Absolute Change | Soil evaporation compensation factor which allows modification of depth distribution to meet soil evaporative demand, considering capillary action, crusting, and cracks. | -0.3, 0.3 | -0.069 |
| epco | 0.0, 1.0 (-) | hru | Absolute Change | Plant uptake compensation factor which allows adjustment of water uptake depth distribution in response to plant transpiration demand and soil water availability. | -0.3, 0.3 | -0.114 |
| biomix | 0.0, 1.0 (-) | hru | Absolute Change | Biological mixing efficiency, determining redistribution of soil constituents by biota activity. | -0.3, 0.3 | -0.048 |
| latq_co | 0.0, 1.0 (-) | hru | Absolute Change | Coefficient for the Plant ET curve number | -0.3, 0.3 | 0.101 |

| | | | | | | |
|---|---|---|---|---|---|---|
| perco | 0.0, 1.0 (fraction) | hru | Absolute Change | Percolation coefficient, adjusting soil moisture for percolation to occur. | -0.3, 0.3 | -0.272 |
| cn2 | 35.0, 95.0 (-) | hru | Percent Change | Curve number for Condition II runoff potential. | -30, 30 | 12.283 |
| cn3_swf | 0.0, 1.0 (-) | hru | Percent Change | Soil water factor for the curve number for condition III runoff potential | -30, 30 | -24.729 |
| ovn | 0.01, 30.0 (-) | hru | Percent Change | Manning's "n" value for overland flow velocity estimation | -30, 30 | 14.865 |
| canmx | 0.0, 100.0 (mm H2O) | hru | Percent Change | Maximum canopy storage, representing the maximum amount of water held in the canopy when fully developed. | -30, 30 | -0.189 |
| lat_ttime | 0.5, 180.0 (days) | hru | Percent Change | Lateral flow travel time allows the model to calculate travel time based on soil hydraulic properties. | -30, 30 | -19.100 |
| revap_min | 0.0, 50.0 (m) | aqu | Percent Change | Threshold depth of water in shallow aquifer for percolation to deep aquifer | -30, 30 | 7.659 |
| Lai_pot | 0.5, 10 ($m^2$ $m^{-2}$) | plt | Absolute Value | Potential maximum leaf area index | NA | Corn: 5<br>Cotton: 2.5<br>Soyb: 2.027 |
| Harv_idx | 0.01, 1.25 (-) | plt | Absolute Value | Harvest index- crop yield/aboveground biomass | NA | Soyb: 0.418 |

### 2.2.2. Best Management Practices Simulation

In this study, we simulated two commonly used best management practices: cover crops and reduced fertilizer application rates. We used winter wheat as the cover crop, which is commonly used in the Tar-Pamlico Basin. We planted the cover crop 14 days after harvesting the main summer cash crop. We terminated the cover crop prior to planting the summer crop the following spring. We applied a 30% reduction in nitrogen fertilizer use to simulate policies related to strict nitrogen application.

### 2.3. Farmers' behavioral model: Econometrics framework

We conducted a survey (Appendix 1) among farmers in the Tar-Pamlico River basin and other coastal areas in eastern North Carolina to gauge farmers' interest in voluntary conservation programs. Our goal was to use survey results to parameterize a behavioral model that predicts farmers' responses to various policy changes, especially concerning the provision of payments for cover crops and reductions in fertilizer usage. By incorporating scenarios that reflect aspects of existing and hypothetical agricultural support programs (i.e. Environmental Quality Incentives Program, or EQIP), the survey sought to capture farmers' perspectives on and likely response to potential policies and economic incentives, thereby bridging the gap between policymakers and farmers.

The survey asked farmers about their specific farming practices, environmental concerns, and the potential impact of policy changes on these practices. This comprehensive approach was intended to gather insights into farmers' current challenges and their willingness to accept different practices in light of new policies or economic conditions. These surveys are increasingly common in agri-environmental policy analysis (Howard & Roe, 2013; Ma et al., 2012; Peterson et al., 2015).

### 2.3.1. Choice Experiment Design in Farmer Preference Survey

The survey incorporated a choice experiment to gauge farmers' preferences for various hypothetical voluntary conservation contracts, aimed at reducing nutrient runoff (Figure 3b.2). This experiment varied five key attributes across different scenarios: cover crop usage (required or not), strict nitrogen application (mandatory or optional), lenient nitrogen application (mandatory or optional), funding agency (State and Federal government agencies or private conservation groups), and the annual payment amount ($10, $40, $70, $100, and $130 per acre; or $25, $99, $173, $247, and $321 per Ha). Each respondent was presented with two scenarios, each containing two conservation contracts and a "neither" option, allowing us to simulate real policy decisions (Figure 3b.2).

**Scenario 1**

**Please consider the terms of Programs A & B below for your field and answer the questions that follow as if a real conservation contract was being offered to you.**

| | **Program A** | **Program B** |
|---|---|---|
| **Limited Nitrogen Application** | Apply No more than 40 lbs. per acre | Apply No more than 60 lbs. per acre |
| **Cover Crops** (Planting a legume crop after harvesting the main cash crop) | Must be planted after 2023 harvest | No Requirement |
| **Funding Source** (who is providing the money and enforcing the contract) | Private Conservation Group | State and Federal Government Agencies |
| **Annual Cost Share Payment to You** | $130/acre | $10/acre |

28. Which program do you prefer?

1 = Program A 2 = Program B 3 = Neither program

29. How Certain are you about your choice?

1 2 3 4 5 6 7 8 9 10

Not at all Certain Very Certain

**Figure 3b.2** Sample cost share contract

We sent surveys to over 1870 farmers through a combination of solicitation via email, solicitation via postal mail, and direct engagement at farmer meetings in eastern North Carolina. Our primary method of contact involved mailings to farmer addresses. We utilized a mixed-mode web push approach that included an initial invitation to participate as well as a follow-up mailing to initial non-responders. This follow-up mailing included a paper survey and a pre-paid return envelope (Dillman et al., 2014). We received 279 responses, with 76 of these providing enough data to include them in the construction of the farmers' behavioral model. The vast majority of responses that did not provide sufficient data involved respondents indicating that they were no longer actively farming. These 76 responses, which represent up to 29 $km^2$ of farmland, are particularly valuable for developing a model that accurately reflects farmer willingness to accept different agricultural practices under a voluntary conservation contract setting.

The provided STATA code (Appendix 1) outlines an econometric analysis of the behavioral responses of farmers in North Carolina, grounded in the Random Utility Maximization (RUM) theory (Habib 2011). RUM theory specifies that the utility farmer *i receives from*, choosing alternative $j$ in time period $t$, denoted $U_{ijt}$, can be described as a function of the observed attributes $X_{ijt}$ and unobserved factors $\epsilon_{ijt}$ (Howard et al., 2024). Thus, the utility function can be expressed as follows:

$$Uijt=Xijt\beta i+\epsilon ijt$$

Where:

- $X_{ijt}$ represents the attributes observed, including state funding presence, payment rate, strict nitrogen regulation, lenient nitrogen regulation, an alternative-specific constant for the “no contract” option, and cover crops utilization.
- $\beta_i$ is a vector that represents preference parameters for the population, with the subscript $i$ indicating that parameters may vary across individuals, thus accounting for heterogeneity in preferences among farmers.

- $\epsilon_{ijt}$ is the unobserved error term.

To incorporate preference heterogeneity directly into the model, we utilize the mixed logit model. In this model, individual-specific deviation parameters $\eta_i$ may be added:

$$U_{ijt}=X_{ijt}(\beta+\eta_i)+\epsilon_{ijt}$$

This means that individual $i$'s preference parameter, $\beta_i$ is equal to the sum of the population average preference parameter a vector $\beta$ and the individual-specific deviation parameter. For each attribute with preference heterogeneity, the model estimates a set of two parameters, one for the average preference in the population and one for the standard deviation of the individual deviation parameters (Gaur et al., 2023).

Assuming the error term follows a Type-1 extreme value distribution with mean zero, the probability $P_{i\{c1,c2,...cT\}}$ of individual $i$'s sequence of choices $[c1,c2,...cT]$ over $T$ time periods (Gaur et al., 2023) is given by:

$$P_{\{c1,c2,...cT\}} = \int \left[\pi_{t=1}^{T} \frac{\exp(X_{imt}\beta_i)}{\sum_{m=1}^{M}\exp(X_{imt}\beta_i)}\right] f(\beta \mid \theta)d\beta$$

where:

- $X_{imt}$ represents the observed attributes of the alternatives available to farmer $i$ in choice situation $t$, which includes factors from the survey such as the presence of state funding, payment rates, strict and lenient nitrogen application regulations, and the requirement of cover crops.

- $\beta_i$ is a vector of coefficients associated with the attributes $X_{imt}$, reflecting the mean preferences of the farmers but allowing for individual-specific deviations to capture preference heterogeneity.
- $f(\beta|\theta)$ is the density function of $\beta$, with $\theta$ being the parameters of the distribution, indicating how the preference parameters $\beta$ are distributed in the population of farmers.
- $M$ is the number of alternatives available in the choice set.

In refining our econometric model, we focused on allowing preference heterogeneity for the alternative specific constant (ASC) and cover crop utilization. Attempts to include heterogeneity for nitrogen application restrictions did not converge, suggesting limited variability in preferences for these attributes among the farmers surveyed.

$$V_{ij} = \beta_{ic1}StateFundingPresence + \beta_{ic2}PaymentRate + \beta_{ic3}StrictNitrogenRegulation + \beta_{ic4}LenientNitrogenRegulation + +\beta_{ic5}AlternativeSpecificConstant + +\beta_{ic6}CoverCrops\_Utilization \quad (3)$$

2.3.2. Estimation of Willingness to Accept (WTA)

In our survey of the farmers in the Tar-Pamlico basin, we presented choices between two hypothetical agricultural assistance programs alongside a status quo option of no contract. This enabled us to examine the impact of specific regulatory or funding conditions on farmers' willingness to implement environmentally beneficial practices. Utilizing the mixed logit model described in the previous section, we analyzed how these variables related to policy interventions, economic incentives, and environmental practices influence farmer choices, thus revealing insights into the decision-making processes that drive the adoption of sustainable agricultural practices (Howard et al., 2024).

The estimation of WTA is a critical element of our econometric framework, serving to gauge the minimum amount a farmer would accept to alter their current agricultural practice to incorporate a practice that is potentially less profitable but more environmentally friendly. It is derived from the utility differences provided by the mixed logit model's coefficients and is expressed mathematically as the monetary compensation required to offset the utility loss incurred by switching from the farmer's current status-quo to a new situation where they accept an offered conservation contract. The WTA for policy j is calculated as:

$$WTA_{ij} = \frac{-(U_{ij} - U_{i\ baseline})}{\beta_{payment,i}}$$

In this formula, $U_{ij}$ represents the utility from accepting the conservation contract, $U_{i\ \mathrm{baseline}}$ is the utility for the current practice, and payment, $\beta_{\mathrm{payment},i}$ is the coefficient for the policy payment attribute, which also represents the marginal utility of income changes.

Our econometric analysis captures individual-specific preference deviations and the inherent randomness in farmers' responses to incentives, thus highlighting unique decision-making processes. The mixed logit model provides coefficients and standard errors for each contract attribute, which are essential for determining the marginal effects on farmer utility and calculating the likelihood of contract acceptance and overall Willingness to Accept (WTA). In essence, each farmer is assigned a draw from the distribution of farmer preferences estimated in the farmer behavioral model, so each farmer can potentially have a different simulated minimum WTA for a specified contract. These insights are vital for developing targeted policies and interventions that promote sustainability and economic efficiency, enhancing our understanding of agricultural practices and supporting resilience in farming communities (Howard et al., 2024).

### 2.4. Hydrological-Econometric models integration

Integrating hydrological and econometric models is a crucial step toward achieving a comprehensive understanding of watershed dynamics and agricultural decision-making processes (Liu et al., 2008). By combining the insights gained from the farmers' behavioral model with the SWAT+ hydrological model, we aim to develop an integrated framework that bridges the gap between policy interventions and on-the-ground agricultural practices (Du et al., 2020). By analyzing farmers' willingness to adopt these practices (cover crops and reduced N-rate application) based on the incentives offered (standard EQIP cost share rates), we aim to estimate the extent of land conversion for cover crops and reduced fertilizer application. This integration allows us to assess the effectiveness of incentive programs in promoting sustainable agricultural practices and inform policymaking for environmental conservation (Cheng & Li, 2015).

Table 3b.2 outlines seven distinct scenarios simulated in this study. Scenario 1 serves as the baseline, involving no implementation of additional Best Management Practices (BMPs). Utilizing the findings from Scenario 1, we identified the top 12% of Hydrological Response Units (HRUs) for highest agricultural surface nitrate export for Scenarios 2 and 4, as well as the top 24% of HRUs for highest agricultural surface nitrate export for Scenarios 3 and 5. From an engineering perspective, these HRUs are considered the most optimal areas for BMP deployment to minimize the watershed's nitrate export effectively (Sheshukov et al., 2016).

Scenarios 2, 3, and 6 explore the impacts of cover crops, while Scenarios 4, 5, and 7 examine the effects of a 30% reduction in N-fertilizer application rates across varying percentages of the Tar-Pamlico watershed. Scenarios 2-5 provide conservation contracts at current EQIP rates ($50 per acre for N reduction, $75 per acre for cover crops) and simulate perfect adoption and land use change in the targeted HRUs. Scenarios 6 and 7 similarly offer the same conservation contracts to the same targeted HRUs but use a farmer behavioral model to predict the proportion of farmers who will accept the offer and consequently, what percentage of HRUs will be converted. A comprehensive cost-benefit analysis was conducted to assess the expenditure associated with implementing these practices and the benefits gained through nitrogen loss reduction.

**Table 3b.2** Policy scenarios for hydrological and socio-hydrological modeling

| Policy Scenario | Type of model | Description |
|---|---|---|
| Scenario 1 | Hydrological Model | Baseline |
| Scenario 2 | Hydrological Model | Cover crops applied on 12% of the total agricultural land |
| Scenario 3 | Hydrological Model | Cover crops applied on 24% of the total agricultural land |
| Scenario 4 | Hydrological Model | 30% reduced N fertilizer application on 12% of the agricultural area |
| Scenario 5 | Hydrological Model | 30% reduced N fertilizer application on 24% of the agricultural area |
| Scenario 6 | Socio-Hydrological Model | Cover crops applied to areas based on the farmers' behavior model. |
| Scenario 7 | Socio-Hydrological Model | 30% reduced N fertilizer application to areas based on the farmers' behavior model. |

## 3. Results and Discussion

### 3.1. SWAT+ model optimization

In this study, we evaluated the performance of the model for simulating monthly nitrate load at the Washington, NC station over two distinct periods (Figure 3b.3), a calibration period from 2003 to 2011 and a validation period from 2012 to 2019. The model's ability to simulate nitrate loads similar to the observed values was assessed using three key performance indices: Nash-Sutcliffe Efficiency (NSE), the Coefficient of Determination ($R^2$), and the Kling-Gupta Efficiency (KGE). During the calibration period, the model demonstrated a good level of accuracy in simulating nitrate loads, considering Tar-Pamlico is a coastal watershed (Upadhyay et al., 2022), achieving an NSE of 0.61, an $R^2$ of 0.61, and a KGE of 0.77. These metrics indicate a strong agreement between the observed and simulated data, suggesting that the model is well-calibrated and capable of capturing the key dynamics governing nitrate transport and retention within the Tar-Pamlico watershed (Upadhyay et al., 2022).

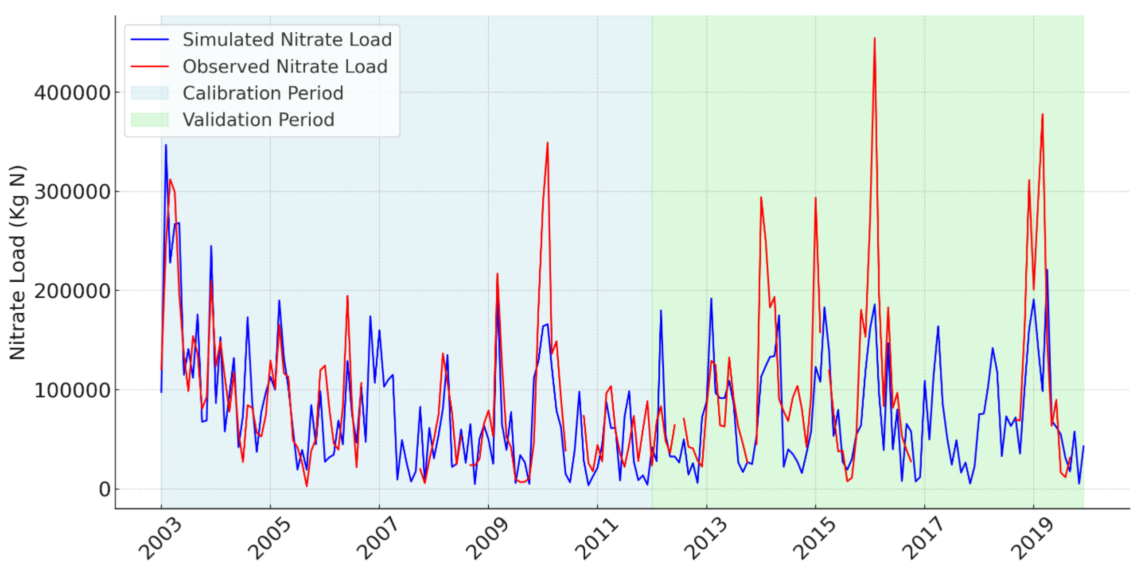


**Figure 3b.3** Simulated and observed nitrate load for calibration and validation

For the validation period, the performance indices indicated a moderate level of model accuracy, with an NSE of 0.33, an $R^2$ of 0.33, and a KGE of 0.39. While these values are lower than those observed during the calibration period, they still demonstrate the model's capacity to provide reasonable nitrate load predictions under varying conditions. The decline in performance indices during the validation period was likely due to uncertainties associated with the reduced frequency of observed data from 2012 to 2019 (Birgand et al., 2011). After 2010, the frequency of nitrate concentration sampling by NCDEQ shifted from daily to monthly. Between January 2003 and December 2011, a total of 1,134 nitrate concentration measurements were collected, compared to only 88 data points during the validation period from January 2012 to December 2019.

### 3.2. Farmers Behavioral Modeling:

The results from the mixed logit model (Table 3b.3), based on 76 farmer survey responses, demonstrate statistically significant factors that influence farmers' choices regarding conservation contracts. Notably, the payment variable (Coef. = 0.0321, $P < 0.000$) indicates that money is a highly significant factor in the farmer's decision to choose a conservation contract. Higher payment rates increase farmer utility and the probability of farmers accepting these contracts. This finding underscores the importance of financial incentives in promoting widespread conservation practices among farmers. The status-quo, or no contract, alternative specific constant (ASC) is also significant (Coef. = 3.161, $P = 0.003$), suggesting a general bias among farmers against choosing a conservation contract.

Table 3b.3: Mixed Logit Model Results

| Variable | Coefficient | Standard Error | z-value | P-value | 95% Confidence Interval |
|---|---|---|---|---|---|
| **Mean** | | | | | |
| State funding presence | .0108 | .535 | 0.02 | 0.984 | -1.037, 1.059 |
| Payment rate ($) | .032 | .009 | 3.54 | 0.000 | 0.014, 0.050 |
| Strict nitrogen regulation (lb/ acre) | -2.134 | .869 | -2.45 | 0.014 | -3.838, -0.430 |
| Lenient nitrogen regulation (lb/ acre) | -1.11 | .873 | -1.27 | 0.203 | -2.824, 0.599 |
| Alternative specific constant | 3.161 | 1.046 | 3.02 | 0.003 | 1.111, 5.211 |
| Cover crops utilization | -.845 | .971 | -0.87 | 0.384 | -2.749, 1.059 |
| **Standard Deviation** | | | | | |
| Alternative specific constant | 3.35731 | 1.188573 | 2.82 | 0.005 | 1.028, 5.687 |
| Cover crops utilization | 2.849883 | 1.294219 | 2.20 | 0.028 | 0.313, 5.387 |

Conversely, the coefficient for the dummy variable representing strict nitrogen application limits (StrictNitrogenRegulation, Coef. = -2.134354, P = 0.014) is negative and statistically significant, indicating that contracts with stringent nitrogen application restrictions are less likely to be chosen by farmers. This result may highlight concerns among farmers about the feasibility or economic implications of significantly reducing nitrogen use on their crops. The standard deviations for ASC (SD = 3.357, P = 0.005) and cover crops (SD = 2.8499, P = 0.028) are significant, illustrating variability in farmers' preferences for these contract attributes. This heterogeneity suggests that while some farmers may be more inclined towards contracts that include these features, others may have a strong preference against them, highlighting the need for flexible policy designs to accommodate diverse farmer preferences (Howard et al., 2024). Although some of the management practice attributes do not achieve statistical significance, all mean coefficient estimates maintain the expected negative sign. This indicates that, all else equal, farmers are reluctant to implement these practices. Notably, the negative coefficient for strict nitrogen (N) limits is larger than that for lenient N limits, aligning with expectations that stricter regulations are less appealing (Howard et al., 2024). Additionally, the high p-values associated with some coefficients may be attributable to the small sample sizes involved in the study. Indeed, we see that, while cover crops are not the norm across fields, 11.7% of our sample report using cover crops currently, and in other watersheds cover crops are voluntarily adopted by a minority of farmers (Burnett et al., 2015).

In contrast, the variable representing state funding (dummystatefunding, Coef. = .0107, P = 0.984) is not statistically significant, suggesting that this factor does not have a discernible impact on farmers' contract choices within the context of this model. Overall, these results indicate that financial incentives and the specifics of conservation practices (such as nitrogen application limits) play crucial roles in influencing farmers' decisions to participate in conservation programs. The heterogeneity in preferences highlighted by the significant standard deviations underscores the importance of designing flexible conservation programs that can cater to a wide range of farmer needs and concerns (Howard et al., 2024).

In the simulation for strict nitrogen (N) restriction policies under the current EQIP rate of $50 per acre or $123.5 per Ha, our analysis reveals a modest enrollment projection. Based on the mixed logit model's outcome and subsequent simulations, it is estimated that only 3.75% of the farmers in our sample would opt to participate in a policy that mandates strict nitrogen application limits under current EQIP rates. The process involved calculating the WTA strict N restrictions at or below a $123.5 per Ha rate, then aggregating the total area farmers are willing to enroll under such conditions. The low percentage of potential enrollees underscores a cautious or reluctant stance among farmers toward adopting strict nitrogen application limits, even when incentivized.

The analysis regarding the adoption of cover crops under the current Environmental Quality Incentives Program (EQIP) rates reveals a more optimistic participation forecast compared to strict nitrogen restrictions. Our simulation indicates that approximately 26.2% of farmers would be willing to enroll in a policy promoting cover crop practices when the WTA threshold is set at or below $75 per acre, or $185.3 per Ha. However, our model suggests that not all of those who enroll in the conservation program would count as new or additional acreage in the practice. While we see a contract acceptance rate of 26.23%, some of these farmers report already utilizing cover crops in the past, so our prediction for the increase in new acreage of the management practice is a more modest 14.5%. This higher inclination towards cover crop adoption suggests that, unlike strict nitrogen application restrictions, farmers perceive cover cropping as a more viable and potentially beneficial conservation practice under the EQIP framework. The significant difference in enrollment projections between these two conservation practices underscores the need for tailored incentive structures that reflect the varying levels of farmer receptivity and the distinct environmental benefits each practice offers (Rossi & Hinrichs, 2011).

Understanding the preferences, constraints, and incentives that influence farmers' decisions to adopt conservation practices is vital for designing effective environmental policies (Liu et al., 2018). These behavioral insights serve as foundational components for simulating policies using hydrological models, ensuring that such models reflect realistic agricultural management scenarios (Kuil et al., 2018).

### 3.3. Effects of reduced N-fertilizer application rate and cover crops on watershed processes and N-load.

#### 3.3.1. Effects of 30% reduced fertilizer application on nitrate load

The effect of a 30 percent reduction in fertilizer application across varying percentages of agricultural land on the total nitrate load at Pamlico Estuary and Washington, NC, for engineering models scenarios is shown in Figure 3b.4.

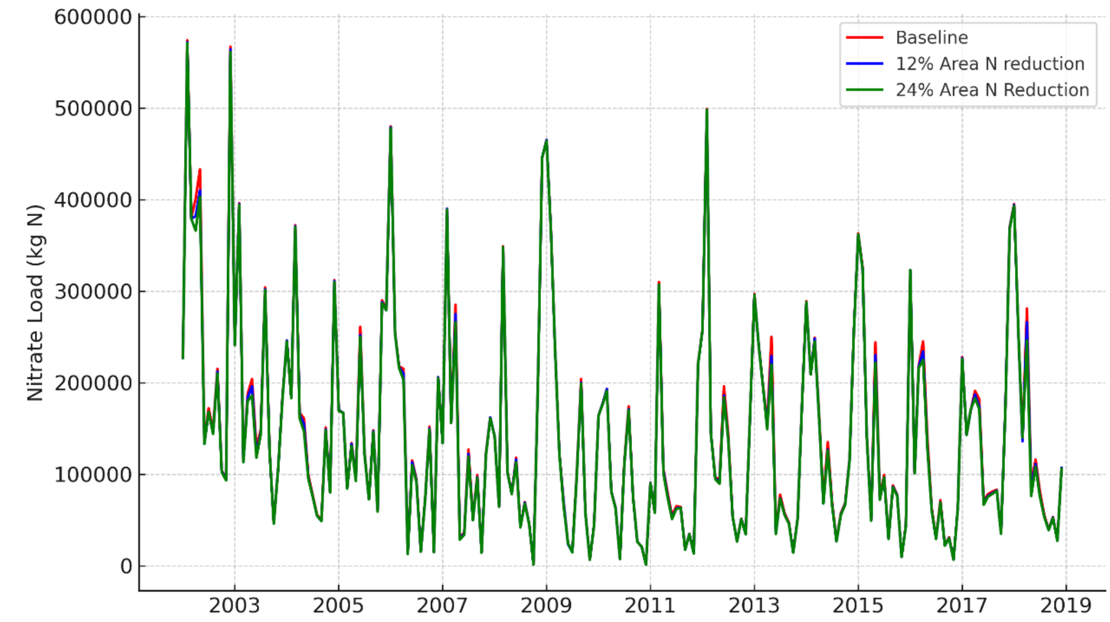


**Figure 3b.4** Effects of reduced fertilizer on nitrate load for the baseline, 12% (scenario 4), and 24% (scenario 5) of total agricultural area in the watershed

At the Pamlico Estuary, the winter season exhibits the highest nitrate loads across the baseline, scenario 4, and scenario 5 (Table 3b.4). In the spring, nitrate loads remain elevated, suggesting significant seasonal runoff (Table 3b.4) and greater nitrate availability from agricultural activity (Bruland et al., 2003). The fall and summer seasons show comparatively lower nitrate loads. As the area with reduced nitrogen fertilization expands, there is a noticeable decrease in nitrate loading, most prominently in the spring and winter seasons. This underscores the potential effectiveness of nitrogen management strategies during periods of increased runoff (Table 3b.4).

In Washington, NC, similar patterns are observed, although with overall lower nitrate loads than the Pamlico Estuary (Table 3b.4). The spring season shows the highest loads, followed by winter, with noticeable reductions in nitrate loading as the area of nitrogen reduction increases.

The least variation across scenarios is seen in summer, suggesting a more stable nitrate input during this season. The more stable nitrate input during summer in Washington, NC, is likely due to consistent agricultural practices, less intense rainfall, increased biological uptake by plants, and more uniform water flows, leading to lower variability in nitrate levels (Dukes & Evans, 2006) across multiple scenarios (Table 3b.4).

**Table 3b.4** Seasonal average flow and nitrate load (Kg N) with reduced fertilizer application rate

| Location | Season | Baseline | 12% Area N reduction | 24% Area N Reduction | Flow ($m^3s^{-1}$) |
|---|---|---|---|---|---|
| Pamlico Estuary | Fall | 221,900 | 219,700 | 218,100 | 116 |
| | Spring | 527,700 | 515,200 | 506,100 | 124 |
| | Summer | 274,400 | 266,700 | 264,100 | 89 |
| | Winter | 736,300 | 734,600 | 733,100 | 155 |
| Washington, NC | Fall | 138,300 | 136,800 | 135,600 | 57 |
| | Spring | 331,100 | 325,100 | 315,100 | 87 |
| | Summer | 158,900 | 155,700 | 154,200 | 44 |
| | Winter | 290,600 | 289,100 | 287,800 | 94 |

To determine if the nitrate loading under all three scenarios (Baseline, scenario 4, and scenario 5) at the Pamlico Estuary are statistically different from each other, we performed an Analysis of Variance (ANOVA) on monthly nitrate load at Pamlico estuary (Table 3b.5). ANOVA is a statistical method used to compare the means of three or more samples to see if at least one of them differs significantly from the others. If the p-value from the ANOVA test is less than a significance level (0.05), we can reject the null hypothesis that all groups have the same mean, suggesting that at least one scenario differs in terms of nitrate loading (St & Wold, 1989).

**Table 3b.5** Reduced fertilizer application ANOVA (single factor) test at Pamlico estuary

SUMMARY

| *Groups* | *Count* | *Sum* | *Average* | *Variance* |
|---|---|---|---|---|
| Baseline | 204 | 29923200 | 146682.3529 | 13625690057 |
| Scenario-4 | 204 | 29514920 | 144680.9804 | 13416121673 |
| Scenario-5 | 204 | 29263940 | 143450.6863 | 13284143139 |

ANOVA

| *Source of Variation* | *SS* | *df* | *MS* | *F* | *P-value* | *F crit* |
|---|---|---|---|---|---|---|
| Between Groups | 1085469390 | 2 | 542734694.8 | 0.040376083 | 0.960431 | 3.01051703 |
| Within Groups | 8.18617E+12 | 609 | 13441984956 | | | |
| Total | 8.18725E+12 | 611 | | | | |

The ANOVA test yielded a p-value of 0.96, which is much greater than the significance level of 0.05. This result indicates that we cannot reject the null hypothesis, suggesting there is not enough statistical evidence (St & Wold, 1989) to say that the mean monthly nitrate loading under the four scenarios at the Pamlico Estuary are significantly different from each other.

It's important to note that while the ANOVA test provides insight into the overall differences across groups, it doesn't specify which groups differ from each other (St & Wold, 1989). However, in this case, the high p-value suggests that the differences in mean nitrate loading between the scenarios are likely not to be significant.

Despite implementing nitrogen reduction strategies across 12%, and 24% areas, the analysis suggests that these measures, within the scope of the study, do not significantly alter the mean monthly nitrate loading when compared to the baseline scenario with no nitrogen reduction (Table 3b.5). The lack of statistically significant differences in nitrate loading under various nitrogen reduction scenarios at the Pamlico Estuary could be attributed to several factors (Barker et al., 2008).

This outcome may indicate that the predominant sources of nitrate loading in the Pamlico Estuary are not primarily agricultural runoff, or that the scale of reduction explored in the scenarios is insufficient to manifest a statistically significant impact given the natural variability of nitrate loading and other contributing factors. Additionally, excessive nitrate leaching from groundwater, possibly from legacy nitrate, could be contributing significantly to the observed levels. The effectiveness of nitrogen reduction strategies might also be influenced by the spatial distribution of runoff sources and the timing of nitrogen applications in agricultural practices (Craswell, 2021).

### 3.3.2. Effects of Cover Crops on Nitrate Load

The results from multiple scenarios reflecting varying degrees of cover crop implementation, aimed at reducing nitrate export to the estuary are shown in Figure 3b.5.

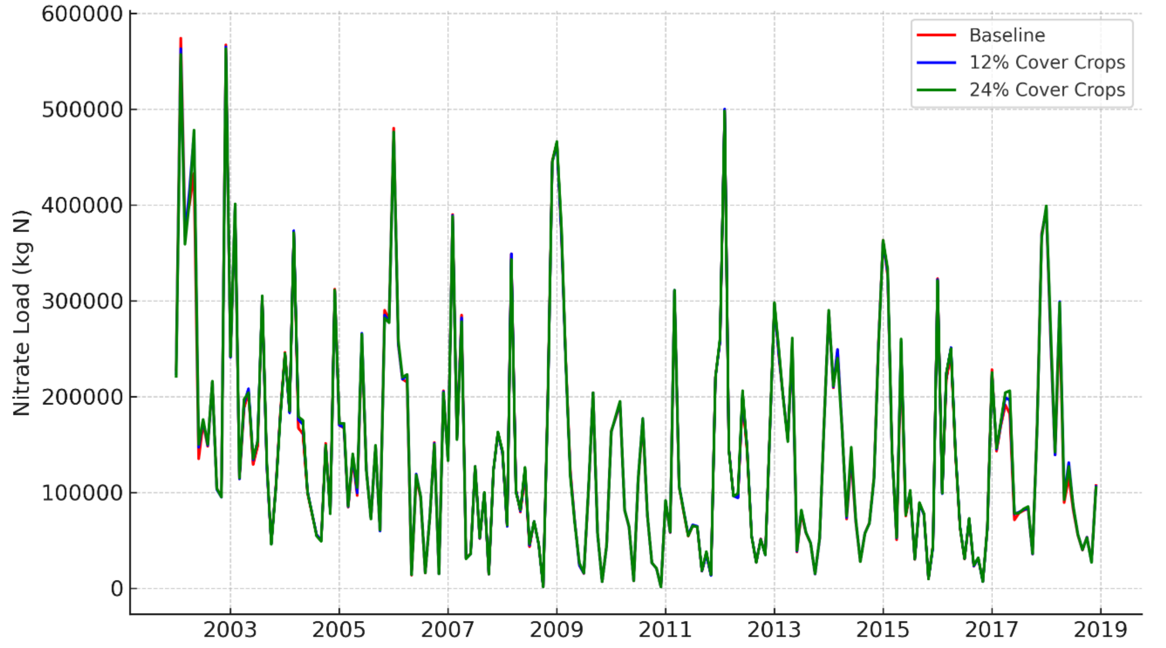


**Figure 3b.5** Effects of reduced fertilizer on monthly nitrate load to the Pamlico estuary for the baseline, 12% (scenario 2), and 24% (scenario 3) coverage with cover crops.

The seasonal average nitrate loads (kg N) under varying cover crop scenarios were assessed at two locations: Pamlico Estuary and Washington, NC (Table 3b.6). In the Pamlico Estuary, winter consistently showed the highest nitrate loads (734,200 to 734,700 kg N) in each scenario, suggesting higher discharge (120 $m^3/s$). Contrary to expectations, the decrease in nitrate loading with the expansion of cover crop areas is not universally observed. For instance, during the spring, an increase in nitrate loads (537,600 kg N) was noted with the highest cover crop coverage (scenario 3, 24% area application of cover crops) compared to the baseline (527,700 kg N), challenging the presumption of uniform effectiveness of cover crops in nitrate load reduction across seasons. For Washington, NC, while echoing a similar trend of high nitrate loads in the spring (327,600 to 331,100 kg N) and winter (288,100 to 290,600 kg N), also underscores a more nuanced response to increased cover crop adoption. The changes in nitrate loading with varying cover crop scenarios were modest, suggesting that the cover crops' role in mitigating nitrate runoff is complex and influenced by many factors (Craswell, 2021).

**Table 3b.6** Seasonal variation of flow and nitrate load (kg N) with cover crops

| Location | Season | Baseline | 12% Cover Crops | 24% Cover Crops | Flow ($m^3$ $s^{-1}$) |
|---|---|---|---|---|---|
| Pamlico Estuary | Fall | 221,900 | 220,600 | 221,400 | 116 |
| | Spring | 527,700 | 537,200 | 537,600 | 124 |
| | Summer | 274,400 | 281,000 | 281,900 | 89 |
| | Winter | 736,300 | 734,200 | 736,700 | 155 |
| Washington, NC | Fall | 138,300 | 138,000 | 137,800 | 57 |
| | Spring | 331,100 | 327,600 | 328,000 | 87 |
| | Summer | 158,900 | 158,700 | 159,200 | 44 |
| | Winter | 290,600 | 288,100 | 289,100 | 94 |

To assess whether the monthly nitrate loading under all four scenarios (Baseline, 12% (scenario 2) Cover Crops, and 24% (scenario 3) Cover Crops) at the Pamlico Estuary significantly differs, we conducted an Analysis of Variance (ANOVA) (Table 3b.7). For cover crop application, the ANOVA test yielded a p-value of 0.991, significantly greater than the significance level of 0.05.

This result indicates that we cannot reject the null hypothesis, suggesting there is not enough statistical evidence to assert that the average monthly nitrate loading under the three scenarios (baseline, 12% cover crops (scenario 2), and 24% (scenario 3) cover crops) at the Pamlico Estuary are significantly different from each other (Table 3b.7).

**Table 3b.7** Summary of ANOVA results for cover crop scenarios

| **ANOVA: Single Factor** | | | | | | |
|---|---|---|---|---|---|---|
| **SUMMARY** | | | | | | |
| **Groups** | Count | Sum | Average | Variance | | |
| **Baseline** | 204 | 29923200 | 146682.4 | 1.36E+10 | | |
| **Scenario-2** | 204 | 30140350 | 147746.8 | 1.37E+10 | | |
| **Scenario-3** | 204 | 30218900 | 148131.9 | 1.37E+10 | | |
| **Source of Variation** | SS | df | MS | F | p-value | F crit |
| **Between Groups** | 2.3E+08 | 2 | 1.15E+08 | 0.008407 | 0.991628 | 3.010517 |
| **Within Groups** | 8.33E+12 | 609 | 1.37E+10 | | | |
| **Total** | 8.33E+12 | 611 | | | | |

While the ANOVA test identifies overall differences across groups, it does not specify which groups, if any, differ from one another (St & Wold, 1989). However, the high p-value suggests that any differences in mean monthly nitrate loading among the various cover crop scenarios are likely not significant. This is further underscored by the detailed summary and ANOVA table (Table 3b.7), which provide counts, sums, averages, and variances for each scenario. Despite minor variations in average nitrate loads, these do not amount to statistically significant differences, as evidenced by the Between Groups sum of squares (SS) of 230004436, a within-groups SS exceeding 8.3 trillion, and a notably small F-value of 0.00841 against an F critical value of 3.0105.

This comprehensive analysis highlights that the variance observed within groups significantly overshadows any minor differences between the groups (St & Wold, 1989). Such a conclusion might indicate that the scale of cover crop implementation explored in the scenarios is insufficient to establish a statistically significant impact on nitrate loading or winter wheat as a cover crop may not be efficient in reducing nitrate loss from agricultural fields (Kaspar et al., 2012; Ritter et al., 1998). It could also that the effectiveness of cover crop strategies might be influenced by factors such as the spatial distribution of runoff sources, the timing of cover crop planting, and management practices, as well as the presence of other nitrogen sources beyond agricultural runoff (Kaspar et al., 2012).

The introduction of winter wheat as a cover crop could elevate nitrate loads due to several interconnected factors (Nouri et al., 2022). The growth cycle of winter wheat, particularly its dormant phase during early winter, may not align well with the timing of nitrate assimilation and soil nitrogen release (Anthoni et al., 2004; Footitt et al., 2014). This misalignment can lead to periods where nitrate, unutilized by the cover crop, becomes prone to leaching during the region's heavy rainfall events, thereby contributing to increased nitrate loads in the watershed (Cordovil et al., 2020; Robertson & Vitousek, 2009). This issue is compounded by the decomposition of winter wheat post-harvest, which can release nitrogen back into the soil, subsequently increasing loss to downstream waters. Furthermore, winter wheat's efficiency in nitrogen uptake might be compromised by environmental conditions and management practices, leaving unused nitrate to leach into the Tar-Pamlico basin. Soil disturbance from the planting and termination of winter wheat exacerbates this problem by disrupting soil structure and potentially enhancing nitrate mobility (McGuire et al., 1998; Moore et al., 2019).

This analysis clearly demonstrates that the relationship between cover crop coverage and nitrate load is multifaceted, reflecting the influence of environmental conditions, management practices, and the inherent characteristics of the watershed (Bindraban et al., 2012; Neumann et al., 2021; Smith et al., 2019). It suggests that even while the literature suggests cover crops are efficient in nutrient (nitrate) management strategies, their effectiveness is conditional, necessitating a tailored approach based on watershed characteristics (Bindraban et al., 2012; Neumann et al., 2021). This calls for continued research to identify the optimal conditions under which cover crops can most effectively contribute to water quality improvement in agricultural landscapes, underscoring the importance of an integrated approach to nutrient management.

### 3.4. Hydrological and Socio-Hydrological Model Comparison

The model simulated minimal variation in nitrate load at the outlet point for multiple BMP scenarios, as detailed in section 3.3. Consequently, we conducted a comparison of Hydrological and Socio-Hydrological models at the field scale. In SWAT+, each field is contained in an HRU with fields of the same crop, management practices, soil type, and slope. Therefore, we compared the nitrate levels leaving the agricultural fields under seven different scenarios at the HRU scale, as shown in Table 3b.8. In this section, we present the economic and environmental implications of cover crop and reduced fertilizer application rate conservation contracts through the use of the hydrological model with naive assumptions of contract adoption (i.e. typical engineering approach) and the Socio-Hydrological model with adoption informed by the farmer behavioral model.

**Table 3b.8** Cost-benefit analysis of different engineering and econometric scenarios

| Policy Scenarios | Additional Area Converted ($km^2$) | Total Budget Spent in million dollars ($) | Area Enrolled ($km^2$) | Total annual average $NO_3$-N (kg) from agriculture | Change total annual average $NO_3$-N (kg) from agriculture | Change in nitrate per enrolled area (kg $km^{-2}$) | Benefit per enrolled area ($ $km^{-2}$) | Benefit-cost ratio |
|---|---|---|---|---|---|---|---|---|
| | | Cover crop ($75 per acre or 18500 per $km^2$) Strict N application ($50 per Acre or $12300 per $km^2$) | | | | | $20.9 per kg (Ribaudo et al., 2005) | |
| Scenario 1 | 0 | 0 | 0 | 1,013,000 | | | | |
| Scenario 2 | 606 | 11.2 | 606 | 958,000 | 55,000 | 91.3 | 1,907 | 0.103 |
| Scenario 3 | 1,212 | 22.4 | 1,212 | 957,000 | 56,000 | 46.5 | 971 | 0.053 |
| Scenario 4 | 606 | 7.4 | 606 | 968,000 | 46,000 | 75.2 | 1,571 | 0.128 |
| Scenario 5 | 1,212 | 15 | 1,212 | 940,000 | 73,000 | 60.5 | 1,265 | 0.103 |
| Scenario 6 | 206 | 3.8 | 319 | 1,024,000 | -11,000 | -33 | -700 | -0.038 |
| Scenario 7 | 46 | 0.6 | 46 | 1,009,000 | 4,000 | 97.3 | 2,033 | 0.165 |

In the context of the hydrological modeling scenarios detailed in the analysis, the 12% and 24% coverage figures represent the total percentage of agricultural land targeted for intervention, assuming that all the farmland in these areas will agree to the offered conservation contract and implement the specified land management practices. This assumption underpins the theoretical maximum impact of the agricultural practices under consideration but may not align with real-world applications. We used farmers' behavioral model results (section 3.2) to develop the socio-hydrological model. In the socio-hydrological model, 3.75% (reduced fertilizer application rate), 14.5% (additional cover crops applied), and 26.2% (total farmland enrolled for cover crops) reflect the actual proportion of farmers willing to adopt these specific practices, based on informed econometric analysis under standard EQIP cost-share rates.

The engineering approach (scenarios 2 through 5) assumed these areas would be targeted and all the farmers in this area would implement the conservation practices. Assuming that all farmers in a targeted area will adopt conservation practices can be overly optimistic, as it overlooks individual differences in economic circumstances, willingness, and ability to change (Howard et al., 2024). Integrating a farmers' behavioral model into the planning process can provide more realistic predictions by accounting for these variations in behavior and receptivity, thereby enhancing the effectiveness and efficiency of policy implementation (Howard et al., 2024). Thus, for the socio-hydrological model implementation, these percentages are calculated relative to the 24% of agricultural land targeted in the hydrological scenarios. This means 3.75%, 14.5%, and 26.2% farmers of 24% of total selected agricultural HRUs will implement these practices on their fields for reduced fertilizer application rate, additional cover crops applied, and total farmland enrolled for cover crops, respectively. In other words, of the targeted farmers (24%), only 3.75% would implement reduced fertilizer application making the practice implemented on 0.9% of the agricultural land in the watershed. This differentiation in percentage base points—from theoretical maximum to likely practical application—highlights the critical need to consider both the absolute and relative scales when assessing the adoption and effectiveness of various agricultural and environmental practices. The socio-hydrological modeling thus provides a more realistic estimate of the area that would actually be converted to the new practices, bridging the gap between theoretical planning and actual implementation (Howard et al., 2024).

### 3.4.1 Area Conversion and Budget Allocation:

The baseline scenario operates with no additional cost and no area conversion, serving as a control for comparing Hydrological and Socio-Hydrological modeling scenarios for cover crops and reduced fertilizer application rate (Table 3b.2).

Introducing cover crops on 12% of the agricultural lands in the watershed entails an expenditure of approximately \$11.2 million (considering the current EQIP rate for cover crops of \$185.3 $ha^{-1}$) and affects over 606 $km^2$. Doubling this coverage to 24% doubles the budget to about \$22.5 million and covers over 1200 $km^2$. In contrast, a strategy focusing on a 30% reduction in nitrogen usage over a similar area demands a lesser budget of around \$7.5 million (considering the current EQIP rate for strict N application of \$123.5 $ha^{-1}$). Based on the enrollment projections from the socio-hydrological modeling scenarios involving cover crops and strict nitrogen (N) application under current EQIP rates, the area converted within the targeted agricultural lands amounts to over 206 $km^2$ for cover crops and over 45 $km^2$ for nitrogen application. Correspondingly, the budgets allocated are more modest \$3.8 million for cover crops and \$0.6 million for nitrogen application.

3.4.2. Agricultural Output and Environmental Impact:

To examine the effect of the practices at the field scale we summed the cumulative annual average agricultural nitrate loss (including surface, lateral, and groundwater nitrate) in kg from the agricultural areas (HRU scale) in the Tar-Pamlico basin where the practices were implemented. To compare the hydrological and socio-hydrological models, we considered only the 24% agricultural area (as used in scenarios 3 and 5) to determine the cumulative annual average nitrate loss from agricultural fields in all scenarios as mentioned in section 2.4.

The baseline scenario maintains agricultural nitrate-nitrogen export at approximately 1,010,000 kg without any interventions, serving as a reference for comparing various conservation strategies. Introducing cover crops across 12% and 24% of the agricultural areas (Scenarios 2 and 3) reduces output slightly to 958,000 kg and 957,000 kg, respectively, which is a reduction of 55,300 and 56,300 kg of nitrate-nitrogen respectively. The extension of these strategies demonstrates the environmental impact of scaling up sustainable practices. In Scenarios 4 and 5, strict fertilizer reduction strategies applied over 12% and 24% of the agricultural areas further influence export, which decreases to 967,800 kg and 935,500 kg, respectively. These changes result in nitrate-nitrogen reductions of 45,600 kg and 77,900 kg, showing the positive environmental effects of reduced nitrogen usage across varying scales. These changes highlight the tradeoff in the farmers' decision between decreased agricultural output, improved water quality, and additional payment as part of the agricultural assistance program.

In Scenario 6, cover crops were applied to an additional 207 $km^2$, bringing the total area under this practice to 319 $km^2$ square meters as part of the Environmental Quality Incentives Program (EQIP). This expansion was guided by a farmers' behavioral model, which suggested practical implementations based on actual farming practices. Implementing cover crops over this extended area resulted in agricultural nitrate-nitrogen export of 1,020,100 kg and a slight increase in nitrate levels by 10,600 kg. This scenario highlighted that even if the theoretical implementation of cover crops reduced nitrogen load by targeting specific agricultural fields (HRU), it might not have been possible in the real world. Engineering models specifically target HRUs that exhibit higher surface nitrate exports, predicting that cover crops in these areas would effectively reduce nitrate loads (scenario 2 & 3). However, when incorporating farmers' behavioral models, the selection of HRUs isn't solely based on nitrate export levels, which means cover crops might be applied to fields where they are less effective at reducing nitrates, as was observed in scenario 6. The effectiveness of winter wheat when used as cover crops varied based on the location it was applied to, which crops were planted on that field as the main summer cash crop, soil conditions, rainfall, elevation, and other characteristics (Kaspar et al., 2012; Ritter et al., 1998). This discrepancy highlights the potential limitations of applying naive hydrological models without considering the practical and behavioral dynamics of the farmers.

In Scenario 7, a strict fertilizer application strategy is employed over an area representing 3.75% of the land managed by farmers willing to adopt this practice, as informed by a behavioral model. This approach reduces the agricultural nitrate loss to 1,009,000 kg by decreasing the nitrate load by 4,400 kg. This demonstrates the positive environmental impact of reducing nitrogen usage.

### 3.4.3 Economic Efficiency:

The benefit-cost analysis across the seven scenarios illustrates varying degrees of economic efficiency, highlighting the effectiveness and cost implications of each agricultural strategy implemented (Table 3b.8). To calculate the benefits for each scenario, we multiply the reduction in nitrogen (N) by the estimated social damages of $20.90 for each additional kilogram of N leaving the farm (Ribaudo et al., 2005).

In the baseline scenario (Scenario 1), no interventions are implemented, thus there is no benefit-cost ratio, serving as a control for comparative purposes. For scenarios involving cover crops, Scenario 2 (12% Cover Crop Application) achieves a benefit-cost ratio of 0.103, indicating a moderate return on investment. This efficiency drops significantly in Scenario 3 (24% Cover Crop Application) to a ratio of 0.052, demonstrating declining returns as the scale of cover crop application increases. This result was expected, as we targeted HRUs in sequence according to their nitrate loss in the hydrological modeling scenarios.

In terms of nitrogen management, Scenario 4 (30% Nitrogen Reduction over 12% Area) shows the highest benefit-cost ratio among the initial assessments at 0.128, suggesting that targeted nitrogen reduction is environmentally beneficial. Expanding this approach to a larger area in Scenario 5 (30% Nitrogen Reduction over 24% Area) yields a lower ratio of 0.1028, indicating reduced economic efficiency at a larger scale because of targeted HRU practice implementation in hydrological modeling scenarios.

Scenario 7 (Strict Fertilizer Application over 3.75% Area), informed by a model of farmer behavior, shows a modest increase in the benefit-cost ratio to 0.165. However, this rise from a previous low of 0.05 is still considered suboptimal. More significantly, the disparity between the hydrological model's predicted benefits for a 24% nitrogen reduction (65,300 kg) and the much lower actual benefits observed in the socio-hydrological model (4,400 kg), which amount to only about 6.8% of the expected reduction, suggests that the hydrological model may greatly overestimate the efficacy of the policy. This overestimation might stem from the model's assumption that farmers uniformly adopt and effectively implement BMPs, whereas in reality, achieving targeted intervention could be challenging and costly, with varying levels of adoption among farmers (Howard et al., 2024). This analysis confirms that while larger-scale interventions may achieve significant environmental impacts, their economic viability can vary, often requiring more nuanced, targeted approaches to maximize both ecological and economic benefits in agricultural policymaking.

## 4. Conclusions

This study offers significant insights into the complexities of managing nutrient loading in coastal watersheds through the integration of socio-hydrological modeling with farmers' behavioral responses. The innovative approach of combining economic and engineering frameworks to address accelerated eutrophication reveals several key findings from the study, offering important considerations for policy and practice.

**Socio-economic Dynamics of Agricultural Practice Adoption:** Integrating farmers' behavioral models into hydrological modeling efforts provided valuable insights into the socio-economic dynamics influencing the adoption of sustainable agricultural practices. The study demonstrated the importance (and limitations) of economic incentives in promoting BMP adoption among farmers, as evidenced by the farmers' willingness to accept (WTA) different practices and the highly significant impact of payment level on contract acceptance. However, the relatively low willingness to adopt strict nitrogen application limits, even with incentives, points to the challenges of changing farming practices and the need for policies that are both economically viable for farmers and effective in environmental protection.

**Limited Impact of Best Management Practices (BMPs) on Nitrate Loading:** The simulation results using the SWAT+ model show that, under the scenarios modeled, both cover crops and reduced nitrogen application rates did not significantly reduce nitrate loading to the Pamlico

Estuary. These outcomes highlight the challenge of achieving measurable improvements in water quality through isolated BMPs at the watershed scale, suggesting that the scale and scope of the BMPs modeled may be insufficient for significant nitrate load reduction.

**Hydrological Models Overestimate Policy Benefits:** Our approach to implementing BMPs in the hydrological models significantly overestimate the benefits of nitrogen reduction policies, predicting a reduction that is 15 times higher than what is actually achieved—a discrepancy where only 6.8% of the expected benefits are realized. This highlights the critical need for models to integrate socio-economic dynamics and farmer behaviors to enhance the accuracy and effectiveness of agricultural environmental policies.

**Identifying diverse sources of nitrate in coastal watersheds:** Our findings reveal the complexity of nutrient transport, suggesting that agricultural practices may not be the main source of nitrate in coastal watersheds. Effective nutrient management calls for a multifaceted approach that goes beyond traditional agricultural BMPs, incorporating considerations of alternative sources such as groundwater and legacy nitrate.

**Importance of Interdisciplinary Approaches:** This research underscores the value of interdisciplinary approaches in tackling complex environmental issues like accelerated eutrophication. By bridging econometric and engineering disciplines, the study provides a comprehensive perspective on the challenges and opportunities for implementing sustainable agricultural practices, emphasizing the need for collaboration across scientific, policy, and farming communities to develop and implement effective strategies.

**Future Directions for Research and Policy:** The study highlights several areas for further research, including the exploration of alternative BMPs, the integration of additional socio-economic factors into modeling efforts, and the examination of the cumulative effects of combined BMPs at larger scales. Policymakers are encouraged to consider these findings in the development of agricultural and environmental policies, recognizing the critical role of economic incentives, farmer engagement, and integrated management strategies in improving ecosystem health.

Lastly, while the study's findings indicate that the modeled BMPs alone may not significantly reduce nitrate loading in the Pamlico Estuary, they importantly illuminate the complex interplay between agricultural practices, watershed hydrology, and ecosystem health. These insights contribute valuable knowledge towards developing more effective strategies for combating eutrophication and enhancing the sustainability of agricultural landscapes.

**Appendix 1:** https://github.com/EtheridgeLab/Tar_Pam_SWAT/blob/main/Appendix1.docx

**Acknowledgements:**

This research was made possible with support from the Center for Sustainable Energy and Environmental Engineering and the Integrated Coastal Sciences Program at East Carolina University. Funding was provided by the National Science Foundation [Grant Numbers: 2009185 and 2052889] and the Environmental Protection Agency [Grant Number: R840181].

**Data Availability:**

The data supporting the conclusions of this research are available upon reasonable request from the corresponding author. The majority of the data utilized in this study is open source.

**LLM Statement:**

We utilized ChatGPT to enhance the grammar and sentence structure. Post-editing, we thoroughly reviewed the entire document for accuracy.

**References:**

Anthoni, P. M., Freibauer, A., Kolle, O., & Schulze, E. D. (2004). Winter wheat carbon exchange in Thuringia, Germany. Agricultural and Forest Meteorology, 121(1-2), 55-67.

Bai, T., Li, L., Mu, P. F., Pan, B. Z., & Liu, J. (2023). Impact of climate change on water transfer scale of inter-basin water diversion project. Water Resources Management, 37(6), 2505-2525.

Barker, T., Hatton, K., O'Connor, M., Connor, L., & Moss, B. (2008). Effects of nitrate load on submerged plant biomass and species richness: results of a mesocosm experiment. Fundamental and Applied Limnology, 173(2), 89.

Behboudian, M., Anamaghi, S., Mahjouri, N., & Kerachian, R. (2023). Enhancing the resilience of ecosystem services under extreme events in socio-hydrological systems: a spatio-temporal analysis. Journal of Cleaner Production, 397, 136437.

Bindraban, P. S., van der Velde, M., Ye, L., Van den Berg, M., Materechera, S., Kiba, D. I., ... & van Lynden, G. (2012). Assessing the impact of soil degradation on food production. Current Opinion in Environmental Sustainability, 4(5), 478-488.

Birgand, F., Appelboom, T. W., Chescheir, G. M., & Skaggs, R. W. (2011). Estimating nitrogen, phosphorus, and carbon fluxes in forested and mixed-use watersheds of the lower coastal plain of North Carolina: Uncertainties associated with infrequent sampling. Transactions of the ASABE, 54(6), 2099-2110.

Bruland, G. L., Hanchey, M. F., & Richardson, C. J. (2003). Effects of agriculture and wetland restoration on hydrology, soils, and water quality of a Carolina bay complex. Wetlands Ecology and Management, 11, 141-156.

Burnett, E. A., Wilson, R. S., Roe, B., Howard, G., Irwin, E., Zhang, W., & Martin, J. (2015). Farmers, phosphorus and water quality: Part II. A descriptive report of beliefs, attitudes and best management practices in the Maumee watershed of the western Lake Erie basin. The Ohio State University, School of Environment & Natural Resources, Columbus, OH.

Celikkol Erbas, B., & Guven Solakoglu, E. (2017). In the presence of climate change, the use of fertilizers and the effect of income on agricultural emissions. Sustainability, 9(11), 1989.

Chang, J., Wang, Y., Istanbulluoglu, E., Bai, T., Huang, Q., Yang, D., & Huang, S. (2015). Impact of climate change and human activities on runoff in the Weihe River Basin, China. Quaternary International, 380, 169-179.

Cheng, G., & Li, X. (2015). Integrated research methods in watershed science. Science China Earth Sciences, 58, 1159-1168.

Cherry, K. A., Shepherd, M., Withers, P. J. A., & Mooney, S. J. (2008). Assessing the effectiveness of actions to mitigate nutrient loss from agriculture: A review of methods. Science of the total environment, 406(1-2), 1-23.

Coopersmith, E. J., Minsker, B. S., & Sivapalan, M. (2014). Patterns of regional hydroclimatic shifts: An analysis of changing hydrologic regimes. Water Resources Research, 50(3), 1960-1983.

Cordovil, Cláudia MdS, Shabtai Bittman, Luis M. Brito, Michael J. Goss, Derek Hunt, João Serra, Cameron Gourley et al. (2020) "Climate-resilient and smart agricultural management tools to cope with climate change-induced soil quality decline." In Climate change and soil interactions, pp. 613-662. Elsevier,

Craswell, E. (2021). Fertilizers and nitrate pollution of surface and ground water: an increasingly pervasive global problem. SN Applied Sciences, 3(4), 518.

Cross, T. K., & Summerfelt, R. C. (1986). BOD dynamics in small eutrophic lakes in relation to artificial mixing. Lake and Reservoir Management, 2(1), 286-292.

Dabney, S. M., Delgado, J. A., & Reeves, D. W. (2001). Using winter cover crops to improve soil and water quality. Communications in Soil Science and Plant Analysis, 32(7-8), 1221-1250.

De Bruijn, J. A., Smilovic, M., Burek, P., Guillaumot, L., Wada, Y., & Aerts, J. C. (2023). GEB v0. 1: a large-scale agent-based socio-hydrological model–simulating 10 million individual farming households in a fully distributed hydrological model. Geoscientific Model Development, 16(9), 2437-2454.

Dillman, D. A., Smyth, J. D., & Christian, L. M. (2014). Internet, phone, mail, and mixed-mode surveys: The tailored design method. John Wiley & Sons.

Du, E., Tian, Y., Cai, X., Zheng, Y., Li, X., & Zheng, C. (2020). Exploring spatial heterogeneity and temporal dynamics of human-hydrological interactions in large river basins with intensive agriculture: A tightly coupled, fully integrated modeling approach. Journal of Hydrology, 591, 125313.

Dukes, M. D., & Evans, R. O. (2006). Impact of agriculture on water quality in the North Carolina Middle Coastal Plain. Journal of irrigation and drainage engineering, 132(3), 250-262.

Footitt, S., Clay, H. A., Dent, K., & Finch-Savage, W. E. (2014). Environment sensing in spring-dispersed seeds of a winter annual A rabidopsis influences the regulation of dormancy to align germination potential with seasonal changes. New Phytologist, 202(3), 929-939.

Gaur, V., Lang, C., Howard, G., & Quainoo, R. (2023). When energy issues are land use issues: estimating preferences for utility-scale solar energy siting. Land Economics, 99(3), 343-363.

Genova, P., & Wei, Y. (2023). A socio-hydrological model for assessing water resource allocation and water environmental regulations in the Maipo River basin. Journal of Hydrology, 617, 129159.

Gibson, C. A., Meyer, J. L., Poff, N. L., Hay, L. E., & Georgakakos, A. (2005). Flow regime alterations under changing climate in two river basins: implications for freshwater ecosystems. River Research and Applications, 21(8), 849-864.

Habib, K. M. N. (2011). A random utility maximization (RUM) based dynamic activity scheduling model: Application in weekend activity scheduling. Transportation, 38(1), 123-151.

Hautier, Y., Niklaus, P. A., & Hector, A. (2009). Competition for light causes plant biodiversity loss after eutrophication. Science, 324(5927), 636-638.

Hawley, M. E., Jackson, T. J., & McCuen, R. H. (1983). Surface soil moisture variation on small agricultural watersheds. Journal of Hydrology, 62(1-4), 179-200.

Hettiarachchi, S., Wasko, C., & Sharma, A. (2018). Increase in flood risk resulting from climate change in a developed urban watershed–the role of storm temporal patterns. Hydrology and Earth System Sciences, 22(3), 2041-2056.

Höök, M., & Tang, X. (2013). Depletion of fossil fuels and anthropogenic climate change—A review. Energy policy, 52, 797-809.

Howard, G., & Roe, B. E. (2013). Stripping because you want to versus stripping because the money is good: a latent class analysis of farmer preferences regarding filter strip programs.

Howard, G., Zhang, W., Valcu-Lisman, A., & Gassman, P. W. (2024). Evaluating the tradeoff between cost effectiveness and participation in agricultural conservation programs. American Journal of Agricultural Economics, 106(2), 712-738.

Howarth, R., Chan, F., Conley, D. J., Garnier, J., Doney, S. C., Marino, R., & Billen, G. (2011). Coupled biogeochemical cycles: eutrophication and hypoxia in temperate estuaries and coastal marine ecosystems. Frontiers in Ecology and the Environment, 9(1), 18-26.

Kapsalis, V. C., & Kalavrouziotis, I. K. (2021). Eutrophication—A worldwide water quality issue. Chemical Lake Restoration: Technologies, Innovations and Economic Perspectives, 1-21.

Kaspar, T. C., Jaynes, D. B., Parkin, T. B., Moorman, T. B., & Singer, J. W. (2012). Effectiveness of oat and rye cover crops in reducing nitrate losses in drainage water. Agricultural Water Management, 110, 25-33.

Kuil, L., Evans, T., McCord, P. F., Salinas, J. L., & Blöschl, G. (2018). Exploring the influence of smallholders' perceptions regarding water availability on crop choice and water allocation through socio-hydrological modeling. Water Resources Research, 54(4), 2580-2604.

Lal, R. (2013). Intensive agriculture and the soil carbon pool. Journal of Crop Improvement, 27(6), 735-751.

Liu, T., Bruins, R. J., & Heberling, M. T. (2018). Factors influencing farmers' adoption of best management practices: A review and synthesis. Sustainability, 10(2), 432.

Liu, Y., Gupta, H., Springer, E., & Wagener, T. (2008). Linking science with environmental decision making: Experiences from an integrated modeling approach to supporting sustainable water resources management. Environmental Modelling & Software, 23(7), 846-858.

Luo, Y., Ficklin, D. L., Liu, X., & Zhang, M. (2013). Assessment of climate change impacts on hydrology and water quality with a watershed modeling approach. Science of the total environment, 450, 72-82.

Ma, S., Swinton, S. M., Lupi, F., & Jolejole-Foreman, C. (2012). Farmers' willingness to participate in Payment-for-Environmental-Services programmes. Journal of Agricultural Economics, 63(3), 604-626.

McGuire, A. M., Bryant, D. C., & Denison, R. F. (1998). Wheat yields, nitrogen uptake, and soil moisture following winter legume cover crop vs. fallow. Agronomy journal, 90(3), 404-410.

Moore, Kenneth J., Robert P. Anex, Amani E. Elobeid, Shuizhang Fei, Cornelia B. Flora, A. Susana Goggi, Keri L. Jacobs et al. (2019) "Regenerating agricultural landscapes with perennial groundcover for intensive crop production." Agronomy 9, no. 8 (2019): 458.

NADP National Atmospheric Deposition Program. (2023). Retrieved December, 2023, from https://nadp.slh.wisc.edu/

Naganur, S., Patil, N. S., Patil, V., & Pujar, G. (2024). Evaluation of best management practices (BMPS) and their impact on environmental flow through SWAT+ model. Modeling Earth Systems and Environment, 1-15.

NCDEQ North Carolina Department of Environmental Quality. (2014). Tar-Pamlico Basin Plan. North Carolina Department of Environmental Quality. https://www.deq.nc.gov/about/divisions/water-resources/water-planning/basin-planning/river-basin-plans/tar-pamlico#2014Tar-PamlicoBasinPlan-4040

NCGAR North Carolina Department of Agriculture and Consumer Services. (2022). Tar-Pamlico Watershed Initiatives. North Carolina Department of Agriculture and Consumer Services. https://www.ncagr.gov/divisions/soil-water-conservation/programs-initiatives/watershed-initiatives/tar-pamlico#Contact-4304

Neumann, A., Dong, F., Shimoda, Y., Arnillas, C. A., Javed, A., Yang, C., ... & Arhonditsis, G. B. (2021). A review of the current state of process-based and data-driven modelling: guidelines for Lake Erie managers and watershed modellers. Environmental Reviews, 29(4), 443-490.

Nolan, B. T., Healy, R. W., Taber, P. E., Perkins, K., Hitt, K. J., & Wolock, D. M. (2007). Factors influencing ground-water recharge in the eastern United States. Journal of Hydrology, 332(1-2), 187-205.

Nouri, A., Lukas, S., Singh, S., Singh, S., & Machado, S. (2022). When do cover crops reduce nitrate leaching? A global meta-analysis. Global Change Biology, 28(15), 4736-4749.

Ouyang, Y., Grace, J. M., Parajuli, P. B., & Caldwell, P. V. (2022). Impacts of multiple hurricanes and tropical storms on watershed hydrological processes in the Florida panhandle. Climate, 10(3), 42.

Palmer, M. A., Reidy Liermann, C. A., Nilsson, C., Flörke, M., Alcamo, J., Lake, P. S., & Bond, N. (2008). Climate change and the world's river basins: anticipating management options. Frontiers in Ecology and the Environment, 6(2), 81-89.

Peterson, J. M., Smith, C. M., Leatherman, J. C., Hendricks, N. P., & Fox, J. A. (2015). Transaction costs in payment for environmental service contracts. American Journal of Agricultural Economics, 97(1), 219-238.

Peterson, T. J., Saft, M., Peel, M. C., & John, A. (2021). Watersheds may not recover from drought. Science, 372(6543), 745-749.

Petry, J., Soulsby, C., Malcolm, I. A., & Youngson, A. F. (2002). Hydrological controls on nutrient concentrations and fluxes in agricultural catchments. Science of the Total Environment, 294(1-3), 95-110.

Reckhow, K. H., & Chapra, S. C. (1999). Modeling excessive nutrient loading in the environment. Environmental Pollution, 100(1-3), 197-207.

Ribaudo, M. O., R. Heimlich, and M. Peters. 2005. “Nitrogen Sources and Gulf Hypoxia: Potential for Environmental Credit Trading.” Ecological Economics 52(2): 159–68.

Ritter, W. F., Scarborough, R. W., & Chirnside, A. E. M. (1998). Winter cover crops as a best management practice for reducing nitrogen leaching. Journal of Contaminant Hydrology, 34(1-2), 1-15.

Robertson, G. P., & Vitousek, P. M. (2009). Nitrogen in agriculture: balancing the cost of an essential resource. Annual review of environment and resources, 34, 97-125.

Rossi, A. M., & Hinrichs, C. C. (2011). Hope and skepticism: Farmer and local community views on the socio-economic benefits of agricultural bioenergy. Biomass and Bioenergy, 35(4), 1418-1428.

Schuerz, C. (2019). chrisschuerz/SWATplusR: SWATplusR 0.2. 7.

Sheshukov, A. Y., Douglas-Mankin, K. R., Sinnathamby, S., & Daggupati, P. (2016). Pasture BMP effectiveness using an HRU-based subarea approach in SWAT. Journal of environmental management, 166, 276-284.

Shibu, M. E., Leffelaar, P. A., Van Keulen, H., & Aggarwal, P. K. (2010). LINTUL3, a simulation model for nitrogen-limited situations: Application to rice. European Journal of Agronomy, 32(4), 255-271.

Singh, S.; Hwang, S.; Arnold, J.G.; Bhattarai, R. Evaluation of Agricultural BMPs' Impact on Water Quality and Crop Production Using SWAT+ Model. Agriculture 2023, 13, 1484. https://doi.org/10.3390/agriculture13081484

Smith, D. R., Macrae, M. L., Kleinman, P. J. A., Jarvie, H. P., King, K. W., & Bryant, R. B. (2019). The latitudes, attitudes, and platitudes of watershed phosphorus management in North America. Journal of environmental quality, 48(5), 1176-1190.

St, L., & Wold, S. (1989). Analysis of variance (ANOVA). Chemometrics and intelligent laboratory systems, 6(4), 259-272.

SWAT+ IO Document. (2020). Input/output file documentation, version 2016 modified on November 16, 2020 according to REV 60.5. Retrieved from https://swatplus.gitbook.io/io-docs

Upadhyay, P., Linhoss, A., Kelble, C., Ashby, S., Murphy, N., & Parajuli, P. B. (2022). Applications of the SWAT model for coastal watersheds: review and recommendations. Journal of the ASABE, 65(2), 453-469.

Veisi, H., Jackson-Smith, D., & Arrueta, L. (2022). Alignment of stakeholder and scientist understandings and expectations in a participatory modeling project. Environmental Science & Policy, 134, 57-66.

Wendling, M., Büchi, L., Amossé, C., Sinaj, S., Walter, A., & Charles, R. (2016). Influence of root and leaf traits on the uptake of nutrients in cover crops. Plant and Soil, 409, 419-434.

Wurtsbaugh, W. A., Paerl, H. W., & Dodds, W. K. (2019). Nutrients, eutrophication and harmful algal blooms along the freshwater to marine continuum. Wiley Interdisciplinary Reviews: Water, 6(5), e1373.